2014

# BEYOND PEROXISOME: ABCD2 MODIFIES PPARα SIGNALING AND IDENTIFIES A SUBCLASS OF PEROXISOMES IN MOUSE ADIPOSE TISSUE

Xiaoxi Liu
*University of Kentucky*, xiaoxi.liupharmsci@gmail.com

STUDENT AGREEMENT:

I represent that my thesis or dissertation and abstract are my original work. Proper attribution has been given to all outside sources. I understand that I am solely responsible for obtaining any needed copyright permissions. I have obtained needed written permission statement(s) from the owner(s) of each third-party copyrighted matter to be included in my work, allowing electronic distribution (if such use is not permitted by the fair use doctrine) which will be submitted to UKnowledge as Additional File.

I hereby grant to The University of Kentucky and its agents the irrevocable, non-exclusive, and royalty-free license to archive and make accessible my work in whole or in part in all forms of media, now or hereafter known. I agree that the document mentioned above may be made available immediately for worldwide access unless an embargo applies.

I retain all other ownership rights to the copyright of my work. I also retain the right to use in future works (such as articles or books) all or part of my work. I understand that I am free to register the copyright to my work.

REVIEW, APPROVAL AND ACCEPTANCE

The document mentioned above has been reviewed and accepted by the student's advisor, on behalf of the advisory committee, and by the Director of Graduate Studies (DGS), on behalf of the program; we verify that this is the final, approved version of the student's thesis including all changes required by the advisory committee. The undersigned agree to abide by the statements above.

Xiaoxi Liu, Student

Dr. Gregory Graf, Major Professor

Dr. Jim Pauly, Director of Graduate Studies

# BEYOND PEROXISOME: ABCD2 MODIFIES PPARα SIGNALING AND IDENTIFIES A SUBCLASS OF PEROXISOMES IN MOUSE ADIPOSE TISSUE

Dissertation

A dissertation submitted in partial fulfillment of the requirements for the degree of Doctor of Philosophy in the Graduate School at the University of Kentucky

By

Xiaoxi Liu

Lexington, Kentucky

Director: Dr. Gregory Graf, Associate Professor,

Pharmaceutical Sciences

Lexington, KY

2014

ABSTRACT OF DISSERTATION

# BEYOND PEROXISOME: ABCD2 MODIFIES PPARα SIGNALING AND IDENTIFIES A SUBCLASS OF PEROXISOMES IN MOUSE ADIPOSE TISSUE

ABCD2 (D2) has been proposed as a peroxisomal long-chain acyl-CoA transporter that is essential for very long chain fatty acid metabolism. In the livers of mice, D2 is highly induced by fenofibrate, a PPARα ligand that has been widely used as a lipid lowering agent in the treatment of hypertriglyceridemia. To determine if D2 is a modifier of fibrate responses, wild-type and D2 deficient mice were treated with fenofibrate for 14 days. The absence of D2 altered expression of gene clusters associated with lipid metabolism, including PPARα signaling. Using 3T3-L1 adipocytes, which express high levels of D2, we confirmed that knock-down of D2 modified genomic responses to fibrate treatment. We next evaluated the impact of D2 on effects of fibrates in a mouse model of diet-induced obesity. Fenofibrate treatment opposed the development of obesity, hypertriglyceridemia, and insulin resistance. However, these effects were unaffected by D2 genotype. We concluded that D2 can modulate genomic responses to fibrates, but that these effects are not sufficiently robust to alter the effects of fibrates on diet-induced obesity phenotypes.

Although proposed as a peroxisomal transporter, the intracellular localization of D2, especially in adipose tissue, has not been validated with direct experimental evidence. Sequential centrifugation of mouse adipose homogenates generated a fraction enriched with D2, but lacked well-known peroxisome markers including catalase, PEX19, and ABCD3 (D3). Electron microscopic imaging of this fraction confirmed the presence of D2 protein on an organelle with evidence of a dense matrix and a diameter of ~200 nm, the typical structure and size of a microperoxisome. D2 and PEX19 antibodies recognized distinct structures in mouse adipose. Immunoisolation of the D2-containing compartment from adipose tissue confirmed the scarcity of PEX19. Proteomic profiling of the D2 compartment revealed the presence of proteins associated peroxisome, endoplasmic reticulum (ER), and mitochondria. We conclude that D2 is localized to a distinct subclass of peroxisomes that lack many peroxisome proteins and may physically associate with mitochondria and the ER.

KEYWORDS: ABC Transporter, Fenofibrate, Peroxisome, Adipose Tissue, Cellular Compartment

Xiaoxi Liu

07/29/2014

# BEYOND PEROXISOME: ABCD2 MODIFIES PPARα SIGNALING AND IDENTIFIES A SUBCLASS OF PEROXISOMES IN MOUSE ADIPOSE TISSUE

By

Xiaoxi Liu

Gregory Graf, PH.D.
Director of Dissertation

Jim Pauly, PH.D.
Director of Graduate Studies

07/29/2014

ACKNOWLEDMENTS

First and foremost I would like to express my sincerest appreciation to my mentor Dr. Gregory Graf. He has set up the best example of a scientist who devotes his greatest enthusiasm to scientific research. I am deeply grateful to him for his patient guidance and insightful advice that helped me in overcoming the difficulties and completing the projects. I am thankful to him for my training in scientific writing and presentation skills which will benefit me in a long way for my career development.

I would also like to acknowledge my committee members, Dr. Markos Leggas, Dr. Charles Loftin and Dr. Dennis Bruemmer, who has provided helpful discussions that accelerated the progression of my projects.

I would like to thank my lab members, Yuhuan Wang, Dr. Jingjing Liu, Dr. Nadezhda Steliyanova Sabeva, Dr. Shuang Liang, Dr. Kai Su, Sonja Pijut, Jianing Li, Amanda Harrison, Jeannie Haak, Andrew Brown and Joshua Lester, for their help and assistance.

Lastly but not least, I would like to thank my loving girlfriend Yuhuan Wang, for sharing the happiest moments in my life, and for her love, support and accompany over the most difficult times in my career.

TABLE OF CONTENTS

LIST OF TABLES

LIST OF FIGURES

# CHAPTER 1: INTRODUCTION

## 1.1 METABOLIC SYNDROME, DYSLIPIDEMIA AND CARDIOVASCULAR DISEASE

### 1.1.1 Metabolic syndrome

#### 1.1.1.1 Definition

Metabolic syndrome (MtS) is a group of medial disorders that raise the risk of developing type 2 diabetes and cardiovascular disease [1]. There have been several definitions of metabolic syndrome historically. The most commonly used criteria were proposed by World Health Organization (WHO) [2], the European Group for the study of Insulin Resistance (EGIR) [3], the National Cholesterol Education Program Adult Treatment Panel III (NCEP ATP III) [4], American Association of Clinical Endocrinologists (AACE) [5], and the International Diabetes Federation (IDF) [1]. Although the criteria of each definition slightly differ (Table 1.1), the common characteristics include central obesity, atherogenic dyslipidemia, high blood pressure, and insulin resistance.

#### 1.1.1.2 Epidemiology

The international prevalence of MtS ranges from less than 10% to 84%, depending on the region, sex, age, race and ethnicity of the population studied [6-9]. The MtS is significantly associated with higher economic status, sedentary lifestyle, and high body mass index and quite prevalent in developed countries such as US and Europe [1]. The observed prevalence of MtS is highly correlated with obesity, with the occurrence of 5% in normal weight, 22% in overweight, and 60% in obese populations [10]. The prevalence

of MtS varies from 8% to 43% in men whereas from 7% to 56% in women around the world [9]. The occurrence of MtS increases with age, with 40–59 years of age about three times as prevalent as those 20–39 years of age, 60 years of age and over more than four times as prevalent in males and six times in females [11].

| Clinical Diagnostics | WHO | EGIR | ATPIII | AACE | IDF |
|---|---|---|---|---|---|
| Insulin Resistance | IGT, IFG, T2DM, or lowered insulin Sensitivity plus any 2 of the following | Plasma insulin >75th percentile plus any 2 of the following | None, but any 3 of the following 5 features | IGT or IFG plus any of thefollowing based on the clinical judgment | None |
| Central Obesity | Men: waist-to-hip ratio >0.90; women: waist-to-hip ratio >0.85 and/or BMI > 30 kg/$m^2$ | WC ≥94 cm in men or ≥80 cm in women | WC ≥102cm inmen or ≥88 cm in women | BMI ≥ 25 kg/$m^2$ | IncreasedWC (population specific) plus any 2 of the following |
| Dislypidemia | TGs ≥150mg/dL and/or HDL-C <35 mg/dL in men or <39 mg/dL in women | TGs ≥150mg/dL and/or HDL-C <39 mg/dL in men or women | TGs ≥150mg/dL HDL-C <40mg/dL in men or <50mg/dL in women | TGs ≥150mg/dL and HDL-C <40mg/dL in men or <50mg/dL in women | TGs ≥150mg/dL or on TGs Rx. HDL-C <40mg/dL in men or <50mg/dL in women or on HDL-C Rx |
| Hypertension | ≥140/90mmHg | ≥140/90mmHg or on hypertension Rx | ≥130/85mmHg | ≥130/85mmHg | ≥130mmHg systolic or ≥85 mm Hg diastolic or on hypertension Rx |
| Hyperglycemia | IGT, IFG, or T2DM | IGT or IFG (but not diabetes) | >110mg/dL (includes diabetes) | IGT or IFG (but not diabetes) | ≥100mg/dL (includes diabetes) |
| Other | Microalbuminuria: Urinary excretion rate of >20mg/min or albumin: creatinine ratio of >30mg/g. | | | Other features of insulin resistance | |

**Table 1.1 Clinical diagnostic criteria for metabolic syndrome [12].**

1.1.1.3 Central obesity

Central obesity is clinically characterized as excessive abdominal or visceral fat deposition around the stomach and abdomen. Generally, obesity is due the excessive consumption of high energy food and lack of physical activity. Although obesity is a risk factor for insulin resistance, type 2 diabetes and cardiovascular disease, some obese patients are “protected” from these disease by unknown mechanism [13]. On the other

hand, individuals with excess of visceral fat is at substantially higher risk of insulin resistance and MtS compared with those with similar amount of total body fat, indicating a strong correlation of central obesity and MtS [14, 15]. However, it is still controversial whether visceral fat is a causal factor or just a biomarker of MtS.

In centrally obese patients, the intra-abdominal adipocytes are characterized by a hypertrophied and hyperlipolytic state that is resistant to the effects of insulin [16, 17]. This leads to increased non-esterified fatty acid (NEFA) flux to the liver and may impair liver metabolism. In a diet-induced visceral obesity canine model, hepatic insulin resistance was observed with respect to glucose production [18]. Excessive visceral fat is also correlated with circulating NEFA and may contribute to peripheral tissue insulin resistance [19]. An acute exposure to high levels of NEFA induces insulin resistance in skeletal muscle by inhibiting glucose uptake whereas chronic exposure impairs pancreatic β-cell function [20].

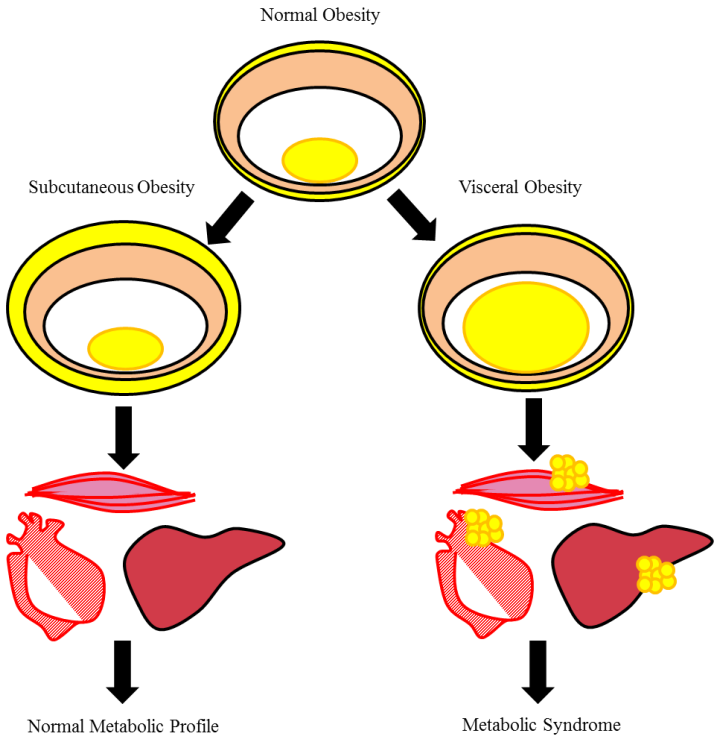


**Figure 1.1 Central obesity and ectopic lipid accumulation in peripheral tissues [21].** Excessive visceral fat accumulation might lead to ectopic lipid accumulation in peripheral tissues such as skeletal muscle, heart and liver, which may eventually increase the risk of metabolic syndrome.

Besides serving as a lipid reservoir, adipose tissue is also an important endocrine organ. The signal molecules secreted from adipose tissue includes TNFα, IL-6, C-reactive protein (CRP), plasminogen activator inhibitor-1 (PAI-1), adipsin, acylation stimulating protein (ASP), adiponectin, leptin and resistin [22]. Abdominally obese patients with excess of visceral fat have elevated plasma CRP, TNFα, and IL-6 concentrations and reduced adiponectin concentrations [23]. CRP is an inflammatory marker that has been demonstrated as an independent predictor of the occurrence of future cardiovascular disease [24]. TNFα is a paracrine mediator in adipocytes and have been suggested to induce adipocyte apoptosis and promote insulin resistance by inhibiting the insulin

receptor substrate 1 signaling pathway [25, 26]. This further tends to exacerbate the NEFA release and induce dyslipidemia [27]. IL-6 has both inflammatory and anti-inflammatory actions. IL-6 impairs insulin sensitivity and also serves as a major determinant of the hepatic production of CRP. IL-6 also suppresses lipoprotein lipase activity [28]. Adiponectin has been shown as a strong inverse independent risk factor for cardiovascular disease and therefore considered as to be 'protective' [29]. Adiponectin has multifaceted functions including, but not limited to, insulin sensitizing, inhibiting hepatic gluconeogenesis, promoting glucose transport and fatty acid oxidation in muscles, and antagonism of TNFα [30–32]. Overall, central obesity is tightly associated with altered NEFA metabolism and adipose endocrine that together promote the development of MtS.

#### 1.1.1.4 Insulin resistance

In the wild environment, nutrient sources are often scarce and caloric demands constantly change. Faced with this challenge, animals develop mechanisms to promote anabolism when energy consumption is excessive and become catabolic when demands override consumption. Insulin acts an efficient solution to adapt to this challenge. However, in modern human society, the common lifestyle has greatly altered with abundant caloric supply but very little caloric demands. Obesity is now an epidemic and often associated with other diseases including metabolic syndrome, type 2 diabetes, nonalcoholic fatty liver disease and cardiovascular disease. Insulin resistance is found with the pathogenesis for many of these modern diseases.

Insulin resistance is defined as a pathological condition in which a normal insulin concentration fails to produce an adequate response in peripheral tissues such as muscle, adipose and liver, which is a key feature of type 2 diabetes. Insulin resistance is a major characteristic of MtS and leads to compensatory elevated insulin secretion from pancreatic β-cells. Intensive insulin therapy may compensate for insufficient insulin action and maintain normal glycemic levels. However, this therapy increases the body weight and the risk of developing cardiovascular disease [33]. Several mechanisms have been proposed to explain the pathogenesis of insulin resistance. Three representative mechanisms include ectopic lipid accumulation, ER stress and systemic inflammation [34].

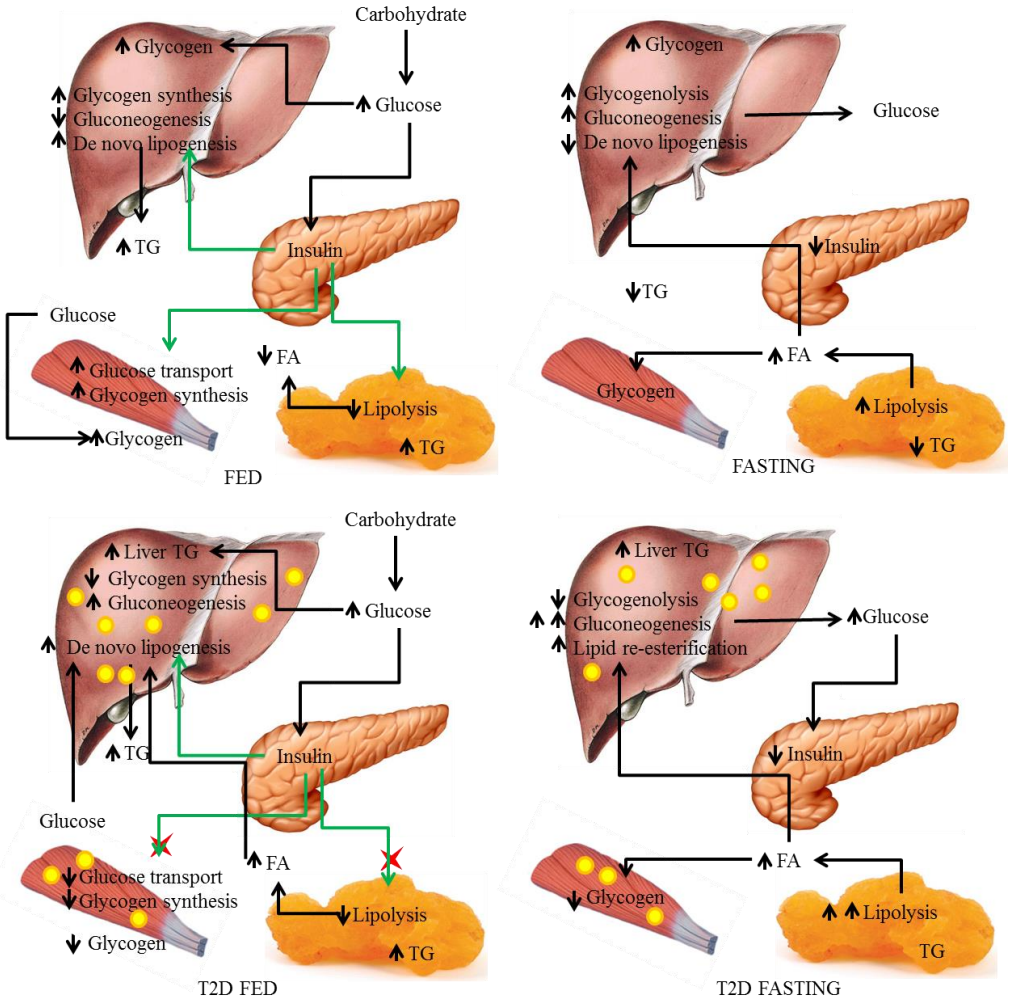


**Figure 1.2 Insulin action in normal and type 2 diabetes conditions [34].** In normal insulin sensitive conditions, during the fed state, dietary carbohydrate leads to elevated plasma glucose levels and triggers insulin secretion from pancreatic β cells. Circulating insulin acts on peripheral tissues including liver, skeletal muscle and adipose. In the liver, insulin increases glycogen synthesis while decreasing gluconeogenesis, and promotes lipogenesis. In the skeletal muscle, insulin promotes glucose transport and glycogen synthesis. In the adipose, insulin promotes triglyceride synthesis while inhibiting lipolysis. During the fasted state, low plasma glucose levels prohibit insulin secretion and therefore plasma insulin level is low. This promotes glycogenolysis and gluconeogenesis and inhibits lipogenesis in the liver, permits the glycogenolysis in the muscle and lipolysis in the adipose. In type 2 diabetic conditions, the insulin signaling is impaired due to ectopic lipid accumulation in peripheral tissues (impaired pathways indicated by 'x'). The results are decreased hepatic glycogen synthesis and increased gluconeogenesis and lipogenesis, decreased glucose transport and glycogen synthesis in liver and increased lipolysis in adipose in both fed and fasted states.

It is widely accepted that the ectopic lipid accumulation is associated with insulin resistance. Early studies demonstrated that acute lipid infusions decreased myocellular glucose utilization by inhibition of pyruvate dehydrogenase, leading to reductions in glucose oxidation and accumulation of glycolytic intermediates [35, 36]. In chronic disease states, however, insulin resistance in skeletal muscle can be attributed to impaired insulin signaling and therefore decreased glucose transport due to impaired GLUT4 translocation, rather than inhibited glycolysis [37, 38]. Since lipids can either circulate in plasma or accumulate within insulin responsive tissues, there were debates concerning which lipids are responsible for insulin resistance. Studies in normal weight, non-diabetic adults have shown that intramyocellular lipid content is a much stronger predictor of muscle insulin resistance than circulating fatty acids [39]. In normal rates infused with lipid emulsion, muscle insulin resistance developed concordantly with the accumulation of intramyocellular diacylglycerol (DAG) and impaired glucose uptake 3-4 hours after the lipid infusion [40]. Insulin resistance occurred independently of changes in muscle triglyceride (TG) content, thus dissociating the TG concentrations from insulin resistance and proposing DAG as the inducer [41]. DAG, a signaling intermediate that activates protein kinase C (PKC) family, was associated with the activation of novel PKC in these experiments. The link between DAG-mediated activation of novel PKC and muscle insulin resistance has been confirmed in human studies, although with some difference in the novel PKC isoforms that was activated [42].

Ectopic lipid accumulation in liver, also known as steatosis is the most common chronic live disease in US. Dietary caloric restriction rapidly reduces hepatic steatosis in patients with poorly controlled type 2 diabetes [43, 44]. After 12 weeks on a hypocaloric diet,

these patients experienced rapid decrease in liver fat content, associated with normalization in hepatic insulin sensitivity and reductions in fasting hyperglycemia. The relationship of hepatic lipid accumulation and insulin resistance has been supported with increasing evidence in genetic rodent models. Lipoprotein lipase (LPL) is a key enzyme that hydrolyzes plasma TG and promotes the tissue uptake of released free fatty acids through fatty acid transport protein (FATP) and CD36. The overexpression of LPL in liver leads to hepatic steatosis and hepatic insulin resistance [45, 46]. The overexpression of hepatic CD36 causes NAFLD even in mice fed with regular chow-diet [47]. Deletion of FATP2 or FATP5 reduces hepatic fatty acid transport and protects against hepatic steatosis and glucose intolerance [48, 49].

#### 1.1.1.5 Hypertension

Individuals with hypertension have two to three fold increased risk for cardiovascular disease compared with non-hypertensive individuals. Essential hypertension is often observed associated with other metabolic disorders, most commonly obesity, insulin resistance and dyslipidemia [50]. At least 75% of the incidence of hypertension is estimated to have a direct relation to obesity [51]. Several mechanisms have been proposed to explain the close relationship between hypertension and obesity. Insulin has been proposed as a mediator for hypertension in obese patients due to the fact that it stimulates the sympathetic nervous system (SNS) and its secretion is considerably elevated by obesity [52-54]. This is supported by studies demonstrating concomitant decreases in blood pressure and SNS activity when insulin is lowered due to low energy diets [55]. There are studies suggesting that hyperglycemia and hyperinsulinemia increase the expression of angiotensinogen, angiotensin II, and the ATI receptor and

therefore activate the renin angiotensin system (RAS). The RAS may give rise to the development of hypertension in insulin resistant patients [56].

### 1.1.2 Dyslipidemia and cardiovascular disease

Atherogenic dyslipidemia comprises a higher proportion of small light-density lipoprotein (LDL) particles, reduced high-density lipoprotein (HDL)-cholesterol and increase triglycerides (TG) [57]. It is commonly seen in patients with obesity, the metabolic syndrome, insulin resistance and type 2 diabetes and has been recognized as an important marker for the increased cardiovascular disease risk [58, 59]. Both lifestyle changes and pharmacological treatments are recommended to control the development of dyslipidemia in patients with metabolic syndrome and type 2 diabetes. The National Cholesterol Education Program (NCEP) adult Treatment Panel (ATP) III recommended lifestyle changes including reduced intake of saturated fats and cholesterol, intake of dietary options to enhance lowering of LDL cholesterol, weight control, and increased physical activity [60]. For individuals at high risk of or currently having developing cardiovascular disease, or persistent atherogenic dyslipidemia, pharmacotherapy may be necessary.

Statins are a class of drugs that are effective in lowering cholesterol levels, improving dyslipidemia and decreasing the risks of cardiovascular diseases. They act as reversible, competitive inhibitors of HMG-CoA reductase, the rate-limiting enzyme for cholesterol biosynthesis. By reducing cholesterol synthesis and decreasing the intracellular cholesterol pool, the statins stimulate the upregulation of cell surface LDL receptors and promote the clearance of apoB100-containing lipoproteins (VLDL, VLDL remnants, IDL

and LDL) [61]. Other functions of statins include inhibiting hepatic VLDL secretion, lowering plasma TG levels, increasing apoA-I expression and HDL secretion [61]. Statins are the first-line option for lowering LDL cholesterol [60]. The LDL cholesterol reducing capacity of specific statins differs and can be summarized as follows: rosuvastatin 45–63% (5–40mg/day); atorvastatin 26–60% (10–80 mg/day); simvastatin 26–47% (10–80 mg/day); lovastatin 21–42% (10–80mg/day); fluvastatin 22–36%(10–20mg/day); and pravastatin 22–34% (10–80 mg/day). Therefore, the selection of specific statin and dose are generally based on the targeted reduction of LDL cholesterol [62].

Ezetimibe is primarily used as a secondary therapy to statins to further reduce LDL cholesterol. It acts by binding to the Niemann-Pick C1-like 1 protein (NPC1L1), a sterol transporter that is responsible for cholesterol and phytosterol absorption in intestine, and therefore inhibiting cholesterol absorption [63, 64]. Ezetimibe alone decreases plasma LDL cholesterol by 20% and has an additive lowering effect when combined with statins [65, 66]. Although there is no clinical trial evidence that ezetimibe treatment alone beneficially impacts the risk for cardiovascular an event, statin/ezetimibe combination offers an option for patients who don’t tolerate moderate to high doses of statins.

Bile acid sequestrants (BAS) are a group of anion exchange resins that bind bile acids in the gastrointestinal tract. BASs are polymeric compounds that are not absorbed by the gut. Thus, BAS along with any bile acids bound to the drug are excreted through feces, which prevent the reabsorption of bile acids across the terminal ileum and lower their concentration in the enterohepatic circulation [61]. With reduced bile acids reabsorbed, there is increased consumption of cholesterol due to the upregulation of 7-a-hydroxylase, the rate-limiting enzyme for the conversion of cholesterol into bile acids. With increased

intrahepatic cholesterol consumption, hepatocytes increase their surface expression of LDL receptors and therefore promote the clearance of apoB100-containing lipoproteins from plasma. The BAS decrease plasma LDL cholesterol by 15-30% and increase HDL cholesterol by 3-5%. Statins should be used in combination with BAS because BAS stimulate HMG-CoA reductase activity and offset the effects over time.

Niacin, also known as nicotinic acid, vitamin B3, is the oldest lipid lowering drug which reduces LDL cholesterol, TG and increases HDL cholesterol [67]. The efficacy of niacin therapy in reducing cardiovascular events was first described in the Coronary Drug Project [68]. Niacin alone or combined with other lipid lowering drugs can significantly reduce the risk of cardiovascular disease [69]. The mechanism of niacin effects is complex and not completely characterized. Niacin stimulates hepatic production of apolipoprotein A1 and HDL and inhibits HDL uptake and catabolism by hepatocytes [70, 71]. Niacin decreases fatty acids flux from visceral adipose to liver by inhibiting hormone-sensitive lipase activity and therefore reduces the substrate for hepatic TG synthesis [72]. It also inhibits diacylglycerol acyltransferase, an enzyme that esterifies fatty acid to glycerol, and therefore reduces TG formation with hepatocytes and VLDL formation [73].

## 1.2 PPARα AND FIBRATES

### 1.2.1 PEROXISOME PROLIFERATOR-ACTIVATED RECEPTORS

Introduction

Peroxisome proliferator-activated receptors (PPARs) are a group of nuclear receptor proteins that functions as transcription factors [74]. When activated by endogenous and/or synthetic ligands, PPARs bind to the peroxisome proliferator response element (PPRE) motifs of regulated gene promoter regions and induce the transcription of downstream target genes that have various biological roles [75].

Peroxisome proliferation was first reported in rats in the 1960s [76]. A number of compounds were later discovered to induce the peroxisome proliferation and named as peroxisome proliferators. The first receptor for peroxisome proliferators was cloned from mouse liver in 1990 and named as peroxisome proliferator-activated receptor [77]. Shortly afterwards, it was realized that the PPARs are a group of three receptors $\alpha$, $\beta/\delta$ and $\gamma$ [78]. They all function as transcription factors and regulate the expression of genes involved in a variety of biological processes including glucose and lipid metabolism, energy homeostasis, insulin sensitivity, immune responses, and cell growth and cell differentiation [79]. A variety of endogenous ligands for PPARs have been identified while a series of synthetic agonists have been discovered and commercialized [80]. Based on the tissue distribution and ligand specificity, the activation of PPARs usually results in diverse effects including adipogenesis, fatty acid oxidation, and anti-inflammation [81].

All three isoforms of PPAR possesses similar structures. They contain four functional domains: A/B, C, D and E/F. The N-terminal domain (A/B) is responsible for the phosphorylation of the receptor [82]. The C domain is the DNA binding domain that is required for the binding of the receptor to peroxisome-proliferator response element (PPRE) in the promoter region of target genes [83]. The D domain or co-FBD is the site

for co-factors coupling. The ligand-binding domain or E/F domain is responsible for specific ligand binding and activation of PPARs [84]. AF-2 domain is associated with E/F domain and promotes the recruitment of cofactors for the initiation of gene transcription process [84].


**Figure 1.3: Functional domains of PPARs [85].** The PPARs consist of four functional domains. The N-terminal region contains the A/B domain that is preceded with AF-1 which is responsible for phosphorylation. C domain (DBD) is responsible for DNA binding. The D domain is the region of cofactors binding (Co-FBD). The E/F domain is the ligand binding domain (LBD) followed by the AF-2 which recruits cofactors for gene transcription.

PPAR forms a heterodimer with RXR and binds to the PPRE region of target gene's promoter. In the absence of ligands, the activation of transcription is blocked by associated corepressor proteins. These proteins include G-protein pathway suppressor 2 (GPS2), nuclear receptor corepressors (NCoR), and histone deacetylases (HDAC) [86, 87]. Ligand binding leads to the dissociation of the corepressor proteins and recruits coactivators such as PPAR coactivator (PGC-1), the histone acetyltransferase p300, CREB binding protein (CBP), and steroid receptor coactivator (SRC)-1. Formation of the PPAR activation complex causes histone modification (e.g., through acetylation) and initiation of gene transcription [88, 89].

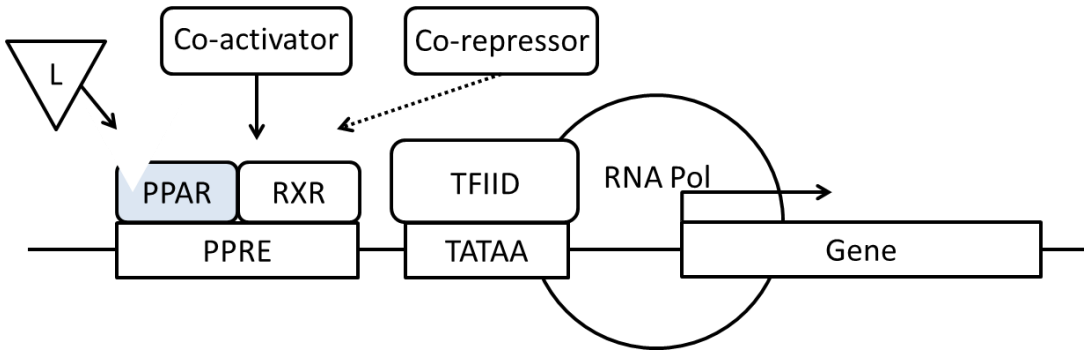


**Figure 1.4: PPAR regulates gene transcription [85].** Without ligand binding, the PPAR is in the inactivated state and interacts with the corepressor. The complex inhibits the initiation of transcription through its histone deacetylase activity. With ligand binding, PPAR is activated and heterodimerizes with RXR. The heterodimer recruits coactivators and promotes gene transcription due to its histone acetylase activity.

PPARγ

PPARγ is expressed in immune cells, mucosa of colon and cecum, placenta, but is most widely expressed in adipose tissue. PPARγ is the master regulator for differentiation and functioning of adipocytes [90]. There are three isoforms of PPARγ identified. All three isoforms are derived from the same gene but transcribed using alternative promoters [91, 92]. PPARγ 1 is ubiquitously expressed, while PPARγ2 is restricted to adipose tissue and PPARγ3 is abundant in adipose tissue, macrophages and large intestine [93, 94]. Genetic ablation studies in cells have shown that PPARγ1 has adipogenic action but PPARγ2 is more potent in this function [95].

Like most nuclear receptors, functions as a ligand-activated transcription factor. The biological ligands for PPARγ are still not characterized. It has been shown that polyunsaturated fatty acids and related molecules can activate PPARγ, although the response to native fatty acids is poor [96]. Certain oxidized fatty acids found in oxidized

LDL activate PPARγ with increased potency and efficacy relatively and are present significantly in atherosclerotic lesions [97]. However, it is unclear if oxidized fatty acids are activators in other tissues. Nitrated fatty acids and lysophosphatidic acid have also been reported to activate PPARγ [98, 99]. The impact of these molecules in PPARγ biology needs further validation.

Thiazolidinediones (TZD) are a class of synthetic agonists that activate PPARγ and are known for their anti-diabetic effects. The TZDs were initially discovered to lower glucose levels in rodents. They were later confirmed to improve insulin sensitivity in human subjects [100]. Rosiglitazone and pioglitazone are currently widely used in clinic for the treatment of type 2 diabetes. TZDs take their effects by primarily acting on adipose tissue through a 'lipid steal' mechanism [101, 102]. Type 2 diabetes is associated with elevated plasma free fatty acids (FFA) and ectopic lipid accumulation in peripheral tissues other than adipose, such as liver and skeletal muscle. Activation of PPARγ in adipose tissue increases its capability to store dietary fatty acids through upregulation of aP2, LPL, CD36, FATP, PEPCK and the glycerol transporter aquaporin 7. This results in the shift of fatty acids into adipose from other peripheral tissues where ectopic lipid accumulation has deleterious effects on insulin action. Another mechanism by TZDs sensitize insulin response is by altering the production of adipokines. TZD administration in rodents and humans induced the mRNA and plasma protein levels of adiponectin, of which amount is inversely correlated with insulin sensitivity [103-105]. Activation of PPAR in adipocytes is also associated with decreased TNFα and resistin which cause insulin resistance [106].

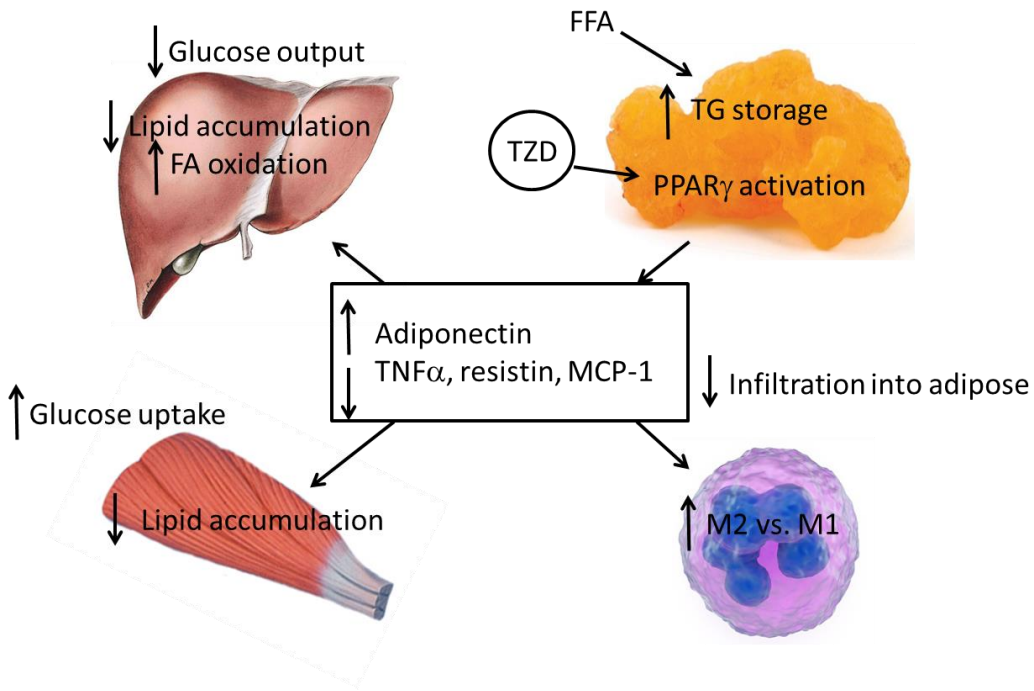


**Figure 1.5 Thiazolidinedione (TZD) activates PPARγ in adipose tissue and increases insulin sensitivity [90].** PPARγ activation in adipose tissue promotes lipid uptake from plasma and storage in adipocytes. Activation of PPARγ also alters the production of adipokines (i.e. adiponectin, TNFα, MCP-1, and resistin). This leads to suppression of hepatic glucose uptake and stimulation of skeletal muscle glucose uptake. Activation of PPARγ also tilts the population of macrophages toward the anti-inflammatory M2 phenotype and reduces macrophage infiltration into adipose. FA, fatty acid; FFA, free fatty acid; TG, triglyceride.

PPARβ/δ

PPARβ or δ is highly expressed in many tissues including colon, small intestine, liver, keratinocytes, heart, adipose, spleen, skeletal muscle, lung, brain and thymus [107]. Although expressed all over the body, its pharmacology is less understood than the other subtypes [108]. PPARβ is the most abundant isoform of all the three PPARs in skeletal muscle. Given the large percentage of skeletal muscle in whole body weight (~50%), it was proposed that activation of PPARβ may greatly promote fatty acid catabolism in

skeletal muscle and therefore improve plasma lipid profiles [85]. However, very little evidence has been reported to support this hypothesis. Nonetheless, a number of synthetic compounds are being developed as selective PPARβ ligands and have shown potential application in treating dyslipidemia. In insulin-resistant middle-aged obese rhesus monkey, a selective PPARβ agonist GW501516 causes a dramatic increase in plasma HDL cholesterol and reductions in LDL and TG in a dose dependent manner, suggesting its hypolipidemic and antidiabetic properties [109]. In humans, however, there are conflicting reports as to whether PPARβ polymorphisms are associated with plasma lipoprotein profiles [110, 111].

## 1.2 PPARα AND FIBRATES

### 1.2.1 PPARα

Introduction

PPARα was the first identified PPAR isoform and named based on its ability to be activated by peroxisome proliferators in rodents. PPARα is expressed in numerous tissues including liver, kidneys, heart, skeletal muscle and brown adipose [94, 112]. PPARα expression is also detected in immune cells such as T-cells and macrophages [113, 114]. Evidence suggests that rodents and humans have similar tissue distribution pattern of PPARα [115, 116] . PPARα is a key modulator of fatty acid oxidation, which occurs in mitochondria, peroxisomes and microsomes in the liver. It controls many aspects of hepatic lipid metabolism, including fatty acid uptake and activation, intracellular fatty acid trafficking, fatty acid oxidation and ketogenesis and triglyceride storage and lipolysis [117, 118].

PPARα target genes

The first identified PPARα direct target was acyl-CoA oxidase, the rate-limiting enzyme in peroxisomal long-chain fatty acid oxidation [78]. It catalyzes the first step of b-oxidation of straight-chain acyl-CoAs which is followed by one of two enzymes carrying both enoyl-CoA hydratase and 3-hydroxyacyl-CoA dehydrogenase activity (Ehhadh and Hsd17b4) and eventually peroxisomal 30ketoacyl-CoA thiolase (Acca1a and Acca1b) [119-128]. All these genes are PPARα targets. Additionally, PPARα also regulates the expression of genes involved in fatty acid uptake (Abcd2 and Abcd3), conversion of fatty acid to acyl-CoA (Crot), and thioesterases (Acots). In mitochondrial β-oxidation, PPARα induces genes regulating fatty acid import (Slc25a20, Slc22a5, Cpt1, and Cpt2). PPARα also regulates the major enzymes in the β-oxidation pathway, including acyl-CoA dehydrogenases (Acad), trifunctional enzyme (Hadh), and genes responsible for the β-oxidation of unsaturated fatty acid (Dci, Decr) [120-124, 129-134]. In addition, synthesis of ketone bodies via mitochondrial HMG-CoA synthase (Hmgcs2) and HMG-CoA lyase (Hmgcl) is governed by PPARα. PPARα also regulates the expression electron transferring flavoprotein and the corresponding dehydrogenase (Etfa, Etfb, Etfdh) [122, 124]. Finally, PPARα induces uncoupling proteins Ucp2 and Ucp3, which have been proposed to transport nonesterified fatty acid anions out of mitochondrial matrix [135-139].

Cyp4A gene expression is also regulated by PPARα in both mice and humans. Cyp4A enzymes belong to the cytochrome P450 monoxygenase superfamily and are in charge of

catalyzing microsomal ω-hydroxylation of fatty acids [140, 141]. Using PPARα deficient mice, studies demonstrated an almost complete dependence on PPARα for the expression of Cyp4a genes (Cyp4a10, Cyp4a12, Cyp4a14 in mice, Cyp4a1, Cyp4a3 in rat, and Cyp4a11 in human) [122, 123, 129, 140, 142]. In these experiments, gene expression is extremely sensitive to PPARα ligand treatment, suggesting that Cyp4a genes may be PPARα downstream targets. The ω-hydroxylation of saturated and unsaturated fatty acids may cause the production of high affinity endogenous PPARα ligands (i.e. hydroxyeicosatetraenoic acids (HETEs)) and create a positive feedback loop [143]. Alternatively, the promotion of ω-oxidation by PPARα has been suggested to accelerate the degradation of the PPARα agonist leukotriene B4 as a feedback mechanism to control the duration of the inflammatory response [144].

While PPARα is best known for its ability to induce fatty acid oxidation, PPARα also plays important roles in regulation of lipogenesis. Functional PPREs were identified in the promoter of a number of lipogenic genes including Δ6 desaturase (Fads2), malic enzyme (Mod1), phosphatidate phosphatase (Lpin2) and Δ9 desaturase (Scd1) [145-148]. In contrast to de novo fatty acid synthesis, the synthesis of triglycerides may be directly regualted by PPARα. Several genes within these pathways are promoted by PPARα activation, including Gpam, Agpat genes, Mogat1, Dgat1, and Lpin2 [122, 124, 134, 149]. This may reflect a role of PPARα in neutralizing incoming adipose tissue-derived free fatty acids in response to fasting. The activation of PPARα also upregulates fatty acid transport proteins including Slc27a1, Slc27a2, Slc27a4, Fabp1, Fabp2, Fabp3, and Fabp4 in the liver [122, 124].

There is a large number of evidence from clinical studies showing that fibrates effectively lower plasma TG and raise plasma HDL [150-152]. Since fibrates act as synthetic agonist for PPARα, PPARα have been indicated to play important roles in the control of lipoprotein metabolism. Plasma TG is lowered by PPARα partly due to the reduction in VLDL [153]. This effect of PPARα is largely attributed to the induction of genes involved in fatty acid oxidation and the reduction in available lipid for VLDL production. However, in addition to its role in fatty acid catabolism, PPARα also influences intracellular lipid trafficking and metabolism as mentioned earlier, some of which may accelerate hepatic lipid importing. On the other hand, PPARα also positively regulates the expression of microsomal triglyceride transfer protein (Mttp). Mttp is an enzyme involved in formation of nascent VLDL particle using apoB100 [154]. With positive roles in both VLDL uptake and secretion from liver, the activation of PPARα accelerates the lipid turnover rate within the body.

In addition to suppressing VLDL secretion, PPARα agonists are also known to stimulate clearance of TG-rich lipoproteins [153]. Lipoprotein lipase (LPL) is attached to the capillary endothelium of peripheral tissues such as skeletal muscle and adipose and mediates the clearance of TG-rich lipoproteins VLDL and chylomicrons. Expression of Lpl in liver is restricted to Kupffer cells [155, 156]. No evidence is available supporting a stimulatory effect of PPARα on the expression of LPL in tissues such as heart and skeletal muscle, which account for the majority of triglyceride clearance from plasma [155, 157]. However, the post-translational regulation influences most for the activity of LPL activity. LPL-modulating factors include apolipoprotein C-III (Apoc3), apolipoprotein A-V (Apoa5). Angiopoietin-like protein 3 (Angptl3) and Angiopoietin-

like protein 4 (Angptl4) have also been indicated as LPL-modulators. It is now clear that PPARα agonists increase LPL activity by altering the secretion of these proteins. PPARα downregulates the expression of LPL inhibitor APOC3 [158]. PPARα increases hepatic expression and secretion of APOA5, which is a positive regulator of LPL activity [159]. A functional PPRE has been validated in the promoter region of the APOA5 gene, confirming APOA5 as a direct PPARα target [160, 161]. PPARα promotes the expression of Angptl4 in plasma and liver. Anpgtl4 converts active LPL dimers to inactive monomers and therefore inhibits its activity [162]. The PPRE is located to one of the introns of the Angptl4 gene [163]. With pharmacological PPARα activation, PPARα regulates the aforementioned gene expression and promotes LPL activity and therefore stimulates plasma TG clearance.

Other than TG clearance, activation of PPARα also raises plasma HDL levels in humans. This is achieved through promotion of apolipoprotein A-I (Apoa1) and A-II (Apoa2) expression [164, 165]. In rodents, however, gene expression of Apoa1 is not promoted by PPARα, because of disabling mutations within the PPRE [166]. PPARα activation in mouse downregulates Apoa1 mRNA expression and plasma concentrations [166-168].

### 1.2.2 Fenofibrate

Introduction

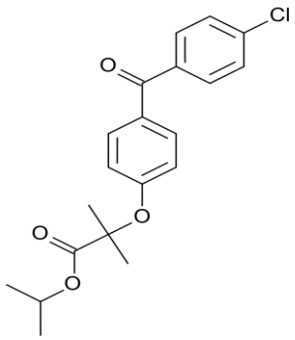


**Figure 1.6. Chemical structure of fenofibrate.**

Fenofibrate is a fibric acid derivative and has been available for decades as a treatment for dyslipidemia [169]. It is recommended in addition to diet restriction and other non-pharmacological approaches such as physical exercise for the treatment of severe hypertriglyceridemia and mixed hyperlipidemia in patients with statins intolerance. It is also prescribed as a secondary or combined therapy to statins in patients with mixed hyperlipidemia when TGs and HDL cholesterol are not satisfactorily controlled by statins therapy alone [169].

Mechanism of action

Fenofibrate is an orally administered prodrug that is converted to fenofibric acid by esterases following absorption, which is its pharmacologically active metabolite [170]. The lipid-lowering effects of fenofibrate are mediated through the activation of peroxisome proliferator-activated receptor-α (PPARα) [171]. Briefly, PPARα heterodimerizes with retinoid X receptor (RXR), and binds to specific peroxisome proliferator response elements (PPRE), thereby modulating the expression of genes involved in lipid metabolism [170-172]. Activation of PPARα results in increased

lipolysis and clearance of TG-rich lipoproteins from circulation. Molecular mechanism involves the promoted activation of lipoprotein lipase and reduced production of the lipoprotein lipase inhibitor ApoCIII from liver [155, 173-175]. Fenofibrate also promotes fatty acid β-oxidation, which reduces the availability of free fatty acids for TG synthesis [155, 173-175]. De novo fatty acid synthesis is also inhibited by fenofibrate through the reductions in acetyl-CoA carboxylase and fatty acid synthase activity, which also reduces the available fatty acid pool in liver for TG synthesis [175, 176]. Hepatic ApoB and VLDL production and secretion are reduced by fenofibrate treatment [175, 176]. Fenofibrate increases LDL clearance and reduces small dense LDL levels in plasma [177-180]. However, larger LDL particles have a high binding affinity for LDL receptors, which makes them less susceptible to oxidation [173, 177, 178]. PPARα activation also increases the synthesis of ApoAI and ApoAII, which are the major protein components in HDL particles [164, 175, 176, 181]. It enhances the expression of ATP-binding cassette transporter A1 (ABCA1) and scavenger receptor-B1 (SRB1), which leads to HDL-mediated cholesterol efflux from macrophages [170, 171, 173, 182, 183]. Fenofibrate treatment causes the increase in plasma HDL cholesterol levels [173, 177, 184], which is the results of reductions in the activity of cholesteryl ester transfer protein (CETP), the key enzyme that mediates the lipid transfer from HDL to VLDL [173, 177].

Therapeutic efficacy

The therapeutic efficacy of fenofibrate has been demonstrated in large amounts of clinical studies in adults [185-197]. In the FIELD trial, the comparison of fenofibrate monotherapy was compared with placebo in patients with type 2 diabetes [185]. Patients

generally had no indication for other hypolipidemic therapy although considered to be at higher risk of coronary heart disease. They also showed good glycemic control. There was 24% relative reduction in nonfatal myocardial infarction in patients on fenofibrate vs those on placebo. Fenofibrate also reduced 11% total cardiovascular disease events and 20% coronary revascularization compared with placebo. Based on a post hoc subgroup analysis, fenofibrate treatment exhibited the greatest effects in patients with significant baseline hypertriglyceridemia or dyslipidemia. In another two trials, the effects of fenofibrate were compared with gemfibrizol with regards to improvement in TG and HDL cholesterol [186, 187]. No significant difference was observed between two treatment approaches, although total cholesterol and LDL cholesterol was reported to drop greater in fenofibrate treated patients. In comparison with statins, fenofibrate consistently showed greater improvements in TG and HDL cholesterol levels in patients with hypercholesterolemia, while fenofibrate was less effective in reducing total cholesterol and LDL cholesterol [188-193]. Compared with niacin, fenofibrate improved TG and HDL cholesterol with more significance but less effectively in improving total cholesterol and LDL cholesterol in patients with mixed dyslipidemia [194]. In the ACCORD Lipid trial, the treatment effects were compared between fenofibrate plus simvastatin and placebo plus simvastatin in patients with type 2 diabetes who were at higher risk of cardiovascular diseases [195, 196]. No significant difference was observed in either primary nor secondary endpoints between the two groups. However, fenofibrate plus simvastatin significantly improved the total cholesterol, HDL cholesterol and TG levels compared with placebo plus simvastatin. In a trail to evaluate the additive effect of fenofibrate to the combination of stain and ezetimibe, fenofibrate further improved lipid

profiles in patients with mixed dyslipidemia after 12 week of treatment [197]. Addition of fenofibrate significantly further improved HDL cholesterol and TG than statin/ezetimibe combined treatment alone [197].

## 1.3 PEROXISOMAL ABC TRANSPORTERS

### 1.3.1 PEROXISOMES

Introduction

Peroxisomes are subcellular organelles that are present in almost all eukaryotic cells. They are characterized by a single layer membrane containing granular matrix and a crystalline core [198]. The first reported discovery of these organelles dates back to 1950s when subcellular particles bound by a single membrane containing matrix and a crystalline core were observed in kidney and live cells [199]. The term 'peroxisome', however, was not proposed until 1960s with the identification of oxidases and catalases within these organelles [200]. Early studies on peroxisomes focused on their functions on hydrogen peroxide metabolism and were greatly facilitated by the utilization of 3, 3'-diaminobenzadine (DAB) staining [201]. Later on, peroxisomes were reported to exist in a large number in tissues with active lipid metabolism, including liver, intestine, brain and adipose [202, 203]. The shape and size of peroxisomes vary in different tissues, with the diameter ranging from 0.1um to 0.5um. Peroxisomes tend to be smaller in adipocytes and often observed without a crystalline core. Therefore, adipose peroxisomes were referred to as 'microperoxisomes' [202]. Besides oxidative catalytic functions, peroxisomes are actively involved in a variety of metabolic processes, including β-

oxidation of very long chain fatty acids (VLCFA), α-oxidation of branched chain fatty acids and biosynthesis of ether-phospholipids [204].

Biogenesis of Peroxisomes

Peroxisomes are highly dynamic and plastic organelles that readily respond to environmental change and metabolic stress. Although the origin of peroxisomes still remains controversial, there are currently two alternative theories that describe the generation and population of peroxisomes. In a classical model, peroxisomes are autonomous and generate from existing peroxisomes [205]. Some peroxisomes exhibit a dumbbell shape in fixed tissues, reflecting the ongoing dividing process that was captured histologically [206]. Such structures are more often observed in rodent livers after peroxisome proliferator treatments, which greatly induce the peroxisome division and growth [207].

In a relatively new model, peroxisomes are described as semiautonomous organelles that derive their matrix protein from cytosolic ribosomal synthesis and import their membrane proteins and lipid components from the endoplasmic reticulum (ER) [208]. Peroxisomes were observed in contact with smooth ER in guinea pig intestine and were suggested to arise from local ER regions containing high concentrations of catalases [207, 209]. Using fluorescent labeled peptides fused to peroxisomal proteins, it was shown that precursors of peroxisomes dissociating from ER in a 'budding' pattern [210]. Two preperoxisomal vesicles underwent heterotypic fusion and formed a new organelle that continued to import matrix proteins from cytosol [210].

The assembly of peroxisomes, especially that of the membrane protein and components requires the assistance of a group of proteins called peroxins. The majority of studies on peroxisomal biogenesis are done using yeast as a model because of its ease to manipulate and proliferate [211]. Over 30 peroxins have been identified in yeast, at least 23 of which are essentially required for the peroxisomal biogenesis [212, 213]. There are at least a dozen of peroxins conserved in mammals. The peroxisomal membrane and membrane protein assembly critically requires at least three proteins, which are Pex3, Pex16, and Pex19. As a chaperone protein, Pex19 functions as an import receptor for newly synthesized proteins [214]. Pex3 is localized in a preperoxisomal vesicle budding from ER and serves as a docking receptor for peroxisomal membrane proteins [215]. Pex16 assists Pex19 for the recruitment of Pex3 and carried peroxisomal proteins [216]. The peroxisomal matrix proteins are imported through a different mechanism. These proteins have a sequence of amino acids, called PTS, at carboxyl (PTS1) or amino (PTS2) terminus that directs newly translated protein from the cytosolic ribosomes to peroxisomes [217, 218] . Pex5 and Pex7 are the import receptors for PTS1-and PTS2-containing matrix proteins, respectively [219, 220]. They first deliver proteins from cytoplasm to docking sites at peroxisomal membrane and then recycle back to the cytoplasm [221].

Fatty Acid Oxidation in Peroxisomes

Both peroxisomes and mitochondria are sites for fatty acid oxidation in animal cells. Although both organelles metabolize fatty acyl-CoAs, their roles are not interchangeable. Peroxisomes are the major place for β-oxidation of very long chain fatty acids (VLCFA), α-oxidation of branched chain fatty acids and biosynthesis of ether-phospholipids [204].

The overall mechanism of β-oxidation is the same in peroxisomes and mitochondria and contains four consecutive enzymatic steps which include dehydration, hydration, oxidation and thiolysis. Although the chemical reactions are essentially the same in the two organelles, they use different enzymatic machineries to catalyze these reactions. Mitochondria use acyl-CoA dehydrogenase to catalyze the first step of β-oxidation and generate a molecule of $FADH_2$ whose energy is used to produce two molecules of ATP. The peroxisomes, on the other hand, use acyl-CoA oxidase to catalyze the first step and produce one molecule of $FADH_2$. However, since peroxisomes don't have a respiratory chain, electrons from $FADH_2$ are directly passed to $O_2$ and creating $H_2O_2$. Instead of being used to generate ATP, the energy is released as heat. Therefore, fatty acid oxidation in peroxisomes is less energy efficient. In addition, the major results of fatty acid oxidation in peroxisomes is to shorten very long chain fatty acids rather than complete oxidized them [222, 223]. Fatty acids of 26 carbon or more are oxidized exclusively in peroxisomes, while fatty acids with less carbon can be oxidized in both organelles [224]. Peroxisomes also transport fatty acyl-CoA in a different pattern than mitochondria. Mitochondria utilize a carnitine exchange system to uptake fatty acyl-CoA across membrane which consists of carnitine palmitoyl-transferases 1 and 2 (CPT1 and CPT2) and carnitine-acylcarnitine translocase (CACT). CPT1 is localized on the outer membrane and replaces the CoA with carnitine, generating a fatty acid carnitine, which is transferred across the inner membrane to mitochondrial matrix by CACT. CPT2 then convert fatty acid carnitine back to fatty acyl-CoA by replacing the carnitine with CoA. However, peroxisomes use three ATP binding cassette transporters on the membrane to uptake substrates [225].

Peroxisomal ABC Transporters

To transport metabolites across the membrane, peroxisomes need the facilitation of different metabolic transporters. One of the transporter families is the ATP-binding cassette (ABC) transporter subfamily D which contains four members: adrenoleukodystrophy protein (ALDP/ABCD1), ALDP-related protein (ALDRP/ABCD2), a peroxisomal membrane protein (PMP70/ABCD3) and PMP70-related protein (P70R/ABCD4). The first three has been identified as peroxisomal transporters while the last was reported to be localized to endoplasmic reticulum (ER) [226].

ABCD1 (D1) is involved in the peroxisomal uptake of a variety of VLCFA-CoA [227, 228]. Dysfunction of D1 leads to impaired peroxisomal β-oxidation and causes the human genetic disorder X-linked adrenoleukodystrophy (X-ALD), which is characterized by the accumulation of VLCFA in plasma and tissues. Transfection of *ABCD1* cDNA into X-ALD skin fibroblasts restored the VLCFA oxidation and brought the VLCFA content to normal [229, 230]. Besides closely related to fatty acid metabolism, *ABCD1* gene expression was also reported to respond to cholesterol level in human THP-1 cells and primary macrophages [231]. In wild-type mice, cholesterol feeding increased the plasma cholesterol level while this response was lost in *Abcd1* deficient mice [232]. Although the mechanism by which cholesterol affects D1 expression has not been elucidated, these findings suggest a possible link between D1 function and cellular cholesterol metabolism.

ABCD2 (D2) shares 66% amino acid identity with D1 and is presumed to have overlapping substrate specificity based on complementation studies in yeast [228, 233]. Additionally, a ubiquitous promoter-controlled D2 transgene corrected both biochemical and neurological phenotypes in D1 deficient mice, indicating that they share overlapping functions [234, 235]. Mice lacking D2 are characterized by late-onset cerebellar and sensory ataxia with loss of cerebellar Purkinje cells and accumulation of VLCFA in dorsal root ganglia cells [236]. D2 deficient mice also showed evidence of oxidative stress with spontaneous and premature ceroid deposition in adrenal medulla cells [237], reduced rates of VLCFA (C26:0) and PUFA (C24:6ω3) oxidation, as well as altered LCFA and VLCFA levels (C20:0, 22:1ω9, 22:6ω3 and 22:5ω6) in the cerebral cortex [238]. D1 and D2 appear to cooperate in monounsaturated C26:1ω9 import [239] and serum levels of C22:1ω9, a fatty acid associated with disruptions in lipid metabolism in rats and other species [240], were elevated in fed and fasting states [238, 241]. The absence of D2 sensitized mice to dietary erucic acid, resulting in the rapid onset of obesity and insulin resistance [242].

The expression of D2 is dynamically regulated by several transcription factors, including PPARα, sterol regulatory element binding proteins SREBP1a and SERBP1c, retinoid X receptor (RXR), thyroid hormone receptor (TR), LXRα, and TCF4/β-catenin [130, 232, 243-245]. D2 expression levels in liver are near the lower limit of rtPCR and immunoblotting detection, but are dramatically up-regulated by PPARα agonists and in genetic and high fat feeding obesity models [242, 246]. Although no functional peroxisome proliferator response element has been identified in the D2 promoter, the expression of D2 is induced by fibrate treatment and is PPARα dependent [130].

Prolonged fasting for 48 hours was also shown to increase both hepatic D2 expression and the amount of some peroxisomal metabolites (C20:0 and C22:1) in mouse serum [238]. Collectively, these data demonstrate a number of key functions for D2 as a lipid homeostasis regulator. However, the precise physiological role of D2 in lipid metabolism remains largely unknown.

ABCD3 (D3) is one of the most abundant peroxisomal membrane proteins at least in hepatocytes. Overexpression of D3 in CHO cells induced the β-oxidation of plamitic acid (C16:0) and inhibited the β-oxidation of tetracosanoic acid (C24:0), suggesting its role in the metabolic transport of long chain and very long chain fatty acids [247]. In *Abcd3* deficient mice, the bile acid precursors, trihydroxycholestanoic acid (THCA) and dihydroxycholestanoic acid (DHCA), as well as pristanic acid accumulated in plasma [248]. In *Abcd3* deficient mouse fibroblast, the β-oxidation of phytanic and pristanic acid was decreased to 50% of control [248]. These results indicate that D3 is required for the transport of LCFA-CoA, THCA-CoA, DHCA-CoA and branched chain acyl-CoA and essential for bile acid synthesis.

## 1.4 PEROXISOMES IN ADIPOSE TISSUES

More than the major depot for lipid storage as an energy source backup, adipose tissue is also an active endocrine organ that secretes various adipokines and other signal molecules. Peroxisomes tend to be smaller in adipocytes and are often observed with absence of the crystalline core. Therefore, adipose peroxisomes were referred to as ‘microperoxisomes’ [202]. Nevertheless, microperoxisomes are abundant in adipocytes

and are observed in close relationship with lipid droplets. A large number of microperoxisomes are present in cultured 3T3-L1 adipocytes and mouse epididymal fat [203, 249].

Brown adipose tissue also harbors a large amount of ‘catalase-positive particles’ and tend to increase their number dramatically in response to cold exposure [250]. Later studies demonstrated the presence of oxidase in these particles which identified them as peroxisomes [251]. During adipocyte differentiation and exposure to low temperature, the Pex genes increased in a PGC1α dependent manner, indicating potential roles of peroxisomes in brown adipose physiology [252].

Recently, there has been emerging evidence indicating that peroxisome metabolism is critically required for normal adipose function [253, 254]. In Pex7 deficient mice, peroxisome biogenesis is impaired due to the failure of peroxisomal protein import [254]. These mice lack plasmalogens, the synthesis of which strictly relies on peroxisomal metabolism, and had severely reduced adiposity despite similar food intake. The phenotype could be rescued by feeding the mice with alkyl-glycerol and restoring plasmalogen levels [254]. Presumably, exogenous alkyl-glycerol enters the ether lipid synthetic pathway in peroxisomal metabolism and increase the production of plasmalogen. However, the exact amount of endogenous ether phospholipids in adipose tissue was not reported. Although a direct requirement for peroxisome-derived lipids in adipose development was suggested by the authors, it was not confirmed that plasmalogen was the signaling molecule. Moreover, it remains to be further determined whether adipose dysfunction in Pex7 deficient mice is due to defective PPARγ signaling.

In another mouse model in which Pex5 was specifically deleted in adipose using aP2 promoter, peroxisomes were dysfunctional in white adipose tissue, but intact in liver, heart, pancreas, and muscle [253]. Adipose function was impaired resulting in reduced lipolysis and increased fat mass. However, other phenotypes were also observed including failure of catalase import into peroxisomes in the nervous system, impaired shivering thermogenesis, and reduced plasma adrenaline levels, suggesting some adipose phenotypes were due to secondary effect or off-target Pex5 deletion.

# CHAPTER 2: ABCD2 MODIFIES PPARα SIGNALING *IN VITRO* BUT DOES NOT IMPACT RESPONSE TO FENOFIBRATE THERAPY IN A MOUSE MODEL OF DIET-INDUCED OBESITY

## Introduction

Fenofibrate has been widely used clinically to treat dyslipidemia. As an agonist of PPAR (peroxisome proliferator-activated receptor) α, fenofibrate has been shown to significantly reduce TG (triglyceride) levels and raise HDL (high density lipoprotein) cholesterol levels in plasma [176, 255]. However, the clinical response to fenofibrate therapy is highly variable [256]. It has been proposed that response variability may be partially due to fenofibrate therapy and genetic factor interactions [257]. Polymorphisms at several genes have been reported to interact with the lipid-lowering effects of fenofibrate during the postprandial period [258-264]. However, only a limited number of genes have been investigated so far, and the effects of other candidate genes, especially those that play important roles in lipid metabolism, remain unexplored.

ABCD2 (D2) is a mammalian peroxisomal ABC transporter thought to facilitate very long chain fatty acyl-CoA import into peroxisomes for β-oxidation [236, 238, 265]. Impaired peroxisome functions lead to very long chain fatty acid (VLCFA) and branched chain fatty acid (BCFA) accumulation in plasma and tissues, resulting in severe metabolic diseases [266]. X-linked adrenoleukodystrophy is a peroxisomal disorder caused by inactivation of the *ABCD1* (D1) gene [267]. D2 shares 66% amino acid identity with D1 and is presumed to have overlapping substrate specificity based on

complementation studies in yeast [228, 233]. Additionally, a ubiquitous promoter-controlled D2 transgene corrected both biochemical and neurological phenotypes in D1 deficient mice, indicating that they share overlapping functions [234, 235].

D2 protein has been detected in adrenal, brain, kidney, liver, and skeletal muscle, but is most abundant in adipose [241]. Mice lacking D2 are characterized by late-onset cerebellar and sensory ataxia with loss of cerebellar Purkinje cells and accumulation of VLCFA in dorsal root ganglia cells [236]. D2 deficient mice also showed evidence of oxidative stress with spontaneous and premature ceroid deposition in adrenal medulla cells [237], reduced rates of VLCFA (C26:0) and PUFA (C24:6ω3) oxidation, as well as altered LCFA and VLCFA levels (C20:0, 22:1ω9, 22:6ω3 and 22:5ω6) in the cerebral cortex [238]. D1 and D2 appear to cooperate in monounsaturated C26:1ω9 import [239] and serum levels of C22:1ω9, a fatty acid associated with disruptions in lipid metabolism in rats and other species [240], were elevated in fed and fasting states [238, 241]. The absence of D2 sensitized mice to dietary erucic acid, resulting in the rapid onset of obesity and insulin resistance [242].

The expression of D2 is dynamically regulated by several transcription factors, including PPARα, sterol regulatory element binding proteins SREBP1a and SERBP1c, retinoid X receptor (RXR), thyroid hormone receptor (TR), LXRα, and TCF4/β-catenin [130, 232, 243-245]. D2 expression levels in liver are near the lower limit of rtPCR and immunoblotting detection, but are dramatically up-regulated by PPARα agonists and in genetic and high fat feeding obesity models [242, 246]. Although no functional peroxisome proliferator response element has been identified in the D2 promoter, the

expression of D2 is induced by fibrate treatment and is PPARα dependent [130]. Prolonged fasting for 48 hours was also shown to increase both hepatic D2 expression and the amount of some peroxisomal metabolites (C20:0 and C22:1) in mouse serum [238]. Collectively, these data demonstrate a number of key functions for D2 as a lipid homeostasis regulator. However, the precise physiological role of D2 in lipid metabolism remains largely unknown.

Our initial studies revealed that absence of D2 altered the genomic response to fenofibrate treatment in mouse liver, and confirmed that D2 protein levels altered responses to fibrate treatment *in vitro*. This prompted us to propose that D2 may play a role in the regulation of PPARα signaling and response to fenofibrate therapy. We next tested the hypothesis that D2 would alter the effect of fibrate in a model of diet-induced obesity. Fibrates decreased weight gain, adiposity, hyperlipidemia and insulin resistance, but these effects were not altered by the D2 genotype.

## Materials and Methods

### Analysis of hepatic gene expression and sample preparation

*Animals*

Age-matched (3 month, n=6) wild-type (WT) and *Abcd2* (D2) knock-out (KO) mice on the C57Bl/6J background were gavaged (200 µL/day) with fenofibrate (100 mg/kg/day) dispersed in water containing 3% gum arabic for 14 days. Control mice were gavaged

with vehicle alone (3% gum arabic). Livers were dissected from the mice and total RNA was extracted using RNeasy Kit (Qiagen).

*Microarray*

A cDNA microarray was manufactured at IGBMC (Institut de Génétique et de Biologie Moléculaire et Cellulaire). The array consisted of 20,736 mouse cDNA clones representing approximately 15,000 Unigene clusters. The clone selection, cDNA amplification, spotting, and labelling in two colors (dUTP-Cy3 and dUTP-Cy5) has previously been described [268]. Arrays were scanned using ScanArray 4000 (Packard Biochips, Billerica, MA, USA) and images quantified using Imagene 5.0 (BioDiscovery Microarray Bioinformatics Software, Marina Del Rey, CA, USA). Detailed information is available on the IGBMC microarray web site (http://www-microarrays.u-strasbg.fr). The microarray experiment has been deposited in the Array Express Database under accession number E-MTAB-2006.

*Hybridization and data processing*

All samples were hybridized in duplicate and analyzed using dye swap to avoid label specific bias. Pre-processing of raw data and statistical analyses were performed using Bioconductor packages in R programming environment [269]. For mouse custom cDNA arrays, background correction was performed using the "normexp" method implemented in the Bioconductor LIMMA package to adjust local median background estimates [270, 271]. Background-corrected intensity data were normalized using the Print-tip loess method to remove the bias within each array and the A-values quantile normalization (Aquantile) to remove the bias between arrays.

*Functional enrichment analysis*

To evaluate which pathways or functional categories were enriched in differentially expressed genes we computed both the Gene set enrichment analysis (G) and Hypergeometric distribution function (H). We used $P<0.05$ as the cut-off point to determine whether the metabolic and cell signalling pathways extracted from The Kyoto Encyclopaedia of Genes and Genomes (KEGG) (http://www.genome.jp/kegg/) [272] were significantly enriched. GeneSetTest function from LIMMA package tests whether a set of genes is enriched for differential expression. Its principle is the same as for Gene Set Enrichment Analysis introduced by [273], but the statistical tests used are different. It is based on a set of probe-wise t-statistics arising for microarray analysis. We have computed three different tests: i) up-regulated genes, with positive t-statistics as indicated by red spots, ii) down-regulated genes, with negative *t*-test statistics as indicated by green spots, and iii) genes differentially expressed regardless of the direction as indicated by black spots. The sizes of spots are scaled positively with the probability values in a semi-quantitative pattern. We used the "phyper" hypergeometric distribution function from stats package to determine enriched KEGG pathways in the subset of genes differentially expressed at $P<0.05$.

**Impact of D2 on fibrate response *in vitro***

*Generation of D2 deficient 3T3-L1 cell line*

3T3-L1 cells were propagated as fibroblasts in sub-confluent cultures in DMEM/F12 supplemented with antibiotics and 10% newborn calf serum. One day post-confluence, cells were infected with lentiviral particle expressing short hairpin RNA directed against

D2 (sequence: 5′-CCGGCCTCGGACTTTCATCATCAAACTCGAGTTTGATGATGAAAGTCCGAGGTTTTTG-3′, Sigma MISSION® shRNA Lentiviral Transduction Particles TRCN0000105346) and a control shRNA in the presence of hexadimethrine bromide (polybrene, 8 ug/ml). Cell-viral particle mixtures were incubated in 37°C overnight. Medium was replaced with DMEM/F12 containing antibiotics and 10% newborn calf serum. 2ug/ml puromycin was added to select successfully transduced cells. Medium was replaced every three days until resistant clones could be identified. Several puromycin-resistant colonies were selected by limiting dilution, expanded separately in medium containing reduced amount of puromycin (1 ug/ml), and frozen in liquid nitrogen. Cell lysates of each expanded colony were prepared and subjected to immunoblot analysis to confirm knockdown of D2.

*Adipocyte differentiation and fenofibrate treatment*

D2 deficient 3T3-L1 and control cells were propagated as fibroblasts in sub-confluent cultures in DMEM/F12 supplemented with antibiotics and 10% newborn calf serum. Two days post-confluence (Day 2), cells were treated with a 1.7 µM insulin, 0.5 µM dexamethasone, 0.5 mM isobutylmethylxanthine, and 1 µM rosiglitizone in DMEM/F12 supplemented with 10% fetal calf serum and antibiotics for 48 hours to promote differentiation to adipocytes as previously described [241]. Thereafter, cells were cultured in DMEM/F12 supplemented with 10% fetal calf serum. Four days post-confluence (Day 4), the medium was replaced with DMEM/F12 supplemented with antibiotics, 10% fetal calf serum, and 1 ug/ml insulin. Fresh medium was replaced every two days. 3T3-L1 adipocytes were analyzed between 8-12 days post-confluence. Eight

days post-confluence (Day 8), adipocytes were treated with carrier (DMSO) or fenofibrate (500mM) for 16 hours. Cells were washed with PBS (4°C) and total RNA was extracted using RNeasy kit (Qiagen, Valencia, CA).

*Protein sample preparation and immunoblotting*

Cell lysates were prepared by incubating the cells in triton lysis buffer (80 mM NaCl, 50 mM Tris, 2 mM $CaCl_2$, 1% Triton, pH 8.0) at 4°C for 30 min, scraped off the dish, and homogenized with polytron homogenizer. Samples were added with protein sample buffer (30mM Tris base, 10mM EDTA, pH 6.8, 3% SDS, 20% glycerol, and 0.00625% bromphenol blue) to achieve uniform concentrations. β-mercaptoethanol was added to a final concentration of 1.2% (v/v). Samples were heated to 95 °C for 5 min before loading. Proteins were size-fractionated on 10% SDS-polyacrylamide gels and transferred to nitrocellulose membranes. Membranes were incubated in buffer A (20 mM Tris, 137mM NaCl, 0.2% Tween 20 and 5% non-fat milk, pH 7.6) for 30 min at room temperature. Anti-ABCD2 antibody [241] was diluted in buffer A and incubated with membranes for 60 min at room temperature. Membranes were washed 3 times for 5 min in buffer B (20 mM Tris, 137mM NaCl and 0.2% Tween 20, pH 7.6). Horseradish peroxidase-conjugated goat anti-rabbit IgG were diluted in buffer B and incubated with membranes for 30 min at room temperature. Membranes were washed 3 times for 5 min in buffer B and visualized by enhanced chemiluminescence (SuperSignal West Pico, Thermo Scientific).

*Quantitative real-time PCR*

Total RNA was reverse transcribed using SuperScriptTM First Strand Synthesis system (Invitrogen). Quantitative RT-PCR was performed on an Applied Biosystems 7900HT

sequence detection system. Standard reaction volume was 30 ul containing 1X SYBR Green PCR master mix (Applied Biosystems), 1 ul of cDNA template, and 150 nM concentrations of each oligonucleotide. Initial steps of RT-PCR were 10 min at 95°C. Cycles (n=40) consisted of a 15-s melt at 95°C followed by a 1-min annealing/extension at 60°C. All reactions were performed in triplicate. Means of the differences in threshold cycle ($C_T$) values from cyclophilin and their S.D. were calculated for each treatment group ($\Delta C_T$). The relative abundance of each transcript within treatment groups was determined by subtracting the control group mean difference from the remaining treatment groups ($\Delta\Delta C_T$) and calculated according to the expression $2^{-\Delta\Delta CT}$. The S.D. of the difference between control and each treatment group was calculated as the square root of the sums of squares for the S.D. of the $\Delta C_T$ means.

**Impact of D2 on fibrate response *in vivo***

At 8 weeks of age, *Abcd2* knock-out (KO) and wild-type (WT) male mice were provided free access to a high fat diet (control, 60% kCal, Research Diets Inc., New Brunswick, NJ) or the same diet formulated with fenofibrate (Fibrate, 60% kCal plus 0.05% w/w fenofibrate, Cayman Chemical 10005368). Mice were housed in a 10 hour dark/14 hour light cycle. Every week, mice were weighed and food was replaced. Fasting blood glucose levels and body composition (analyzed by MRI, EchoMRI) were measured at the initiation (8 weeks of age) and every 4 weeks of the study. A glucose tolerance test was conducted at the mid-point (8 weeks on diet) and the end (16 weeks on diet) of the study.

At 17 weeks, a subgroup of mice was placed in the metabolic cages to record metabolic parameters. Each mouse was housed separately and provided with free access to diet and water. Mice were allowed to acclimatize for 48 hours. Metabolic data were collected for the next 72 hours. Air flow rate (Flow, l/ml), oxygen percentage ($dO_2$, %), carbon dioxide percentage ($dCO_2$, %), food and water consumption and locomotor activity were measured. Mean values of energy expenditure (H) in the active (dark), resting (light) phase, and whole day average were calculated for each mouse. Since the data displayed the same pattern for both active and resting phases, we only show the whole day average data in this paper.

Blood samples of these mice were taken using heparinized capillary tubes before and 0.5, 1, 2, and 3 hours after tail vein injection of 650mg/kg body weight of Triton WR-1339 (Sigma). Total plasma triglyceride (TG) concentrations of all time points were determined and TG secretion rates were calculated using linear regression analysis.

At 16 weeks, mice were anesthetized with ketamine/xylazine (9/1, w/w) for tissue collection. Tissues were snap-frozen in liquid nitrogen, embedded in Tissue-Tek O.C.T, formalin-fixed (10% in PBS), and stored at -80°C until subsequent analysis. All animal procedures were performed with the approval of the Institutional Animal Care and Use Committee.

*Statistical Analysis of Data*

Data were analyzed by two-way ANOVA and presented as mean with standard error of the mean. Bonferroni post-hoc tests were employed where indicated. All statistical analyses were conducted using GraphPad Prism statistical analysis software.

**Impact of D2 polymorphisms on fibrate responses in human subjects**

*Study Population*

The Genetics of Lipid Lowering Drugs and Diet Network (GOLDN) study, described in detail in previous publications [274, 275], was designed to identify genetic markers associated with response to fenofibrate therapy in a population of related metabolically healthy individuals of European American ancestry. Participants were asked to discontinue use of lipid-lowering medications, fast for at least 8 hours, and abstain from alcohol prior to study visits. Circulating plasma lipids were measured at baseline and after three weeks of daily treatment with 160 mg of micronized fenofibrate. Genotype information was collected on 906,600 single nucleotide polymorphisms (SNPs) using the Affymetrix Genome-Wide Human 6.0 array and Human Genome Build 36 was used as the reference to impute untyped SNPs. After imputation and quality control, a hybrid set of 2,543,887 SNPs was created, with complete genotype and covariate information available on 861 participants.

*SNP Selection*

Of the three *ABCD2* variants previously implicated in affecting gene expression in humans [276], the GOLDN data set had genotyped variants that were in perfect linkage disequilibrium (R2=1) with two of them, rs7309234 and rs11172592, used as proxies for rs4285917 and rs4284427, respectively. The third SNP, rs10783969, was neither typed nor in linkage disequilibrium with any of the GOLDN variants and was excluded from the analysis.

*Statistical Analysis of SNP data*

Linear mixed models were used to assess the association of each *ABCD2* variant with the fenofibrate-induced change in plasma triglycerides, defined as area under the curve calculated using the trapezoidal rule. The models were adjusted for age, sex, and study site as fixed effects, and pedigree as a random effect. Sensitivity analyses were conducted using the alternative phenotype definition of log-transformed plasma triglyceride concentration ratios comparing post- to pre-fenofibrate treatment levels.

**Results**

*Identification of ABCD2-regulated pathways with and without fenofibrate treatment*

To evaluate the influence of D2 on genomic responses to fibrate treatment, age-matched WT and D2 KO mice (n=6) were administered fenofibrate for 14 days. Total RNA was extracted from liver and subjected to microarray analysis. To determine which pathways or functional categories were enriched among differentially expressed genes, we computed both the Gene Set Enrichment analysis (G) and Hypergeometric distribution function (H) (Fig. 2.1). Red indicates significance with a preponderance for up-regulated genes within the pathway or gene cluster. Green indicates significant down-regulation. Black spots indicate significance within the cluster, but without overall up or down trend. Open circles indicate no significant differences. The size of the symbols is scaled to the magnitude of the *P*-value. The influence of genotype alone was assessed by comparing WT and KO mice without fenofibrate treatment (WT vs. KO, -/- fenofibrate). The effect of fibrate treatment was determined by comparing WT mice with or without fibrate (WT

vs. WT, -/+ fenofibrate). The interaction between genotype and treatment was evaluated by comparing WT and KO mice treated with fenofibrate (WT vs. KO +/+ fenofibrate).

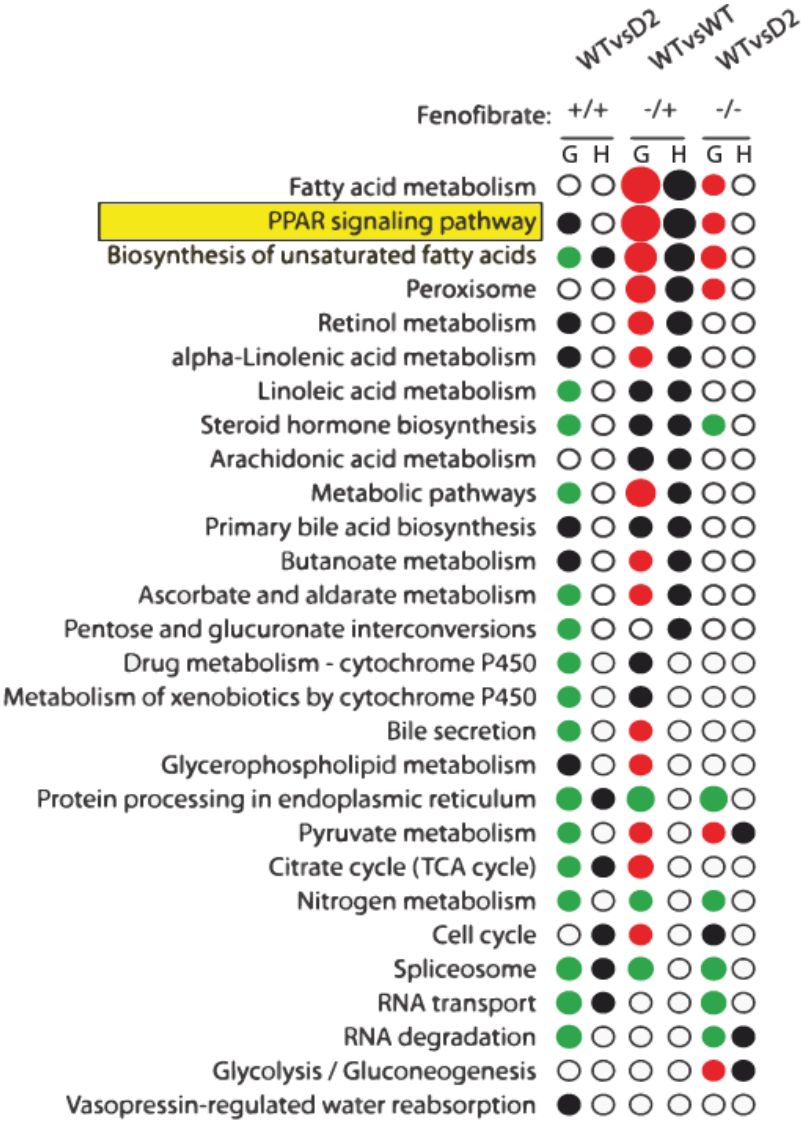


**Figure 2.1. Dysregulated pathways in liver samples of KO mice with (+) or without (-) fenofibrate treatment.** Biosynthesis of the unsaturated fatty acids pathway is the most affected pathway in KO mice with or without fenofibrate. Significant KEGG pathways were identified by using the statistics GSEA (G) and Hypergeometric distribution function (H). Black spots represent dysregulated pathway when probability

value P<0.05, according to the H test that detects change,s but does not inform about their up or down direction. Red and green spots represent up- and down- regulated pathway expression based on G test when probability value is P<0.05. Black spots in G test column indicate significantly dysregulated pathway but without up- or down- trend. Spot size scales with the probability value.

In the absence of fibrate, most pathways were either not affected or only modestly influenced by the loss of D2 (WT vs. KO, -/-) in both G and H tests. Fibrate treatment in WT mice resulted in altered gene expression in a collection of pathways, including fatty acid metabolism, PPAR signaling and biosynthesis of polyunsaturated fatty acids (WT vs. WT, -/+). The PPAR signaling pathway was the most significantly influenced by fenofibrate as indicated by the size of spots denoting significance in both statistical tests, $p$ < 3.27E-21 (Supplemental Table 1). Notably, the PPAR signaling pathway was altered in KO mice under basal conditions (without fenofibrate), as shown in G (WT vs. KO, -/-, $P$<0.0009; Supplemental Table 1). With fibrate treatment, the change of gene expression in KO mice was still maintained; although the pattern of dysregulation was different (WT vs. KO +/+, $P$<0.001, Supplemental Table 1). This observation indicates that loss of D2 not only influenced PPAR signaling itself, but also modulated the genomic response to fibrates. Similar results were observed for biosynthesis of polyunsaturated fatty acids (Supplemental Table 1). Alterations in selected in the biosynthesis of PUFAs pathway were confirmed by rtPCR (Fig. 2).

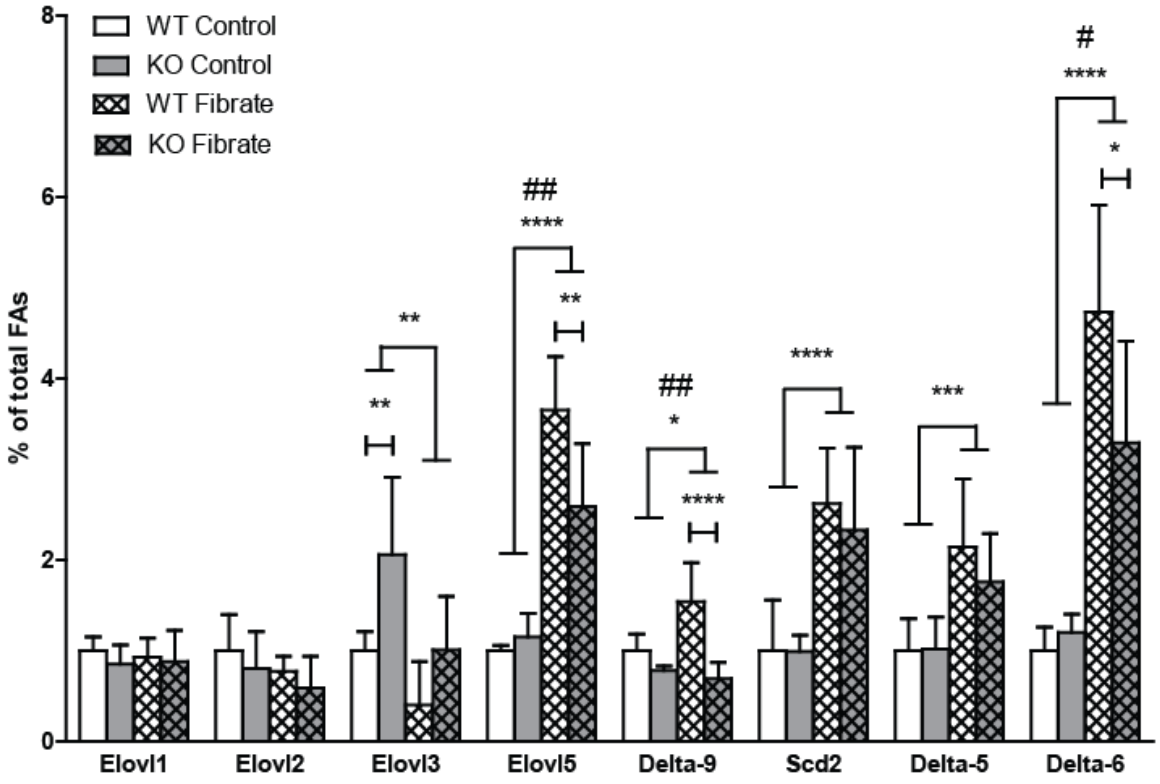


**Figure 2.2. D2 modulates fenofibrate effects on hepatic fatty acid biosynthesis.** Relative mRNA abundance for fatty acid elongases and desaturases as determined by rtPCR. Data were analyzed by two-way ANOVA with genotype and treatment as factors. # over lines terminating in horizontal bars indicates significant genotype by treatment interaction. * over lines terminating in horizontal bars indicates an overall effect of fibrate treatment. * over bars terminating in vertical lines indicates effect of genotype within treatment. Bonferonni post-hoc tests were conducted within treatment. # $P<0.05$, ## $P<0.01$, ### $P<0.005$, #### $P<0.001$. * $P< 0.05$, ** $P<0.01$, *** $P<0.005$, **** $P<0.001$.

*Cellular response to fenofibrate treatment is dependent on ABCD2 in 3T3-L1 cells*

Based on alterations in gene expression in mice, we hypothesized that the lack of ABCD2 may impact PPAR signaling and responses to fibrate treatment. First, we evaluated the influence of D2 on these responses *in vitro*. We selected NIH3T3-L1 adipocytes because they are the only cell line known to express D2 at high levels and respond to fibrate treatment [241, 277].

We developed a stable clone harboring a shRNA directed against D2 to repress expression. Parent 3T3-L1 cells, stable clones with D2 shRNA and control shRNA were differentiated to adipocytes. Levels of D2 were confirmed by immunoblotting. Fat from WT and KO mice were used as positive (+) and negative (-) controls (Fig. 2.3A). Our D2 antibody cross reacts with a protein with similar size to D2 in a number of tissues and in 3T3-L1 adipocytes, but this protein is absent in fat [241]. Total RNAs of shD2 and control cells were extracted and analyzed by quantitative real-time PCR to determine the expression levels of PPAR family members. Interestingly, the lack of D2 specifically suppressed the expression of PPARα, but the other two members of PPAR family, β and γ, were unchanged (Fig. 2.3B).

Control and shD2 cells were differentiated to adipocytes and treated overnight with either carrier or fenofibrate. Expression of PPARα and its target genes were determined using real-time PCR (Fig. 2.3C). The mRNA levels of PPARα, CPT1 (carnitine palmitoyltransferase 1), UCP2 (uncoupling protein 2) and UCP3 were significantly increased in response to fenofibrate treatment in control cells, but the elevation of gene expression was blunted in the shD2 cells. Conversely, fenofibrate treatment decreased the

expression levels of SCD1 (stearoyl-CoA desaturase 1), SCP2 (sterol carrier protein 2), PPARγ and ChREBP (carbohydrate-responsive element-binding protein) in control cells, but that effect was not influenced by the loss of D2. This suggests D2 modulates genomic response to fibrate by influencing the expression of some, but not all the genes in the PPAR signaling pathway.

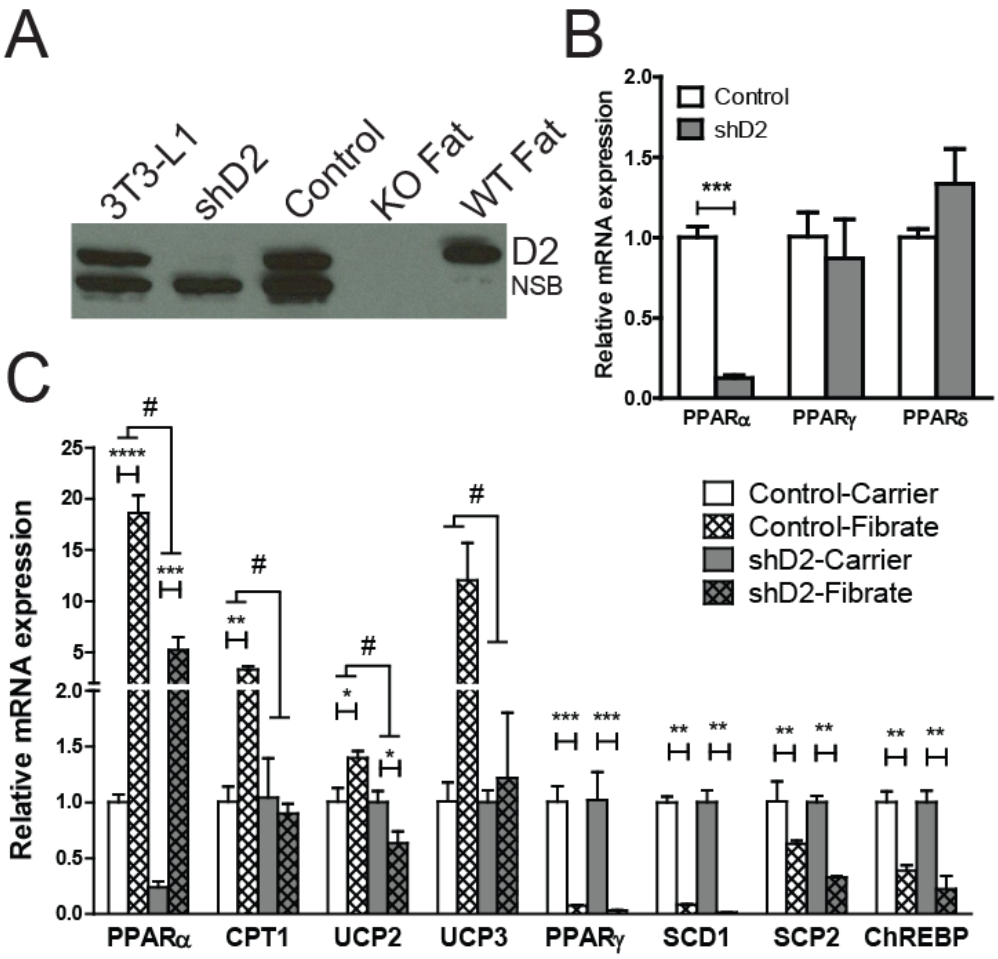


**Figure 2.3. D2 modulates PPARα and fibrate responses in 3T3-L1 adipocytes.** (A) 3T3-L1 cells and two stable subclones infected with lentiviral particles expressing short hairpin RNAs directed against D2 (shD2) or a control shRNA (Control) were differentiated into adipocytes that express endogenous D2. Cell lysates were analyzed

for D2 expression by immunoblotting. Membrane preparations from epididymal fat dissected from KO and WT mice were used as negative and positive controls. NSB indicates non-specific band in 3T3-L1 cells. (B) Expression levels of PPAR family members were determined in control and 3T3-L1 adipocytes by rtPCR. Data were analyzed by unpaired t-test (n=3 independent wells) (C) Control and shD2 3T3-L1 adipocytes were treated with fenofibrate (500 mM) or Carrier (DMSO) for 16 hr. Gene expression was determined by rtPCR. Data were analyzed by two-way ANOVA # over lines indicate a detection of a significant interaction at $P<0.01$. Bonferonni post-hoc tests were conducted within treatment. * $P< 0.05$, ** $P<0.01$, *** $P<0.001$.

*Triglyceride secretion from liver is accelerated by loss of ABCD2*

Fibrate therapy has been shown to successfully oppose diet-induced obesity in mice [278]. To investigate the impact of D2 on fibrate response *in vivo*, we challenged KO and WT mice with high fat diet (control, 60% kcal) or the same diet formulated with 0.05% (w/w) fenofibrate (Fibrate) for 16 weeks starting at 8 weeks of age. No significant differences in body weight, body composition, insulin sensitivity, or other measures of lipid metabolism between genotypes were observed at 8 weeks. After high fat diet feeding, both KO and WT mice in untreated (control) group developed obesity and hyperglycemia with elevated body weight, fat mass percentage, and blood glucose levels (Fig. 2.4). Fenofibrate treatment mitigated the increase in body weight and adiposity, but these effects were not influenced by loss of D2 (Fig. 2.4A, 4B). Blood glucose levels were measured at the initiation (0 weeks on diet), midpoint (8 weeks on diet), and end of the study (16 weeks on diet) (Fig. 2.4C). Control KO mice tended to have higher blood glucose levels compared to their WT littermates at 8 and 16 weeks of age. However, the

difference between genotypes was lost in fibrate treated animals whose blood glucose levels were normalized. A glucose tolerance test was done at the endpoint of the study (Fig. 2.4D). Glucose tolerance was compromised by the absence of D2. Fibrate lowered blood glucose and improved glucose tolerance, but this effect was not altered by the absence of D2.

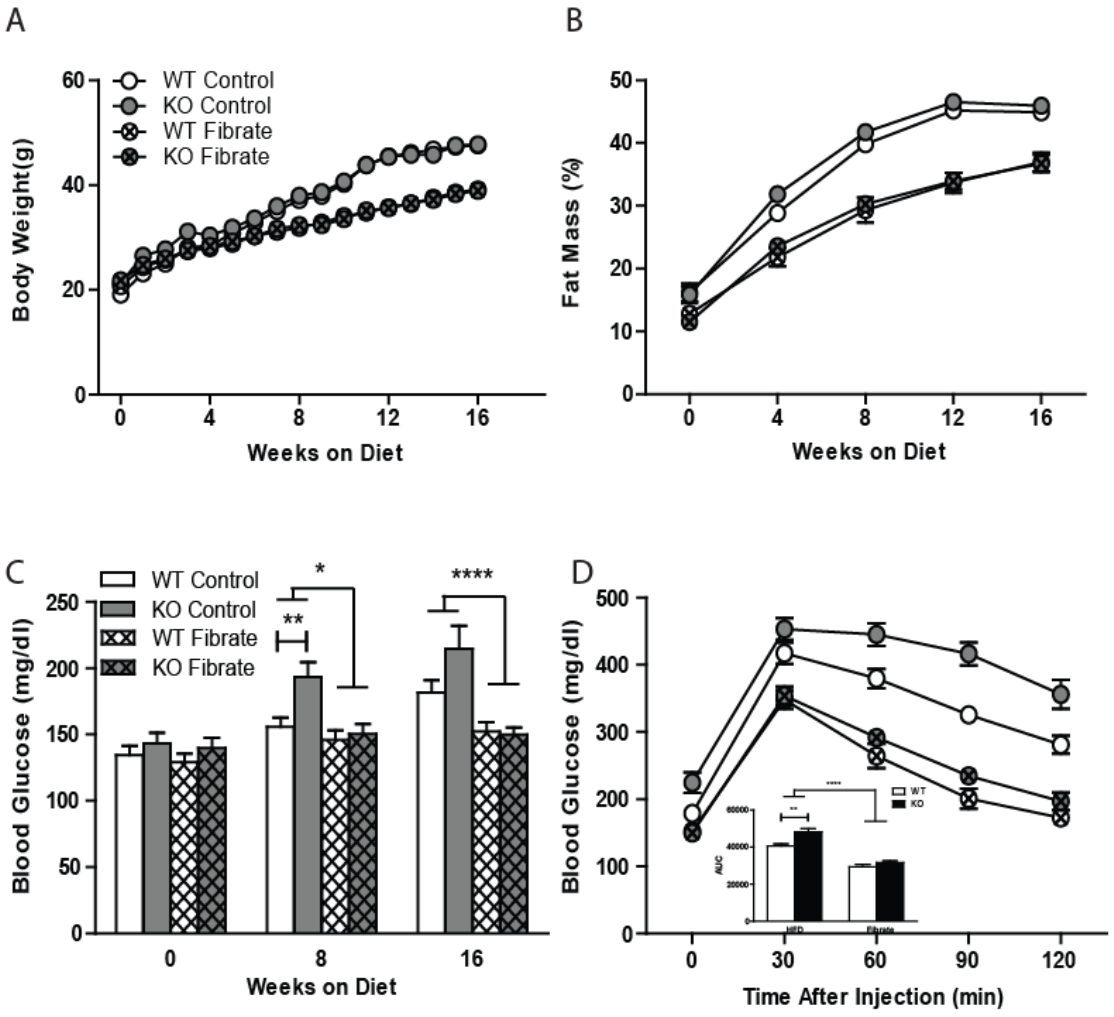


**Figure 2.4. Measurement of physiological parameters.** Body weights (A) were recorded for wild-type mice on high fat diet (WT Control, n=12) and high fat diet containing 0.05% fenofibrate (WT Fibrate, n=17), and D2 knock-out mice on high fat

diet (KO Control, n=8) and high fat diet containing 0.05% fenofibrate (KO Fibrate, n=17). Fat mass percentage (B) of these mice were measured by MRI every four weeks (mean±SEM, n=8~17). Blood glucose concentrations (C) were measured every four weeks (mean±SEM, n=8~17). Glucose tolerance tests (D) were performed by intraperitoneal injection of glucose (1 g/kg) and measurement of blood glucose concentration (mean±SEM, n=8~17). AUC for the GTT measurement was also listed within panel (D). Statistical comparison was made between two treatment groups using two-way ANOVA (mean±SEM, n=8~17, P*<0.05, P****<0.0001). Statistical comparison between genotypes within each group was made using Student's t-test (mean±SEM, n=8~17, P**<0.01).

We analyzed plasma and hepatic lipids from both WT and KO mice with and without fenofibrate treatment (Fig. 2.5A-D). Neither genotype nor fibrate treatment altered plasma or hepatic cholesterol (Fig. 2.5A and B). Fenofibrate reduced the triglyceride levels of plasma and liver, but neither of these effects was altered by the absence of D2 (Fig. 2.5C and D). KO mice exhibited significantly higher triglyceride secretion rates than their WT littermates in both control (WT, 243.0 ± 33.49 mg/dl/hr; KO, 337.7 ± 27.86 mg/dl/hr) and fibrate (WT, 175.8 ± 17.24 mg/dl/hr; KO, 285.8 ± 21.56 mg/dl/hr) groups (Fig. 2.5E and F). However, there was no significant interaction between the genotype and the fibrate treatment. This observation suggests that although the static plasma triglyceride level was not affected, secretion rate of triglyceride from liver was accelerated by loss of D2 with and without fibrate treatment.

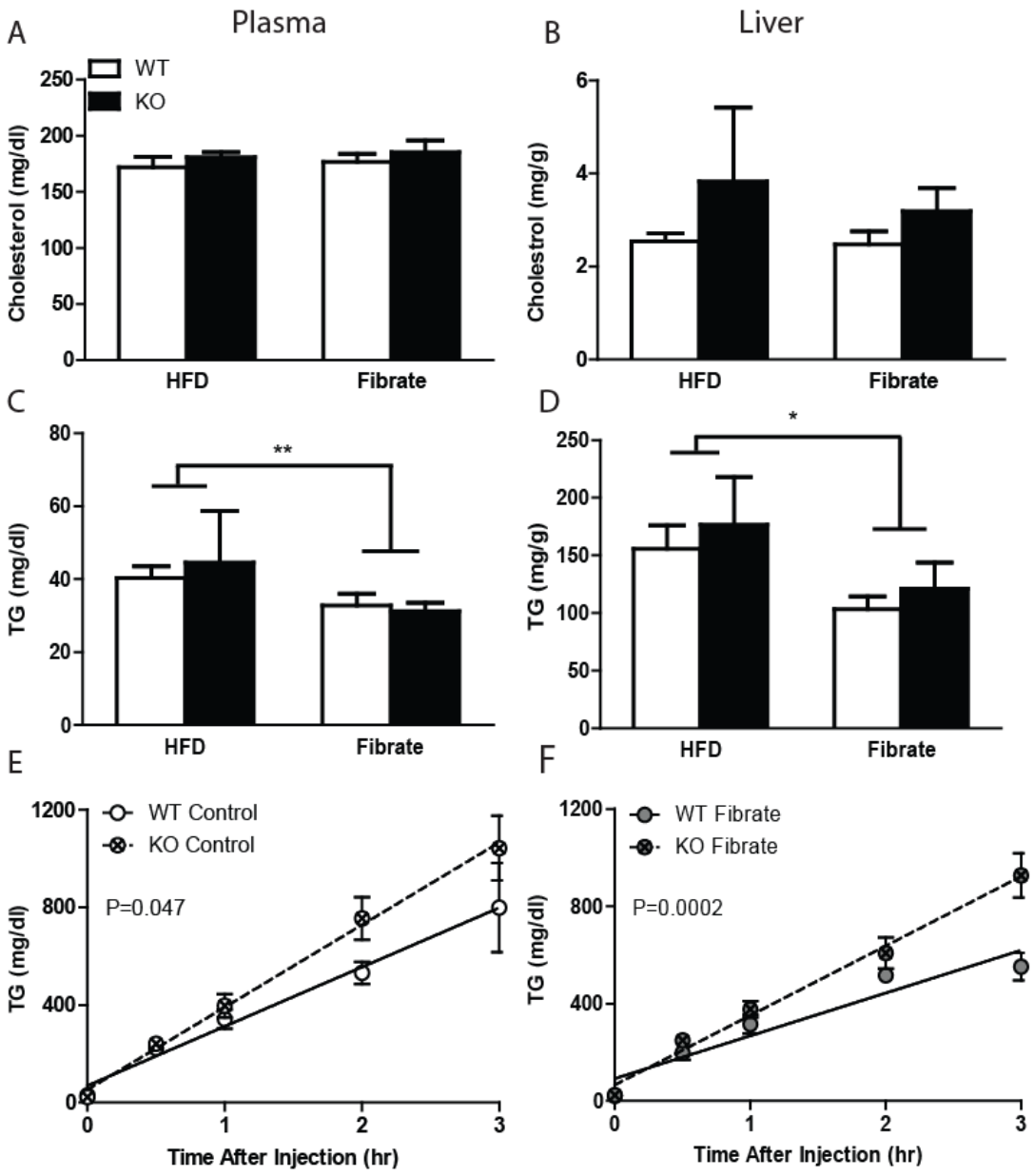


**Figure 2.5. Lipid lowering effect of fibrates dependent on ABCD2.** Total cholesterol and triglyceride concentrations in plasma (A and C respectively, mean±SEM, n=4~17) and liver (B and D respectively, mean±SEM, n=4~5) were measured. Statistical analysis was done using two-way ANOVA (P*<0.05, P**<0.01). Triglyceride secretion rates of control and fibrate treatment were determined using linear regression analysis (n=3~6).

The TG secretion rate was calculated as the slope and the significance of difference between two genotypes was demonstrated as P-value.

We placed a subgroup of mice in the metabolic cages by the end of the experiment. Fenofibrate treatment suppressed food intake and promoted energy expenditure, but these effects were almost equal for both genotypes (Fig. 2.6).

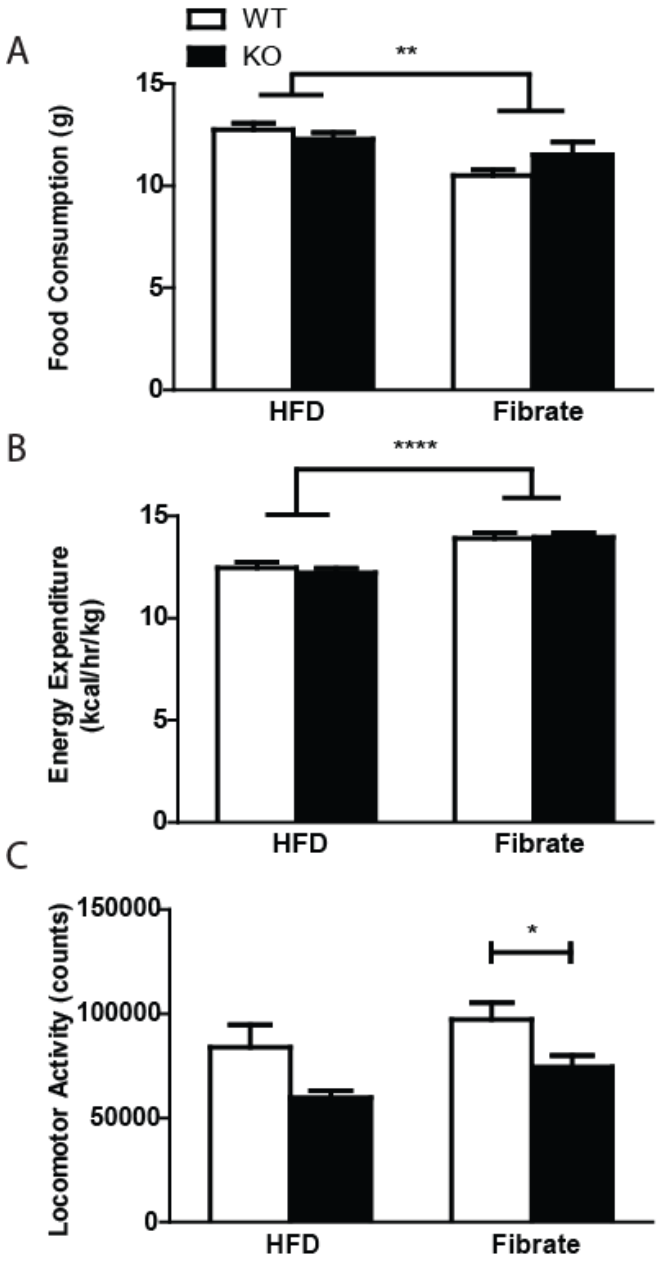

**Figure 2.6. Metabolic parameters.** Accumulative food consumption (A) and locomotor activity (C) of a subgroup of mice were recorded during 72 hour stay in metabolic cages. Energy expenditure (B) was calculated based on recorded oxygen and carbon dioxide flow. Statistical comparison between fibrate treatment and control groups was made using two-way ANOVA (mean±SEM, n=3~6, P**<0.01, P****<0.0001). Significance of difference between two genotypes within each group was analyzed using Student's t-test (mean±SEM, n=3~6, P*<0.05).

*Single nucleotide polymorphisms in ABCD2 do not associate with hypolipidemic effects of fenofibrate*

Efficacy of fibrate treatment for dyslipidemia in human subjects is highly variable between individual patients [256]. To evaluate the association of single nucleotide polymorphisms in *ABCD2* to fenofibrate treatment efficacy, we analyzed the data from the GOLDN study in a population of related metabolically healthy individuals of European American ancestry (Table 1). Three SNPs in *ABCD2* are associated with alterations in expression levels of D2, suggesting they may alter D2 activity in human subjects [276]. Two variants genotyped in GOLDN data set analysis, rs7309234 and rs11172592, were selected and used as proxies for corresponding D2 variants, rs4285917 and rs4284427, as each is in linkage disequilibrium with these expression-associated SNPs, respectively. Neither variant was associated with responses to fibrate among GOLDN participants, suggesting D2 expression is unlikely to alter fibrate responses in human subjects.

**Table 2.1. Association of *ABCD2* variants with fenofibrate effects.** Linear mixed models were used to assess the association of two *ABCD2* variants, rs7309234 and rs11172592, with the fenofibrate-induced change in plasma triglycerides based on the data from the GOLDN study in a population of related metabolically healthy individuals of European American ancestry.

| SNP | Beta | S.E. | *P*-value |
|---|---|---|---|
| rs7309234 | 0.009792360 | 0.0183794364 | 0.5943369 |
| rs11172592 | 0.010279890 | 0.0084339715 | 0.4983299 |

## Discussion

The major finding of this study is that D2 modulates PPARα signaling and genomic response to fibrate treatment *in vitro* and *in vivo*. However, the absence of D2 did not alter the impact of fibrate in a mouse model of diet-induced obesity. Although not a comprehensive assessment, SNPs associated with altered D2 expression levels were not associated with responses to fibrate therapy in human subjects. D2 has long been known as a PPARα target gene that is upregulated in response to fenofibrate. To the best of our knowledge, this is the first report that demonstrates D2 reciprocally regulates PPARα signaling.

A number of gene clusters are differentially affected by fibrate in the presence or absence of D2. We verified differential expression of selected genes in the PUFA synthesis cluster by rtPCR in mouse liver. Other clusters affected include pathways associated with lipid, bile acid, and steroid metabolism, but have yet to be confirmed by secondary approaches. In the present study, we elected to focus on PPAR signaling due to the use of PPAR agonists as lipid modifying agents and the variability in response to fibrate treatment.

In 3T3-L1 cells, suppression of D2 reduced PPARα mRNA levels as well as the upregulation of several PPARα target genes in response to fibrate treatment. Interestingly, the repression of selected genes by fibrates was unaffected. This effect indicates that D2 selectively modulates fibrate responses and, perhaps PPARα signaling. The molecular mechanism responsible for differential effects is unknown, but is likely related to D2-dependent peroxisomal metabolism of fatty acids, a source of PPAR ligands. Alternatively, these differences may be due to effects of fenofibrate that are independent of PPARα.

In the absence of fibrates, D2 deficiency resulted in a modest, but significant increase in fasting glucose at the midpoint and end of the study, as well as reduced glucose tolerance. This is inconsistent with our previously published work in which differences in glycemic control were not observed in D2 deficient mice following high fat feeding or when crossed onto the ob/ob background [242]. However it should be noted that the previous study utilized a 45% kCal high fat diet as opposed to the 60% kCal diet. Other phenotypes, such as weight gain and body composition, were as previously reported.

The absence of D2 also reduced TG secretion rates in both the presence and absence of fibrate treatment. In the absence of D2, TG secretion rates in fibrate treated mice are indistinguishable from untreated WT mice. However, this difference was insufficient to affect fasting TG levels. MTTP (microsomal triglyceride transfer protein) is known to regulate the TG secretion in mice [279], but its mRNA levels were not influenced by loss of D2 irrespective of fibrate treatment (data not shown). LPL (lipoprotein lipase) mRNA was elevated in the brown adipose tissue in KO mice compared to WT littermates on high fat feeding (data not shown). LPL is an enzyme known to hydrolyze triglyceride in lipoprotein to release free fatty acid for uptake into peripheral tissues for metabolism [280]. Given the role of LPL in TG clearance, the increased LPL expression in the face of elevated TG secretion may account for the absence of differences in steady-state plasma TGs.

A number of genetic and environmental factors influence plasma TGs and responses to lipid lowering drugs. We took advantage of an ongoing effort to identify genetic variants that influence responses to fibrate therapy to determine if polymorphisms in the *ABCD2* gene might be associated with such differences. Neither of the two proxy SNPs analyzed were statistically significant, suggesting that variants in *ABCD2* and alterations in D2 levels are unlikely to contribute to differences in response to fibrate therapy. However, it should be noted that the effects of these SNPs on D2 activity have not been formally characterized. Additional studies are needed to fully elucidate the effect of D2 on TG metabolism and responses to fibrate therapy.

# CHAPTER 3. ABCD2 IDENTIFIES A UNIUE PEROXISOME-LIKE SUBCELLULAR ORGANELLE IN MOUSE ADIPOSE TISSUE

## Introduction

Peroxisomes were initially identified in kidney and liver cells as a subcellular organelle characterized by a single membrane containing a granular matrix and a crystalline core [199]. These dynamic organelles have since been shown to be present in virtually all mammalian tissues and cells including adipocytes [203, 204, 281]. Besides the removal of reactive oxygen species, peroxisomes are also metabolically involved in the β-oxidation of very long chain fatty acids, α-oxidation of branched chain fatty acids and biosynthesis of ether-phospholipids [204].

Peroxisomes in adipose tissues are often referred to as 'microperoxisomes', because they are generally smaller in size and lack a crystalline core [202]. Microperoxisomes dramatically increase in number during differentiation of cultured 3T3-L1 adipocytes and were found to be in the vicinity of lipid droplets [203]. Recently, there has been emerging evidence indicating that peroxisome metabolism is critically required for normal adipose function [253, 254]. In Pex7 deficient mice, peroxisome biogenesis is impaired due to the failure of peroxisomal protein import [254]. These mice lack plasmalogens, the synthesis of which strictly relies on peroxisomal metabolism, and had severely reduced adiposity despite similar food intake. In another mouse model in which Pex5 was specifically deleted in adipose using aP2 promoter, peroxisomes were dysfunctional in white adipose tissue but intact in liver, heart, pancreas and muscle [253]. Adipose function was

impaired resulting in reduced lipolysis and increased fat mass. However, other phenotypes were also observed including failure of catalase import into peroxisomes in the nervous system, impaired shivering thermogenesis and reduced plasma adrenaline levels, suggesting some adipose phenotypes were due to secondary effect or off-target Pex5 deletion.

ABCD2 has been proposed as a peroxisomal ABC transporter that promotes the transport of very long chain fatty acyl-CoA into peroxisomes for β-oxidation [248]. The D2 protein is expressed in brain, skeletal muscle, lung, liver and testis, but is most abundant in adipose tissues in mice and highly expressed in cultured 3T3-L1 adipocytes [241]. The mRNA levels of D2 in mouse white adipose tissue respond to fasting and refeeding and correspond to SREBP1c-stimulated gene expression [282]. D2 deficient adipose tissue showed an increase in the abundance of 20:1 and 22:1 fatty acids. When D2 deficient mice were challenged with dietary erucic acid (C20:1), they exhibited rapid onset of obesity, hepatic steatosis and insulin resistance [283]. While these data support a key role for D2 in lipid metabolism, the function of D2 in adipose and its relationship to adipose peroxisome metabolism remains unclear.

To determine the subcellular localization of D2 and its relationship to adipose peroxisomes, we isolated D2-containing organelles from mouse adipose tissue using two independent approaches. Our data indicates that the D2-compartment lacks some of the well-known peroxisomal proteins such as catalase and PEX19, but possesses other peroxisomal enzymes. These results suggest an association of this organelle with mitochondria and ER. The most strongly-associated protein with D2 is leucine rich repeat

containing protein 59 (LRRC59), a poorly characterized protein implicated in intracellular trafficking of FGF1 [284].

**Materials and methods**

Animals

Age-matched (3 month, n=4) wild-type (WT) and Abcd2 (D2) knock-out (KO) mice on the C57Bl/6J background were provided with free access to water and standard chow diet. Mice were housed in a 10 hour dark/14 hour light cycle.

Immunofluorescence microscopy

Mice were perfused with 10ml 1% fresh paraformaldehyde in phosphate buffered saline (PBS) by direct injection into the left ventricle. Epididymal fat pads were dissected and placed into 1% paraformaldehyde for 10min at room temperature. The tissue was washed in three changes of PBS for 10min each and cut into desired number of samples with approximately finger-nail size. Each sample was put into a 2ml tube and blocked in 500ul 5% bovine serum albumin (BSA) in PBS for 1 hour. Samples were incubated in 500ul of anti-D2 antibody dilution in 5% BSA in PBS for 2-3 hours at room temperature. Samples were washed in three changes of PBS for 10min each. Samples were then incubated in 500ul of fluorescent conjugated secondary antibody dilution in 5% BSA in PBS for 45-60min at room temperature. Samples were washed in three changes of PBS for 10min each and placed in chamber mounted on #1.0 borosilicate coverglass (Lab-Tek, catalog #155383). Samples were covered with ~150 µL Vectashield mounting medium. Images were taken using an inverted standard fluorescence or confocal microscope.

## Peroxisome Isolation

Peroxisomes were isolated based on the protocol used for liver peroxisome preparation [13-15]. Mouse adipose tissue was dissected freshly and homogenized using Potter-Elvehjem homogenizer for 5 strokes in ice-cold SEM buffer (250 mM sucrose, 1 mM EDTA, 50 mM MOPS, pH7.4). The homogenate was centrifuged at 750 x g for 10 min to generate post-nuclear supernatant (PNS). The PNS fraction was then centrifuged at 8500 x g for 10 min to generate mitochondria enriched pellet (heavy mitochondria pellet, HM). The resulting supernatant (heavy mitochondria supernatant, HMS) was then centrifuged at 27,000 x g for 20 min to generate peroxisome enriched pellet (light mitochondria pellet, LM). The resulting supernatant (light mitochondria supernatant, LMS) was centrifuged at 100,000 x g, for 45 min to precipitate all the membrane proteins. All centrifugation was done under 4°C. Generated fractions were resuspended in protein sample buffer (PSB, 30mM Tris base, 10mM EDTA, pH 6.8, 3% SDS, 20% glycerol and 0.00625% bromphenol blue) and the protein concentration was determined.

## Protein sample preparation and immunoblotting

Protein samples in PSB were added with 2% 2-mercaptoethanol and heated to 95 °C for 5 min before loading. Proteins were size-fractionated on 10% SDS-polyacrylamide gels and transferred to nitrocellulose membranes. Membranes were incubated in buffer A (20 mM Tris, 137mM NaCl, 0.2% Tween 20 and 5% non-fat milk, pH 7.6) for 30 min at room temperature. Primary antibodies was diluted in buffer A and incubated with membranes for 60 min at room temperature. Membranes were washed 3 times for 5 min in buffer B (20 mM Tris, 137mM NaCl and 0.2% Tween 20, pH 7.6). Horseradish

peroxidase-conjugated secondary antibodies were diluted in buffer B and incubated with membranes for 45 min at room temperature. Membranes were washed 3 times for 5 min in buffer B and visualized by enhanced chemiluminescence (SuperSignal West Pico, Thermo Scientific).

Electron microscopy

Biochemically generated LMt fraction was fixed in 4% paraformaldehyde and washed 3 times for 5 min with 0.1 M cacodylate buffer. Samples were dehydrated in a series of graded ethanol (70% to absolute) and embedded in Epoxy resin. Ultrathin sections were inspected after contrasting with electron microscope.

Wild-type and D2 KO mice were anaesthetized by intraperitoneal injection and perfused via the left ventricle with a mixture of 4% paraformaldehyde, 2% glutaraldehyde in 0.01M cacodylate buffer (pH7.4). Fixed adipose tissue were dissected, cut in slices with razor blades, post-fixed in 0.5%, 1%, or 2% glutaraldehyde in cacodylate buffer (pH7.4) for 45 min and washed 3 times for 5 min with 0.1 M cacodylate buffer. Fixed adipose tissue was embedded into LR White resin (medium grade). LR White-filled gelatin capsules were polymerized at 50°C for three days. After preparation of semithin sections blocks, ultrathin sections of 80nm were cub, collected on 100 mesh nickel grids and therefore coated on the back side with a 1% formvar film. The grids were dried at 37°C overnight prior to immunostaining. The sections were incubated with blocking solution (1% BSA in TBST) for 30 min at room temperature. Incubation with the primary antibodies was performed on droplets with antibodies (anti-D2 and anti-pex19) in 0.5% BSA in TBST overnight at room temperature. Thereafter the sections were incubated with a

secondary antibodies conjugated with gold particles (12nm particles conjugated with anti-rabbit antibody and 6nm particles conjugated wit anti-mouse antibody) in 0.5% BSA in TBST for 1 hour at room temperature. Negative controls were processed in parallel. The grids were rinsed on droplets of TBST and subsequently contrasted with uranyl acetate for 2 min and lead citrate for 45 sec. The sections were examined using electron microscope.

Immunoisolation of ABCD2-containing compartment and Shotgun proteomics

Adipose tissue freshly collected from WT and KO mice was homogenized in ice-cold SEM buffer. Homogenates were centrifuged at 750 x g for 10 min in 4°C to generate post-nuclear supernatant (PNS). Anti-D2 antibodies were biotinylated (EZ-Link™ Sulfo-NHS-LC-Biotinylation Kit, Thermo Scientific, prod# 21435) and incubated with streptavidin iron beads (MagnaBind™ Streptavidin Beads, Thermo Scientific, prod#21344) for 30min in room temperature to prepare antibody-bead complex. The complex was then mixed with freshly prepared adipose PNS in 4°C overnight for antigen-antibody binding. The mixture was then put under magnetic field to isolate the antigen-antibody-bead complexes from other components. The complex was washed sequentially with SEM buffer, triton lysis buffer (80 mM NaCl, 50 mM Tris pH8.0, 2 mM CaCl2, and 1% Triton), triton lysis buffer with 0.5% SDS on ice and triton lysis buffer with 0.5% SDS in 37°C. Each eluate was saved and analyzed with western blotting. For proteomic samples, only elution with triton lysis buffer with 0.5% SDS at 37°C was applied. Eluates were enriched on a SDS-PAGE gel and processed for proteomic analysis.

The protein sample was digested with trypsin and the tryptic peptides were analyzed by LC-MS/MS using an LTQ Velos Orbitrap mass spectrometer (Thermo Fisher Scientific, Waltham, MA) coupled with a Nano-LC Ultra/cHiPLC-nanoflex HPLC system (Eksigent, Dublin, CA) through a nano-electrospray ionization source [30]. Tandem MS/MS data were acquired using CID fragmentation of selected peptides during the information-dependent acquisition. The LC-MS/MS results were subjected to protein identification and acetylation sites determination using ProteomeDiscoverer 1.3 software (Thermo Fisher Scientific, Waltham, MA) and MASCOT server.

## Results

*Immunofluorescent microscopy of ABCD2 protein in mouse adipose tissue*

To determine the distribution pattern of D2 within the adipose tissue and in adipocytes in vivo, we localized D2 in adipose tissue explants by indirect immunofluorescence microscopy (Fig. 3.1). D2 antibody labeled the thin, cytoplasmic space separating the lipid droplet from the cell surface (Fig. 3.1B). Three dimensional reconstruction of high magnification, confocal images revealed a punctate staining pattern dispersed around the lipid droplet (Fig. 3.1C and D).

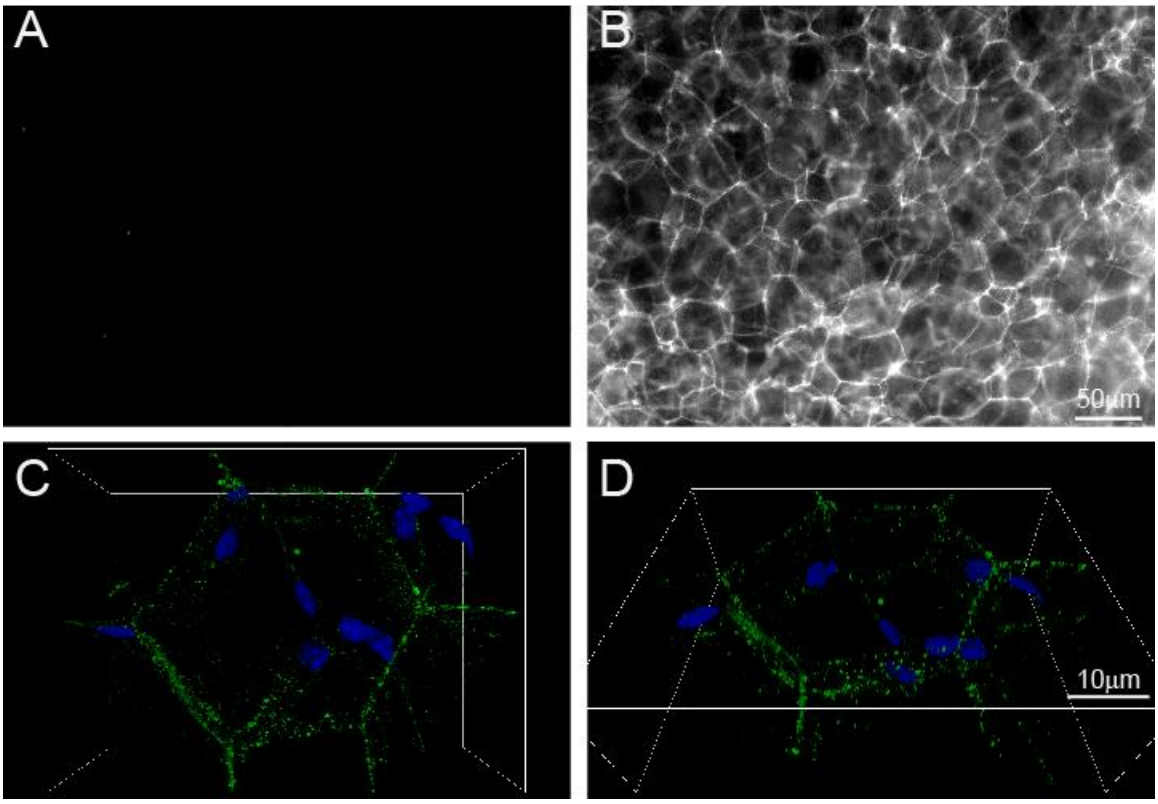


**Figure 3.1. Immunolocalization of D2 in mouse adipose tissue explants.** Mouse epididymal fat pads were fixed with 1% paraformaldehyde, cut into small pieces and processed for indirect immunofluorescence microscopy. A and B) Low power (10X) images of fixed adipose explants labeled with either pre-immune serum (A) or anti-D2 polyclonal antibody (B). C and D) Three dimensional reconstruction of 60 (0.6 mm/slice) high power, confocal images (63X) with 0º (C) or 45º rotation (D) along the z-axis. Green color denotes D2 labeled with AlexaFluor 488. Blue denotes nuclei stained with DAPI. Additional image rotations can be found in supplemental data.

*Localization of D2 and selected peroxisome markers in mouse adipose peroxisome preparations*

To determine the subcellular localization of D2 protein within the adipocytes, mouse adipose tissue was fractionated using a procedure previously published for the isolation of peroxisomes from liver (Fig. 3.2A) [285-287]. Mouse adipose tissue was dissected and homogenized in detergent free buffer. Sequential centrifugation was used to generate the

following fractions: nuclear pellet (NP), post nuclear supernatant (PNS), heavy mitochondria pellet (HMt), heavy mitochondria supernatant (HMS), light mitochondria pellet (LMt), light mitochondria supernatant (LMS), light membranes (LMbn) and cytosol (Cyto). Each fraction was analyzed by western blotting to determine the relative abundance of D2 and selected peroxisome markers in each fraction (Fig. 2B). D2, catalase, D3 (a.k.a PMP70) and PEX19 were all present in the PNS and HMS fractions. However, D2 fractionated with light mitochondria (LMt , 27,000g), while catalase, PEX19 and D3 remained in suspension (LMS) and sequentially precipitated with light membranes (LMbn, 100,000g). Liver peroxisomes generally co-fractionate with light mitochondria and are subsequently separated on a continuous sucrose gradient. However, most peroxisome markers in adipose remained suspended and only D2 came down in the LMt. This is unlikely due to peroxisome rupture since these markers include D3, a protein with multiple membrane spanning segments and that other markers pelleted at 100,000g.

Next, we fixed the LMt pellets from both liver and adipose tissue and processed them for electron microscopy (Fig. 3.2C). We used liver as a positive control to see evidence of both mitochondria (white arrowhead) and peroxisomes (black arrowheads) with their characteristic dense matrix and ~0.2um diameter. LMt pellets from adipose also revealed mitochondria, but in fewer numbers as well as structures with the typical appearance of peroxisomes. However, the fraction was highly enriched with ~0.1um diameter spherical structures, with a clearly defined membrane (white and black arrows). Some contained evidence of matrix (black arrows), but not as electron dense as peroxisomes typical of

liver. With the separation of D2 from catalase and PEX19, we hypothesized that D2 may be localized in a subclass of peroxisome in adipocytes.

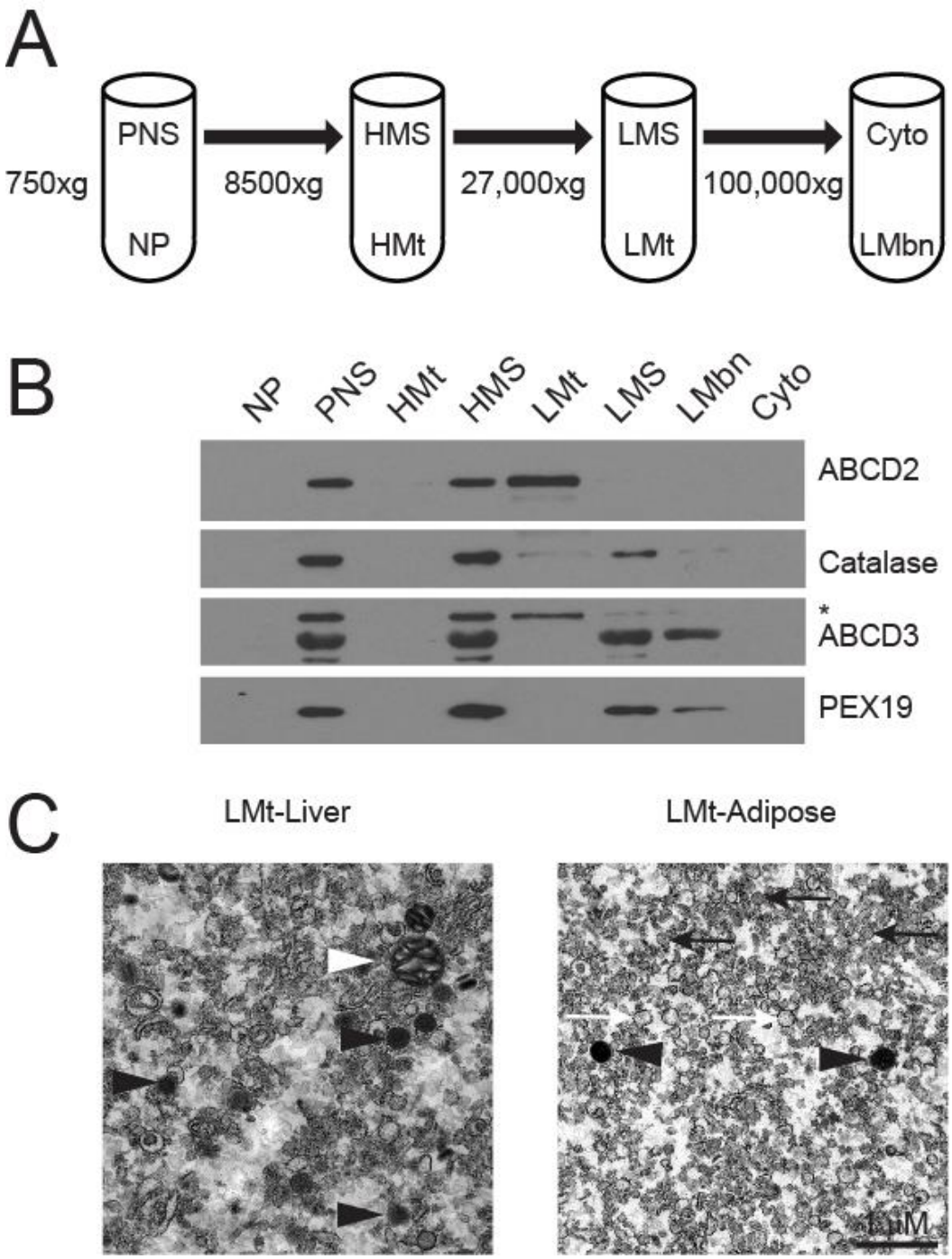


**Figure 3.2. Abundance of D2 and other peroxisome markers in biochemically generated fractions from adipose tissue.** A) Mouse adipose tissue was homogenized in

SEM buffer on ice and sequentially centrifuged using different forces to seperate subcellular fractions. B) 2.3% of each fraction was analysed for the abundance of D2 and other peroxisome marker proteins by western blotting. The asterisk indicates residual signal of D2 from prior blotting. C) Light mitochondrial fractions (LMt) from liver and adipose tissues were fixed in 4% paraformaldehyde and immaged using electron microscopy. Mitochondria are indicated by white arrowheads. Peroxisomes are indicated by black arrowheads. Spherical vesicles with transparent lumen are indicated by white arrows. Spherical vesicles with dense matrix are indicated by black arrows.

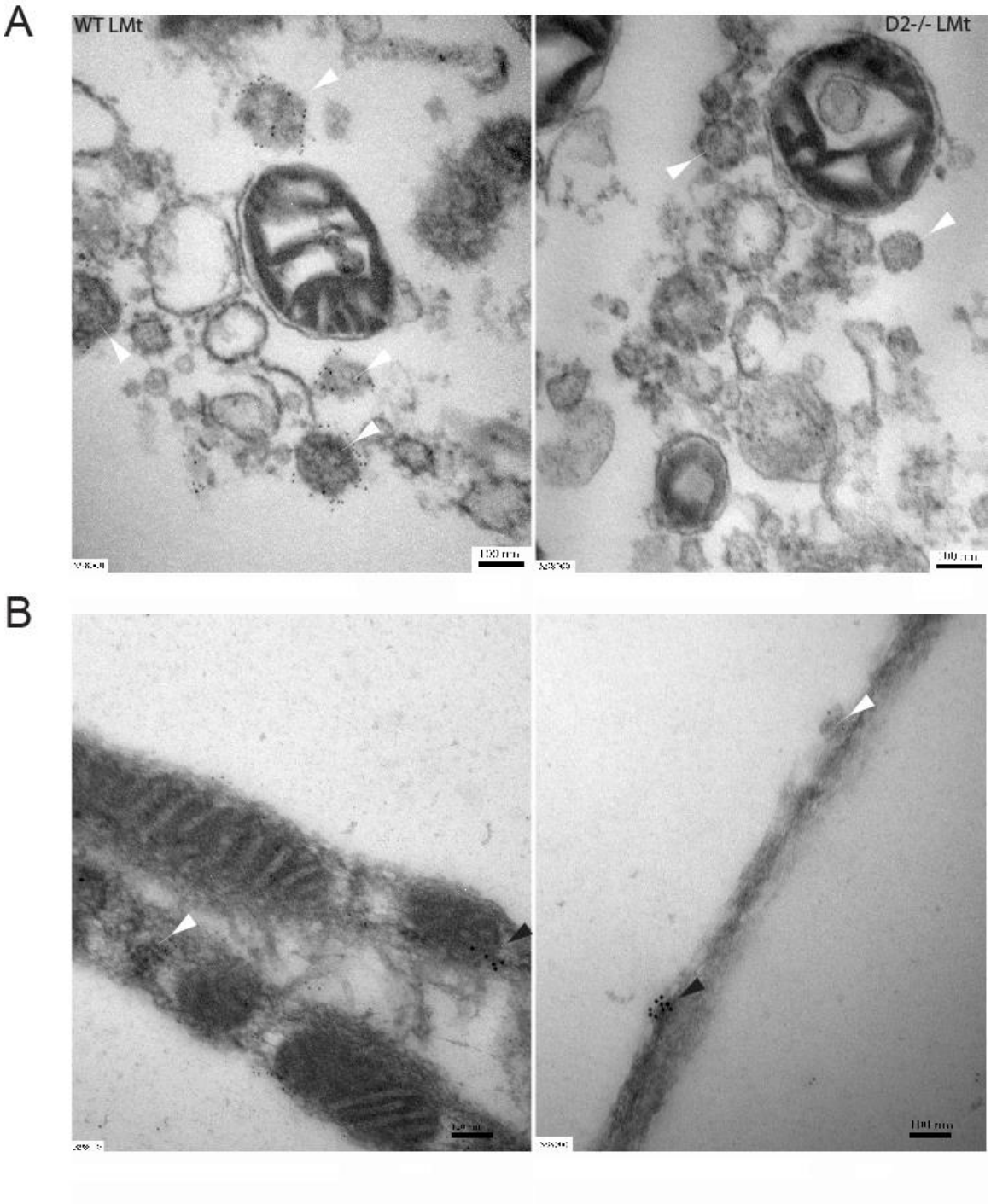


**Figure 3.3. Localization of D2 and PEX19 in fixed mouse adipose tissue.** A) Peroxisome enriched fractions (LMt) were prepared using freshly collected adipose tissue from WT and D2 KO mice by sequential centrifugation. The LMt fractions were fixed in 4% paraformaldehype and embedded in Epoxy resin. Ultrathin sections were cut and immunostained using the polyclonal D2 antibody and secondary antibody (cross-linked with 6nm diameter gold particles). Peroxisome-like compartments are indicated by white arrowheads. B) Fixed mouse epididymal fat samples were cut into ultrathin sections of

80nm, immunostained with D2 antibody and secondary antibody (cross-linked with 6nm gold particles, indicated by empty arrowheads) and PEX19 antibody and secondary antibody (cross-linked with 12nm gold particles, indicated by black arrowheads).

*Localization of D2 and PEX19 in fixed mouse adipose tissues*

Next, we prepared LMt fraction from both WT and D2 knock-out (KO) adipose tissue. The fractions were fixed and immunostained with D2 antibody and detected by secondary antibody cross-linked with gold particles (6nm diameter, Fig. 3.3 A). In the WT sample, the D2 antibody specifically labeled compartments (pointed by white arrowheads) with a more electron dense center distinct from the surrounding vesicular structures, whereas the same compartments were present in the KO sample but not labeled with D2 antibody.

To determine if the D2 compartment was distinct from the PEX19 compartment in vivo, we fixed mouse epididymal adipose explants, cut them into ultrathin sections of 80nm, and immunostained them with the D2 and PEX19 antibodies. D2 (white arrowheads) and PEX19 (black arrowheads) were detected with secondary antibodies linked with 6nm and 12nm gold particles, respectively (Fig. 3.3 B). PEX19 and D2 antibodies recognized distinct structures and exhibited no overlap in adipose sections.

*Immunoisolation and proteomic profiling of the D2-containing compartment*

We next sought to characterize the proteome of the D2-containing compartment. We cross-linked our D2 antibody to biotin and used it to immunoisolate D2-containing organelles from mouse adipose homogenates with avidin-coated magnetic beads. The immunoisolated compartment was eluted sequentially with buffers containing Triton-X 100, Triton-X 100 plus 0.5% SDS at 4°C, and the same buffer at 37°C. Eluted fractions

were processed by SDS-PAGE and analyzed by western blotting (Fig. 3.4). D2 was detected in the starting material (PNS) as well as the supernatant (SupIP) after immunocapture, but with much reduced amount. A modest amount of D2 was eluted with Triton alone (E1). Solubilization of D2 required the addition of SDS in the elution buffer (E2 and E3) and beads. Boiling in SDS under reducing conditions released a small amount of residual D2 from the magnetic beads (data not shown). As in the centrifugation approach, PEX19 did not co-elute with D2. Calnexin was also blotted as a negative control for bulk ER proteins.

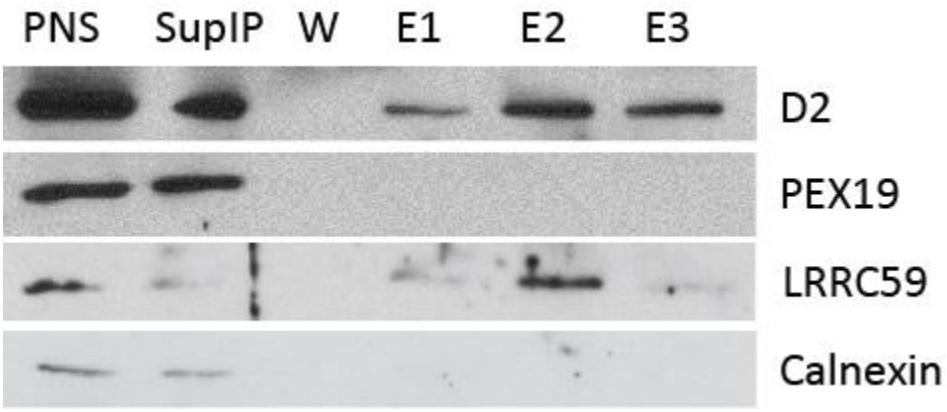


**Figure 3.4. Immunoisolation of the D2-containing compartment.** Avidin-coated magnetic beads were cross-linked with biotin-conjugated D2 antibody. Mouse adipose homogenate (PNS) was incubated with the D2 antibody at 4°C for 16 hours to capture the D2-containing compartment. The captured compartment was isolated from the supernatant (SupIP) under the magnetic field and sequentially washed by SEM buffer on ice (W), triton lysis buffer on ice (E1), triton lysis buffer+0.5% SDS on ice (E2) and triton lysis buffer+0.5% SDS under 37°C (E3). Each fraction was analysed for abundance of D2, PEX19, LRRC59 and calnexin using western blotting.

We next applied shotgun proteomics to analyze the D2-containing organelles from independently prepared WT (n=4) and KO (n=3) adipose tissue. To concentrate proteins

in the D2 compartment, we directly eluted in buffer E3 following the wash step. Eluates were subjected to mass spectrometry analysis to obtain the D2 associated proteome from adipose.

Any peptides present in KO samples were considered as non-specific associations. Uniprot IDs of proteins identified exclusively in the WT samples were analyzed by the DAVID functional annotation tool. Proteins associated with D2 were annotated to peroxisomal, mitochondrial and ER-related (Table 3.1).

| **Peroxisome** |
|---|
| ATP-binding cassette, sub-family D (ALD), member 2 |
| ATP-binding cassette, sub-family D (ALD), member 3 |
| carnitine acetyltransferase |
| dehydrogenase/reductase (SDR family) member 7B |
| enoyl coenzyme A hydratase 1, peroxisomal |
| enoyl-Coenzyme A, hydratase/3-hydroxyacyl Coenzyme A dehydrogenase |
| nephronophthisis 3 (adolescent); acyl-Coenzyme A dehydrogenase family, member 11 |
| sterol carrier protein 2 |
| **Mitochondrion** |
| 3-oxoacid CoA transferase 1 |
| ATP synthase, H+ transporting, mitochondrial F0 complex, subunit b, isoform 1; predicted gene 12231 |
| Cytochrome c oxidase subunit 2 |
| NADH dehydrogenase (ubiquinone) 1 alpha subcomplex, 8 |
| NADH dehydrogenase (ubiquinone) 1 alpha subcomplex, 9 |
| NADH dehydrogenase (ubiquinone) flavoprotein 1 |
| aconitase 2, mitochondrial |
| acyl-Coenzyme A dehydrogenase, medium chain |
| carbonyl reductase 2 |
| carnitine acetyltransferase |
| carnitine palmitoyltransferase 2 |
| citrate synthase |
| cytochrome c oxidase subunit IV isoform 1 |
| cytochrome c oxidase, subunit VI a, polypeptide 1; predicted gene 7795 |
| dihydrolipoamide dehydrogenase |
| fumarate hydratase 1 |
| malate dehydrogenase 2, NAD (mitochondrial) |
| predicted gene 6123; pyruvate dehydrogenase (lipoamide) beta |
| predicted gene 6835; ATP synthase, H+ transporting, mitochondrial F0 complex, subunit f, isoform 2; predicted gene 6581 |
| sideroflexin 1 |
| solute carrier family 25 (mitochondrial carrier, adenine nucleotide translocator), member 4 |
| ubiquinol-cytochrome c reductase, complex III subunit VII |
| **Endoplasmic reticulum** |
| Leucine-rich repeat-containing protein 59 OS=Mus musculus GN=Lrrc59 PE=2 SV=1 - [LRC59_MOUSE] |
| 1-acylglycerol-3-phosphate O-acyltransferase 9 |
| ATPase, Ca++ transporting, cardiac muscle, fast twitch 1 |
| SAC1 (suppressor of actin mutations 1, homolog)-like (S. cerevisiae) |
| SEC22 vesicle trafficking protein homolog B (S. cerevisiae) |
| UDP-glucose ceramide glucosyltransferase-like 1; similar to UDP-glucose ceramide glucosyltransferase-like 1 |
| alpha glucosidase 2 alpha neutral subunit |
| calreticulin |
| dolichyl-di-phosphooligosaccharide-protein glycotransferase |
| endoplasmic reticulum protein 29 |
| heat shock protein 90, beta (Grp94), member 1 |
| peptidylprolyl isomerase B |
| prolyl 4-hydroxylase, beta polypeptide |
| ribophorin II |

**Table 3.1.** Proteins associated with the D2-containing compartment. The D2-containing compartment in adipose homegenates of WT and D2 KO mice was immunoisolated using D2 antibody-cross-linked magnetic beads in detergent free buffer. The compartment was eluted using triton lysis buffer+0.5% SDS and subjected to mass spectromety analysis. Proteins detected exclusively in the WT samples but absent in the KO samples are listed in this table.

One of the proteins with the strongest association with D2 was LRRC59, which was present in all four WT samples. We next re-probed our elution fractions for LRRC59 (Fig.3.4). LRRC59 was detected in PNS and with much reduced amount in SupIP. A modest amount of LRRC59 was present in E1 and E3 and most eluted in E2. These data support strong association of LRRC59 with D2 in adipose peroxisomes.

**Discussion**

In this study, we have shown that D2 is localized in a subclass of peroxisomes that is potentially associated with mitochondria and ER in mouse adipose tissue. To the best of our knowledge, this is the first report that describes the subcellular localization of D2 in mouse adipose tissues.

Our findings indicate that the D2-containing compartment harbors peroxisomal proteins but at the same time lacks some of the well-established markers, therefore distinguishing itself as a subclass of peroxisomes. As early as 1980, the concept of 'microperoxisomes' was proposed with evidence showing their close association with lipid droplets and ER in cultured adipocytes [203]. However, their biological characteristics and functions in adipose tissue have long remained undescribed. In recent years, there has been reemerging interest in the study of these organelles with the discovery that peroxisome dysfunction leads to a series of adipose phenotypes [253, 254]. These findings are generally obtained from peroxin deficient mouse models in which peroxisomal membrane protein assembly is disrupted. In these studies, peroxisomes were not further categorized and no attempt was made to assess tissue-specific effects of peroxisome dysfunction. Our results suggest the existence of distinct subclasses of peroxisomes

within adipose, suggesting that even within a given tissue, peroxisome function may be differentially affected.

D2 has been shown to play essential roles in lipid metabolism [241, 248, 282, 283]. However, D2 is not highly expressed in tissues characterized with high rates of β-oxidation metabolisms, such as liver, heart or skeletal muscle, but is most abundant in white adipose tissue [241]. Given that white adipose is far less metabolically active and contains fewer peroxisomes than liver, the need for such high levels of D2 in adipose is unclear. D2 has been shown to be critical for erucic acid catabolism in mice [283]. However, erucic acid is present in trace amounts in most plant and seed oils, suggesting other essential functions of D2 in endobiotic and xenobiotic metabolism [283]. Given the distinct substrate specificities of peroxisomal transporters, the D2-compartment may differ from other peroxisomes with its unique substrate selection.

Our findings suggest a close relationship between D2-containing peroxisomes and mitochondria and ER. Using immunoisolation approach combined with mass spectrometric, we purified a D2 containing compartments from adipose tissue and determined its proteomic profile. Besides peroxisomal proteins, we also identified mitochondrial and ER proteins. This is consistent with emerging evidence indicating that peroxisomes, mitochondria and ER may be physically associated with each other [210, 288]. Peroxisomes share key components of division machinery with mitochondria in both mammalian cells and yeast [289, 290]. The movement of peroxisomes is coupled with mitochondria but independent of cytoskeleton during cell division in yeast [291]. Peroxisomes derive a portion of their components from mitochondria through a vesicular

transport pathway [292]. The physiological function of this pathway is still unknown, but might involve the transport of lipid metabolites and proteins.

There is also growing evidence suggesting that peroxisomes may form out of ER in a 'budding' pattern and derive some of their proteins and membranes through this mechanism [210]. Vesicles originating from ER were shown to be routed to peroxisomes with the assistance of Pex16 or Pex3 and the ER budding factor Sec16b in human fibroblasts [293-295]. These vesicular structures were referred as 'preperoxisomes' and two biochemically distinct populations have been identified [210]. Preperoxisomes must fuse with other more mature peroxisomes to generate functional organelles [210, 296]. Therefore, there are at least four subpopulations of peroxisomes present within a cell: the two distinct preperoxisomes, the more mature but not fully functional peroxisomes, and the fully mature and functional peroxisomes. However, no attempt has been made to characterize the complete proteomes of these organelles. The D2-containing peroxisome in adipose may be categorized into one of the first three subgroups or even distinguish itself as another subclass of peroxisomes unique to adipocytes.

Finally, we observed that the putative trafficking protein, LRRC59, is closely associated with D2-containing compartment. The biological function of LRRC59 is still poorly understood. A recent report indicates the interaction of LRRC59 with Selenoprotein S (SelS), an ER protein involved in the protein retro-translocation from ER to cytosol and the inflammatory response [297-299]. However, the influence of LRRC59 on SelfS functions was not further investigated [299]. Nonetheless, their interaction indicates a potential role of LRRC59 in the trafficking vesicles originating from the ER. The interaction of LRRC59 and D2 suggests the possible origin of some components of the

D2-conatining peroxisome from the ER. Another group reported that LRRC59 facilitates the intracellular trafficking of fibroblast growth factor 1 (FGF1) into nucleus in cultured cells [284]. Given the importance of FGF1-PPARγ signaling axis in adipocyte metabolism, LRRC59 may be essential for normal adipose functions [300]. Its association with D2 may potentially bridge D2 dependent lipid metabolism and FGF1 signaling in adipose tissue.

# CHAPTER 4. SUMMARY AND CONCLUSION

Of the three identified peroxisomal ABC transporters, ABCD2 is the only one whose functions are still largely unexplored and deserving of more attention. Two fundamental questions need to be addressed to better characterize this transporter: What is its function? Where is it located intracellularly? The work presented in this dissertation will provide some valuable hints on the answers.

The first goal of studies was to determine the role of D2 in modulating PPARα signaling and the impact of D2 on response to PPARα agonist treatment. First, we studied the impact of D2 on response to PPARα agonist fenofibrate treatment in normal mouse model. Based on the microarray analysis, we discovered that various gene pathways were differentially influenced by D2 genotype and fenofibrate. One of the most influenced pathways was the PPAR signaling pathway. Although D2 has long been known as a PPARα target gene, this is the first report to show that lack of D2 reciprocally impacted on PPARα signaling. Next, we examined the effect of D2 on fenofibrate response in cultured 3T3-L1 adipocytes. Fenofibrate treatment induced the expression of PPARα and some of its downstream target genes. This response was blunted by loss of D2 in D2 deficient cells, suggesting D2 modulates genomic response to fibrate by influencing the expression of some of the genes in PPAR signaling pathway. Then, we evaluated the influence of D2 on the lipid-lowering effects of fenofibrate in a mouse model of diet induced obesity. Fenofibrate was effective in controlling the body weight and plasma lipid profiles. Interestingly, the TG secretion rates in D2 KO mice were significantly lower in both treated and control groups. However, it was not sufficient to alter the

overall effects of fenofibrate therapy. Lastly, we looked at the relationship of D2 polymorphism and fenofibrate hypolipidemic effects in humans, but detected no significant correlation.

Our studies have clearly demonstrated the importance of D2 in modulating PPARα signaling. To the best of our knowledge, this is the first report to demonstrate the reciprocal impact of D2 on PPARα signaling. D2 dependent lipid metabolism may impact the endogenous lipid pool and therefore alter the available ligands for PPARα. The differences between genotypes in measured parameters were more evident in untreated group, suggesting the influence may be masked when exogenous ligands are present with considerable amount.

A second goal of studies was to determine the subcellular localization of D2 in mouse adipose tissue and to characterize the D2-containing organelle.

First, we examined the intracellular distribution of D2 within mouse adipocytes using immunofluorescent microscopy. D2 has been known to be most abundantly expressed in adipose tissues. In this study, we discovered a punctuate pattern of D2 distribution surrounding the central lipid droplets within adipocytes. Next, we determined the subcellular localization of D2 using a biochemical approach and discovered that the D2 enriched subcellular fraction didn't have some well-established peroxisomal markers such as catalase and pex19. This indicates D2 may be localized to a subclass of peroxisomes that didn't harbor those markers. Then, using histological and gold labeled immunostaining approach, we verified the distinct localizations of D2 and Pex10 in intact mouse adipose. Lastly, we isolated the D2-containing peroxisome from adipose

homogenates and analyzed its proteomic profile. We discovered a close relationship between this subtype of peroxisome and mitochondria and ER.

Our studies have demonstrated the subcellular localization of D2 in a subclass of peroxisomes. These peroxisomes have a typical structure of microperoxisomes under the electron microscope but lack some well-established marker proteins. These characteristics distinguish it as a unique subclass of peroxisomes that have not been reported before. Proteomic analysis revealed their association with other subcellular organelles including mitochondria and ER. With all the emerging evidence indicating metabolic interplay between these organelles, our findings emphasize the necessity for further investigation of peroxisome dynamics and metabolisms.

In conclusion, the research demonstrated a novel role of D2 in modulating PPARα signaling and fenofibrate response both in vitro and in vivo. The studies also revealed the existence of D2-containing compartments in mouse adipose tissue that potentially represents a subclass of peroxisomes. Further investigation is necessary to elucidate the mechanism by which D2 influences PPARα signaling and to further characterize the D2-containing peroxisome and its relation with other subcellular organelles.

# REFERENCES


1. Zimmet, P., K.G. Alberti, and M. Serrano Rios, *A New International Diabetes Federation (IDF) Worldwide Definition of the Metabolic Syndrome: the Rationale and the Results.* Rev Esp Cardiol (Engl Ed), 2005. **58**(12): p. 1371-5.
2. Alberti, K.G. and P.Z. Zimmet, *Definition, diagnosis and classification of diabetes mellitus and its complications. Part 1: diagnosis and classification of diabetes mellitus provisional report of a WHO consultation.* Diabet Med, 1998. **15**(7): p. 539-53.
3. Balkau, B. and M.A. Charles, *Comment on the provisional report from the WHO consultation. European Group for the Study of Insulin Resistance (EGIR).* Diabet Med, 1999. **16**(5): p. 442-3.
4. Expert Panel on Detection, E. and A. Treatment of High Blood Cholesterol in, *Executive Summary of The Third Report of The National Cholesterol Education Program (NCEP) Expert Panel on Detection, Evaluation, And Treatment of High Blood Cholesterol In Adults (Adult Treatment Panel III).* JAMA, 2001. **285**(19): p. 2486-97.
5. Einhorn, D., et al., *American College of Endocrinology position statement on the insulin resistance syndrome.* Endocr Pract, 2003. **9**(3): p. 237-52.
6. Beltran-Sanchez, H., et al., *Prevalence and trends of metabolic syndrome in the adult U.S. population, 1999-2010.* J Am Coll Cardiol, 2013. **62**(8): p. 697-703.
7. van Vliet-Ostaptchouk, J.V., et al., *The prevalence of metabolic syndrome and metabolically healthy obesity in Europe: a collaborative analysis of ten large cohort studies.* BMC Endocr Disord, 2014. **14**(1): p. 9.
8. Desroches, S. and B. Lamarche, *The evolving definitions and increasing prevalence of the metabolic syndrome.* Appl Physiol Nutr Metab, 2007. **32**(1): p. 23-32.
9. Cameron, A.J., J.E. Shaw, and P.Z. Zimmet, *The metabolic syndrome: prevalence in worldwide populations.* Endocrinol Metab Clin North Am, 2004. **33**(2): p. 351-75, table of contents.
10. Park, Y.W., et al., *The metabolic syndrome: prevalence and associated risk factor findings in the US population from the Third National Health and Nutrition Examination Survey, 1988-1994.* Arch Intern Med, 2003. **163**(4): p. 427-36.
11. Ervin, R.B., *Prevalence of metabolic syndrome among adults 20 years of age and over, by sex, age, race and ethnicity, and body mass index: United States, 2003-2006.* Natl Health Stat Report, 2009(13): p. 1-7.
12. Kaur, J., *A Comprehensive Review on Metabolic Syndrome.* Cardiol Res Pract, 2014. **2014**: p. 943162.
13. Abbasi, F., et al., *Relationship between obesity, insulin resistance, and coronary heart disease risk.* J Am Coll Cardiol, 2002. **40**(5): p. 937-43.
14. Despres, J.P., et al., *Regional distribution of body fat, plasma lipoproteins, and cardiovascular disease.* Arteriosclerosis, 1990. **10**(4): p. 497-511.
15. Despres, J.P., *Is visceral obesity the cause of the metabolic syndrome?* Ann Med, 2006. **38**(1): p. 52-63.
16. Mittelman, S.D., et al., *Extreme insulin resistance of the central adipose depot in vivo.* Diabetes, 2002. **51**(3): p. 755-61.
17. Mauriege, P., et al., *Regional variation in adipose tissue metabolism of severely obese premenopausal women.* J Lipid Res, 1995. **36**(4): p. 672-84.
18. Bergman, R.N., et al., *Why visceral fat is bad: mechanisms of the metabolic syndrome.* Obesity (Silver Spring), 2006. **14 Suppl 1**: p. 16S-19S.

19. Jensen, M.D., *Is visceral fat involved in the pathogenesis of the metabolic syndrome? Human model.* Obesity (Silver Spring), 2006. **14 Suppl 1**: p. 20S-24S.
20. Boden, G., et al., *Effects of acute changes of plasma free fatty acids on intramyocellular fat content and insulin resistance in healthy subjects.* Diabetes, 2001. **50**(7): p. 1612-7.
21. Despres, J.P. and I. Lemieux, *Abdominal obesity and metabolic syndrome.* Nature, 2006. **444**(7121): p. 881-7.
22. Kershaw, E.E. and J.S. Flier, *Adipose tissue as an endocrine organ.* J Clin Endocrinol Metab, 2004. **89**(6): p. 2548-56.
23. Cote, M., et al., *Adiponectinemia in visceral obesity: impact on glucose tolerance and plasma lipoprotein and lipid levels in men.* J Clin Endocrinol Metab, 2005. **90**(3): p. 1434-9.
24. Ridker, P.M., et al., *C-reactive protein, the metabolic syndrome, and risk of incident cardiovascular events: an 8-year follow-up of 14 719 initially healthy American women.* Circulation, 2003. **107**(3): p. 391-7.
25. Xydakis, A.M., et al., *Adiponectin, inflammation, and the expression of the metabolic syndrome in obese individuals: the impact of rapid weight loss through caloric restriction.* J Clin Endocrinol Metab, 2004. **89**(6): p. 2697-703.
26. Hotamisligil, G.S., et al., *IRS-1-mediated inhibition of insulin receptor tyrosine kinase activity in TNF-alpha- and obesity-induced insulin resistance.* Science, 1996. **271**(5249): p. 665-8.
27. Krauss, R.M., *Lipids and lipoproteins in patients with type 2 diabetes.* Diabetes Care, 2004. **27**(6): p. 1496-504.
28. Diamant, M., et al., *The association between abdominal visceral fat and carotid stiffness is mediated by circulating inflammatory markers in uncomplicated type 2 diabetes.* J Clin Endocrinol Metab, 2005. **90**(3): p. 1495-501.
29. Pischon, T., et al., *Plasma adiponectin levels and risk of myocardial infarction in men.* JAMA, 2004. **291**(14): p. 1730-7.
30. Eckel, R.H., S.M. Grundy, and P.Z. Zimmet, *The metabolic syndrome.* Lancet, 2005. **365**(9468): p. 1415-28.
31. Liu, M. and F. Liu, *Transcriptional and post-translational regulation of adiponectin.* Biochem J, 2010. **425**(1): p. 41-52.
32. Ouchi, N., et al., *Adiponectin, an adipocyte-derived plasma protein, inhibits endothelial NF-kappaB signaling through a cAMP-dependent pathway.* Circulation, 2000. **102**(11): p. 1296-301.
33. Wilson, C., *Diabetes: ACCORD: 5-year outcomes of intensive glycemic control.* Nat Rev Endocrinol, 2011. **7**(6): p. 314.
34. Samuel, V.T. and G.I. Shulman, *Mechanisms for insulin resistance: common threads and missing links.* Cell, 2012. **148**(5): p. 852-71.
35. Randle, P.J., et al., *The glucose fatty-acid cycle. Its role in insulin sensitivity and the metabolic disturbances of diabetes mellitus.* Lancet, 1963. **1**(7285): p. 785-9.
36. Jucker, B.M., et al., *13C and 31P NMR studies on the effects of increased plasma free fatty acids on intramuscular glucose metabolism in the awake rat.* J Biol Chem, 1997. **272**(16): p. 10464-73.
37. Cline, G.W., et al., *Impaired glucose transport as a cause of decreased insulin-stimulated muscle glycogen synthesis in type 2 diabetes.* N Engl J Med, 1999. **341**(4): p. 240-6.
38. Griffin, M.E., et al., *Free fatty acid-induced insulin resistance is associated with activation of protein kinase C theta and alterations in the insulin signaling cascade.* Diabetes, 1999. **48**(6): p. 1270-4.

39. Krssak, M., et al., *Intramuscular glycogen and intramyocellular lipid utilization during prolonged exercise and recovery in man: a 13C and 1H nuclear magnetic resonance spectroscopy study.* J Clin Endocrinol Metab, 2000. **85**(2): p. 748-54.
40. Dresner, A., et al., *Effects of free fatty acids on glucose transport and IRS-1-associated phosphatidylinositol 3-kinase activity.* J Clin Invest, 1999. **103**(2): p. 253-9.
41. Yu, C., et al., *Mechanism by which fatty acids inhibit insulin activation of insulin receptor substrate-1 (IRS-1)-associated phosphatidylinositol 3-kinase activity in muscle.* J Biol Chem, 2002. **277**(52): p. 50230-6.
42. Itani, S.I., et al., *Lipid-induced insulin resistance in human muscle is associated with changes in diacylglycerol, protein kinase C, and IkappaB-alpha.* Diabetes, 2002. **51**(7): p. 2005-11.
43. Lim, E.L., et al., *Reversal of type 2 diabetes: normalisation of beta cell function in association with decreased pancreas and liver triacylglycerol.* Diabetologia, 2011. **54**(10): p. 2506-14.
44. Petersen, K.F., et al., *Reversal of nonalcoholic hepatic steatosis, hepatic insulin resistance, and hyperglycemia by moderate weight reduction in patients with type 2 diabetes.* Diabetes, 2005. **54**(3): p. 603-8.
45. Kim, J.K., et al., *Tissue-specific overexpression of lipoprotein lipase causes tissue-specific insulin resistance.* Proc Natl Acad Sci U S A, 2001. **98**(13): p. 7522-7.
46. Merkel, M., et al., *Lipoprotein lipase expression exclusively in liver. A mouse model for metabolism in the neonatal period and during cachexia.* J Clin Invest, 1998. **102**(5): p. 893-901.
47. Koonen, D.P., et al., *Increased hepatic CD36 expression contributes to dyslipidemia associated with diet-induced obesity.* Diabetes, 2007. **56**(12): p. 2863-71.
48. Falcon, A., et al., *FATP2 is a hepatic fatty acid transporter and peroxisomal very long-chain acyl-CoA synthetase.* Am J Physiol Endocrinol Metab, 2010. **299**(3): p. E384-93.
49. Doege, H., et al., *Silencing of hepatic fatty acid transporter protein 5 in vivo reverses diet-induced non-alcoholic fatty liver disease and improves hyperglycemia.* J Biol Chem, 2008. **283**(32): p. 22186-92.
50. Ferrannini, E. and A. Natali, *Essential hypertension, metabolic disorders, and insulin resistance.* Am Heart J, 1991. **121**(4 Pt 2): p. 1274-82.
51. Landsberg, L., et al., *Obesity-related hypertension: pathogenesis, cardiovascular risk, and treatment--a position paper of the The Obesity Society and The American Society of Hypertension.* Obesity (Silver Spring), 2013. **21**(1): p. 8-24.
52. Rowe, J.W., et al., *Effect of insulin and glucose infusions on sympathetic nervous system activity in normal man.* Diabetes, 1981. **30**(3): p. 219-25.
53. Landsberg, L., et al., *Obesity, blood pressure, and the sympathetic nervous system.* Ann Epidemiol, 1991. **1**(4): p. 295-303.
54. Troisi, R.J., et al., *Relation of obesity and diet to sympathetic nervous system activity.* Hypertension, 1991. **17**(5): p. 669-77.
55. Grassi, G., et al., *Body weight reduction, sympathetic nerve traffic, and arterial baroreflex in obese normotensive humans.* Circulation, 1998. **97**(20): p. 2037-42.
56. Malhotra, A., et al., *Angiotensin II promotes glucose-induced activation of cardiac protein kinase C isozymes and phosphorylation of troponin I.* Diabetes, 2001. **50**(8): p. 1918-26.
57. Austin, M.A., et al., *Atherogenic lipoprotein phenotype. A proposed genetic marker for coronary heart disease risk.* Circulation, 1990. **82**(2): p. 495-506.

58. Reaven, G.M., et al., *Insulin resistance and hyperinsulinemia in individuals with small, dense low density lipoprotein particles.* J Clin Invest, 1993. **92**(1): p. 141-6.
59. Kathiresan, S., et al., *Increased small low-density lipoprotein particle number: a prominent feature of the metabolic syndrome in the Framingham Heart Study.* Circulation, 2006. **113**(1): p. 20-9.
60. National Cholesterol Education Program Expert Panel on Detection, E. and A. Treatment of High Blood Cholesterol in, *Third Report of the National Cholesterol Education Program (NCEP) Expert Panel on Detection, Evaluation, and Treatment of High Blood Cholesterol in Adults (Adult Treatment Panel III) final report.* Circulation, 2002. **106**(25): p. 3143-421.
61. Toth, P.P., *Drug treatment of hyperlipidaemia: a guide to the rational use of lipid-lowering drugs.* Drugs, 2010. **70**(11): p. 1363-79.
62. Toth, P.P. and M.H. Davidson, *High-dose statin therapy: benefits and safety in aggressive lipid lowering.* J Fam Pract, 2008. **57**(5 Suppl High-Dose): p. S29-36.
63. Altmann, S.W., et al., *Niemann-Pick C1 Like 1 protein is critical for intestinal cholesterol absorption.* Science, 2004. **303**(5661): p. 1201-4.
64. Kastelein, J.J., et al., *Simvastatin with or without ezetimibe in familial hypercholesterolemia.* N Engl J Med, 2008. **358**(14): p. 1431-43.
65. Bruckert, E., P. Giral, and P. Tellier, *Perspectives in cholesterol-lowering therapy: the role of ezetimibe, a new selective inhibitor of intestinal cholesterol absorption.* Circulation, 2003. **107**(25): p. 3124-8.
66. Davidson, M.H., et al., *Ezetimibe coadministered with simvastatin in patients with primary hypercholesterolemia.* J Am Coll Cardiol, 2002. **40**(12): p. 2125-34.
67. Villines, T.C., et al., *Niacin: the evidence, clinical use, and future directions.* Curr Atheroscler Rep, 2012. **14**(1): p. 49-59.
68. *Clofibrate and niacin in coronary heart disease.* JAMA, 1975. **231**(4): p. 360-81.
69. Bruckert, E., J. Labreuche, and P. Amarenco, *Meta-analysis of the effect of nicotinic acid alone or in combination on cardiovascular events and atherosclerosis.* Atherosclerosis, 2010. **210**(2): p. 353-61.
70. Lamon-Fava, S., et al., *Extended-release niacin alters the metabolism of plasma apolipoprotein (Apo) A-I and ApoB-containing lipoproteins.* Arterioscler Thromb Vasc Biol, 2008. **28**(9): p. 1672-8.
71. Kamanna, V.S. and M.L. Kashyap, *Nicotinic acid (niacin) receptor agonists: will they be useful therapeutic agents?* Am J Cardiol, 2007. **100**(11 A): p. S53-61.
72. Tunaru, S., et al., *PUMA-G and HM74 are receptors for nicotinic acid and mediate its anti-lipolytic effect.* Nat Med, 2003. **9**(3): p. 352-5.
73. Kamanna, V.S., S.H. Ganji, and M.L. Kashyap, *Recent advances in niacin and lipid metabolism.* Curr Opin Lipidol, 2013. **24**(3): p. 239-45.
74. Desvergne, B. and W. Wahli, *Peroxisome proliferator-activated receptors: nuclear control of metabolism.* Endocr Rev, 1999. **20**(5): p. 649-88.
75. Lee, C.H., P. Olson, and R.M. Evans, *Minireview: lipid metabolism, metabolic diseases, and peroxisome proliferator-activated receptors.* Endocrinology, 2003. **144**(6): p. 2201-7.
76. De Duve, C., *Evolution of the peroxisome.* Ann N Y Acad Sci, 1969. **168**(2): p. 369-81.
77. Issemann, I. and S. Green, *Activation of a member of the steroid hormone receptor superfamily by peroxisome proliferators.* Nature, 1990. **347**(6294): p. 645-50.
78. Dreyer, C., et al., *Control of the peroxisomal beta-oxidation pathway by a novel family of nuclear hormone receptors.* Cell, 1992. **68**(5): p. 879-87.

79. Feige, J.N., et al., *From molecular action to physiological outputs: peroxisome proliferator-activated receptors are nuclear receptors at the crossroads of key cellular functions.* Prog Lipid Res, 2006. **45**(2): p. 120-59.
80. Michalik, L., et al., *International Union of Pharmacology. LXI. Peroxisome proliferator-activated receptors.* Pharmacol Rev, 2006. **58**(4): p. 726-41.
81. Rosen, E.D., et al., *Transcriptional regulation of adipogenesis.* Genes Dev, 2000. **14**(11): p. 1293-307.
82. Werman, A., et al., *Ligand-independent activation domain in the N terminus of peroxisome proliferator-activated receptor gamma (PPARgamma). Differential activity of PPARgamma1 and -2 isoforms and influence of insulin.* J Biol Chem, 1997. **272**(32): p. 20230-5.
83. Kliewer, S.A., et al., *Convergence of 9-cis retinoic acid and peroxisome proliferator signalling pathways through heterodimer formation of their receptors.* Nature, 1992. **358**(6389): p. 771-4.
84. Berger, J. and D.E. Moller, *The mechanisms of action of PPARs.* Annu Rev Med, 2002. **53**: p. 409-35.
85. Monsalve, F.A., et al., *Peroxisome proliferator-activated receptor targets for the treatment of metabolic diseases.* Mediators Inflamm, 2013. **2013**: p. 549627.
86. Horlein, A.J., et al., *Ligand-independent repression by the thyroid hormone receptor mediated by a nuclear receptor co-repressor.* Nature, 1995. **377**(6548): p. 397-404.
87. Chen, J.D. and R.M. Evans, *A transcriptional co-repressor that interacts with nuclear hormone receptors.* Nature, 1995. **377**(6548): p. 454-7.
88. Zhu, Y., et al., *Cloning and identification of mouse steroid receptor coactivator-1 (mSRC-1), as a coactivator of peroxisome proliferator-activated receptor gamma.* Gene Expr, 1996. **6**(3): p. 185-95.
89. Zhu, Y., et al., *Isolation and characterization of PBP, a protein that interacts with peroxisome proliferator-activated receptor.* J Biol Chem, 1997. **272**(41): p. 25500-6.
90. Tontonoz, P. and B.M. Spiegelman, *Fat and beyond: the diverse biology of PPARgamma.* Annu Rev Biochem, 2008. **77**: p. 289-312.
91. Fajas, L., et al., *The organization, promoter analysis, and expression of the human PPARgamma gene.* J Biol Chem, 1997. **272**(30): p. 18779-89.
92. Fajas, L., J.C. Fruchart, and J. Auwerx, *PPARgamma3 mRNA: a distinct PPARgamma mRNA subtype transcribed from an independent promoter.* FEBS Lett, 1998. **438**(1-2): p. 55-60.
93. Ricote, M., et al., *Expression of the peroxisome proliferator-activated receptor gamma (PPARgamma) in human atherosclerosis and regulation in macrophages by colony stimulating factors and oxidized low density lipoprotein.* Proc Natl Acad Sci U S A, 1998. **95**(13): p. 7614-9.
94. Braissant, O., et al., *Differential expression of peroxisome proliferator-activated receptors (PPARs): tissue distribution of PPAR-alpha, -beta, and -gamma in the adult rat.* Endocrinology, 1996. **137**(1): p. 354-66.
95. Rosen, E.D., et al., *C/EBPalpha induces adipogenesis through PPARgamma: a unified pathway.* Genes Dev, 2002. **16**(1): p. 22-6.
96. Kliewer, S.A., et al., *Fatty acids and eicosanoids regulate gene expression through direct interactions with peroxisome proliferator-activated receptors alpha and gamma.* Proc Natl Acad Sci U S A, 1997. **94**(9): p. 4318-23.
97. Nagy, L., et al., *Oxidized LDL regulates macrophage gene expression through ligand activation of PPARgamma.* Cell, 1998. **93**(2): p. 229-40.

98. Schopfer, F.J., et al., *Nitrolinoleic acid: an endogenous peroxisome proliferator-activated receptor gamma ligand.* Proc Natl Acad Sci U S A, 2005. **102**(7): p. 2340-5.
99. Zhang, C., et al., *Lysophosphatidic acid induces neointima formation through PPARgamma activation.* J Exp Med, 2004. **199**(6): p. 763-74.
100. Nolan, J.J., et al., *Improvement in glucose tolerance and insulin resistance in obese subjects treated with troglitazone.* N Engl J Med, 1994. **331**(18): p. 1188-93.
101. Rangwala, S.M. and M.A. Lazar, *Peroxisome proliferator-activated receptor gamma in diabetes and metabolism.* Trends Pharmacol Sci, 2004. **25**(6): p. 331-6.
102. Ye, J.M., et al., *Direct demonstration of lipid sequestration as a mechanism by which rosiglitazone prevents fatty-acid-induced insulin resistance in the rat: comparison with metformin.* Diabetologia, 2004. **47**(7): p. 1306-13.
103. Hu, E., P. Liang, and B.M. Spiegelman, *AdipoQ is a novel adipose-specific gene dysregulated in obesity.* J Biol Chem, 1996. **271**(18): p. 10697-703.
104. Yu, J.G., et al., *The effect of thiazolidinediones on plasma adiponectin levels in normal, obese, and type 2 diabetic subjects.* Diabetes, 2002. **51**(10): p. 2968-74.
105. Pajvani, U.B., et al., *Complex distribution, not absolute amount of adiponectin, correlates with thiazolidinedione-mediated improvement in insulin sensitivity.* J Biol Chem, 2004. **279**(13): p. 12152-62.
106. Steppan, C.M., et al., *The hormone resistin links obesity to diabetes.* Nature, 2001. **409**(6818): p. 307-12.
107. Girroir, E.E., et al., *Quantitative expression patterns of peroxisome proliferator-activated receptor-beta/delta (PPARbeta/delta) protein in mice.* Biochem Biophys Res Commun, 2008. **371**(3): p. 456-61.
108. Bishop-Bailey, D., *Peroxisome proliferator-activated receptors in the cardiovascular system.* Br J Pharmacol, 2000. **129**(5): p. 823-34.
109. Oliver, W.R., Jr., et al., *A selective peroxisome proliferator-activated receptor delta agonist promotes reverse cholesterol transport.* Proc Natl Acad Sci U S A, 2001. **98**(9): p. 5306-11.
110. Skogsberg, J., et al., *Evidence that peroxisome proliferator-activated receptor delta influences cholesterol metabolism in men.* Arterioscler Thromb Vasc Biol, 2003. **23**(4): p. 637-43.
111. Gouni-Berthold, I., et al., *The peroxisome proliferator-activated receptor delta +294T/C polymorphism in relation to lipoprotein metabolism in patients with diabetes mellitus type 2 and in non-diabetic controls.* Atherosclerosis, 2005. **183**(2): p. 336-41.
112. Auboeuf, D., et al., *Tissue distribution and quantification of the expression of mRNAs of peroxisome proliferator-activated receptors and liver X receptor-alpha in humans: no alteration in adipose tissue of obese and NIDDM patients.* Diabetes, 1997. **46**(8): p. 1319-27.
113. Marx, N., et al., *PPAR activators as antiinflammatory mediators in human T lymphocytes: implications for atherosclerosis and transplantation-associated arteriosclerosis.* Circ Res, 2002. **90**(6): p. 703-10.
114. Chinetti, G., et al., *Activation of proliferator-activated receptors alpha and gamma induces apoptosis of human monocyte-derived macrophages.* J Biol Chem, 1998. **273**(40): p. 25573-80.
115. Escher, P., et al., *Rat PPARs: quantitative analysis in adult rat tissues and regulation in fasting and refeeding.* Endocrinology, 2001. **142**(10): p. 4195-202.
116. Bookout, A.L., et al., *Anatomical profiling of nuclear receptor expression reveals a hierarchical transcriptional network.* Cell, 2006. **126**(4): p. 789-99.

117. Guan, Y., Y. Zhang, and M.D. Breyer, *The Role of PPARs in the Transcriptional Control of Cellular Processes.* Drug News Perspect, 2002. **15**(3): p. 147-154.
118. Neve, B.P., J.C. Fruchart, and B. Staels, *Role of the peroxisome proliferator-activated receptors (PPAR) in atherosclerosis.* Biochem Pharmacol, 2000. **60**(8): p. 1245-50.
119. Vanden Heuvel, J.P., et al., *Comprehensive analysis of gene expression in rat and human hepatoma cells exposed to the peroxisome proliferator WY14,643.* Toxicol Appl Pharmacol, 2003. **188**(3): p. 185-98.
120. Aoyama, T., et al., *Altered constitutive expression of fatty acid-metabolizing enzymes in mice lacking the peroxisome proliferator-activated receptor alpha (PPARalpha).* J Biol Chem, 1998. **273**(10): p. 5678-84.
121. Richert, L., et al., *Effects of clofibric acid on mRNA expression profiles in primary cultures of rat, mouse and human hepatocytes.* Toxicol Appl Pharmacol, 2003. **191**(2): p. 130-46.
122. Rakhshandehroo, M., et al., *Comprehensive analysis of PPARalpha-dependent regulation of hepatic lipid metabolism by expression profiling.* PPAR Res, 2007. **2007**: p. 26839.
123. Leone, T.C., C.J. Weinheimer, and D.P. Kelly, *A critical role for the peroxisome proliferator-activated receptor alpha (PPARalpha) in the cellular fasting response: the PPARalpha-null mouse as a model of fatty acid oxidation disorders.* Proc Natl Acad Sci U S A, 1999. **96**(13): p. 7473-8.
124. Rakhshandehroo, M., et al., *Comparative analysis of gene regulation by the transcription factor PPARalpha between mouse and human.* PLoS One, 2009. **4**(8): p. e6796.
125. Goldberg, C., *The pursuit of the fictional self.* Am J Psychother, 2004. **58**(2): p. 209-19.
126. Corton, J.C., et al., *Peroxisome proliferators alter the expression of estrogen-metabolizing enzymes.* Biochimie, 1997. **79**(2-3): p. 151-62.
127. Alvares, K., et al., *An upstream region of the enoyl-coenzyme A hydratase/3-hydroxyacyl-coenzyme A dehydrogenase gene directs luciferase expression in liver in response to peroxisome proliferators in transgenic mice.* Cancer Res, 1994. **54**(9): p. 2303-6.
128. Guo, Y., et al., *Underlying mechanisms of pharmacology and toxicity of a novel PPAR agonist revealed using rodent and canine hepatocytes.* Toxicol Sci, 2007. **96**(2): p. 294-309.
129. Hashimoto, T., et al., *Peroxisomal and mitochondrial fatty acid beta-oxidation in mice nullizygous for both peroxisome proliferator-activated receptor alpha and peroxisomal fatty acyl-CoA oxidase. Genotype correlation with fatty liver phenotype.* J Biol Chem, 1999. **274**(27): p. 19228-36.
130. Fourcade, S., et al., *Fibrate induction of the adrenoleukodystrophy-related gene (ABCD2): promoter analysis and role of the peroxisome proliferator-activated receptor PPARalpha.* Eur J Biochem, 2001. **268**(12): p. 3490-500.
131. Hunt, M.C., et al., *Characterization of an acyl-coA thioesterase that functions as a major regulator of peroxisomal lipid metabolism.* J Biol Chem, 2002. **277**(2): p. 1128-38.
132. Kersten, S., et al., *Peroxisome proliferator-activated receptor alpha mediates the adaptive response to fasting.* J Clin Invest, 1999. **103**(11): p. 1489-98.
133. Guo, L., et al., *Differential gene expression in mouse primary hepatocytes exposed to the peroxisome proliferator-activated receptor alpha agonists.* BMC Bioinformatics, 2006. **7 Suppl 2**: p. S18.
134. Yamazaki, K., J. Kuromitsu, and I. Tanaka, *Microarray analysis of gene expression changes in mouse liver induced by peroxisome proliferator- activated receptor alpha agonists.* Biochem Biophys Res Commun, 2002. **290**(3): p. 1114-22.

135. Kelly, L.J., et al., *Peroxisome proliferator-activated receptors gamma and alpha mediate in vivo regulation of uncoupling protein (UCP-1, UCP-2, UCP-3) gene expression.* Endocrinology, 1998. **139**(12): p. 4920-7.
136. Armstrong, M.B. and H.C. Towle, *Polyunsaturated fatty acids stimulate hepatic UCP-2 expression via a PPARalpha-mediated pathway.* Am J Physiol Endocrinol Metab, 2001. **281**(6): p. E1197-204.
137. Tsuboyama-Kasaoka, N., et al., *Up-regulation of liver uncoupling protein-2 mRNA by either fish oil feeding or fibrate administration in mice.* Biochem Biophys Res Commun, 1999. **257**(3): p. 879-85.
138. Jaburek, M., et al., *Hydroperoxy fatty acid cycling mediated by mitochondrial uncoupling protein UCP2.* J Biol Chem, 2004. **279**(51): p. 53097-102.
139. Schrauwen, P., et al., *Uncoupling protein 3 as a mitochondrial fatty acid anion exporter.* FASEB J, 2003. **17**(15): p. 2272-4.
140. Johnson, E.F., et al., *Role of the peroxisome proliferator-activated receptor in cytochrome P450 4A gene regulation.* FASEB J, 1996. **10**(11): p. 1241-8.
141. Honkakoski, P. and M. Negishi, *Regulation of cytochrome P450 (CYP) genes by nuclear receptors.* Biochem J, 2000. **347**(Pt 2): p. 321-37.
142. Gutgesell, A., et al., *Mouse carnitine-acylcarnitine translocase (CACT) is transcriptionally regulated by PPARalpha and PPARdelta in liver cells.* Biochim Biophys Acta, 2009. **1790**(10): p. 1206-16.
143. Cowart, L.A., et al., *The CYP4A isoforms hydroxylate epoxyeicosatrienoic acids to form high affinity peroxisome proliferator-activated receptor ligands.* J Biol Chem, 2002. **277**(38): p. 35105-12.
144. Devchand, P.R., et al., *The PPARalpha-leukotriene B4 pathway to inflammation control.* Nature, 1996. **384**(6604): p. 39-43.
145. Sanderson, L.M., et al., *Peroxisome proliferator-activated receptor beta/delta (PPARbeta/delta) but not PPARalpha serves as a plasma free fatty acid sensor in liver.* Mol Cell Biol, 2009. **29**(23): p. 6257-67.
146. Tang, C., et al., *Regulation of human delta-6 desaturase gene transcription: identification of a functional direct repeat-1 element.* J Lipid Res, 2003. **44**(4): p. 686-95.
147. Castelein, H., et al., *The peroxisome proliferator activated receptor regulates malic enzyme gene expression.* J Biol Chem, 1994. **269**(43): p. 26754-8.
148. Miller, C.W. and J.M. Ntambi, *Peroxisome proliferators induce mouse liver stearoyl-CoA desaturase 1 gene expression.* Proc Natl Acad Sci U S A, 1996. **93**(18): p. 9443-8.
149. Knight, B.L., et al., *A role for PPARalpha in the control of SREBP activity and lipid synthesis in the liver.* Biochem J, 2005. **389**(Pt 2): p. 413-21.
150. Frick, M.H., et al., *Helsinki Heart Study: primary-prevention trial with gemfibrozil in middle-aged men with dyslipidemia. Safety of treatment, changes in risk factors, and incidence of coronary heart disease.* N Engl J Med, 1987. **317**(20): p. 1237-45.
151. Rubins, H.B., et al., *Gemfibrozil for the secondary prevention of coronary heart disease in men with low levels of high-density lipoprotein cholesterol. Veterans Affairs High-Density Lipoprotein Cholesterol Intervention Trial Study Group.* N Engl J Med, 1999. **341**(6): p. 410-8.
152. Bezafibrate Infarction Prevention, s., *Secondary prevention by raising HDL cholesterol and reducing triglycerides in patients with coronary artery disease.* Circulation, 2000. **102**(1): p. 21-7.
153. Kersten, S., *Peroxisome proliferator activated receptors and lipoprotein metabolism.* PPAR Res, 2008. **2008**: p. 132960.

154. Ameen, C., et al., *Activation of peroxisome proliferator-activated receptor alpha increases the expression and activity of microsomal triglyceride transfer protein in the liver.* J Biol Chem, 2005. **280**(2): p. 1224-9.
155. Schoonjans, K., et al., *PPARalpha and PPARgamma activators direct a distinct tissue-specific transcriptional response via a PPRE in the lipoprotein lipase gene.* EMBO J, 1996. **15**(19): p. 5336-48.
156. Camps, L., et al., *Lipoprotein lipase in lungs, spleen, and liver: synthesis and distribution.* J Lipid Res, 1991. **32**(12): p. 1877-88.
157. Carroll, R. and D.L. Severson, *Peroxisome proliferator-activated receptor-alpha ligands inhibit cardiac lipoprotein lipase activity.* Am J Physiol Heart Circ Physiol, 2001. **281**(2): p. H888-94.
158. Hertz, R., J. Bishara-Shieban, and J. Bar-Tana, *Mode of action of peroxisome proliferators as hypolipidemic drugs. Suppression of apolipoprotein C-III.* J Biol Chem, 1995. **270**(22): p. 13470-5.
159. Schultze, A.E., et al., *Administration of a PPARalpha agonist increases serum apolipoprotein A-V levels and the apolipoprotein A-V/apolipoprotein C-III ratio.* J Lipid Res, 2005. **46**(8): p. 1591-5.
160. Prieur, X., H. Coste, and J.C. Rodriguez, *The human apolipoprotein AV gene is regulated by peroxisome proliferator-activated receptor-alpha and contains a novel farnesoid X-activated receptor response element.* J Biol Chem, 2003. **278**(28): p. 25468-80.
161. Vu-Dac, N., et al., *Apolipoprotein A5, a crucial determinant of plasma triglyceride levels, is highly responsive to peroxisome proliferator-activated receptor alpha activators.* J Biol Chem, 2003. **278**(20): p. 17982-5.
162. Kersten, S., et al., *Characterization of the fasting-induced adipose factor FIAF, a novel peroxisome proliferator-activated receptor target gene.* J Biol Chem, 2000. **275**(37): p. 28488-93.
163. Mandard, S., et al., *The direct peroxisome proliferator-activated receptor target fasting-induced adipose factor (FIAF/PGAR/ANGPTL4) is present in blood plasma as a truncated protein that is increased by fenofibrate treatment.* J Biol Chem, 2004. **279**(33): p. 34411-20.
164. Berthou, L., et al., *Opposite regulation of human versus mouse apolipoprotein A-I by fibrates in human apolipoprotein A-I transgenic mice.* J Clin Invest, 1996. **97**(11): p. 2408-16.
165. Lussier-Cacan, S., et al., *Lipoprotein composition changes induced by fenofibrate in dysbetalipoproteinemia type III.* Atherosclerosis, 1989. **78**(2-3): p. 167-82.
166. Vu-Dac, N., et al., *The nuclear receptors peroxisome proliferator-activated receptor alpha and Rev-erbalpha mediate the species-specific regulation of apolipoprotein A-I expression by fibrates.* J Biol Chem, 1998. **273**(40): p. 25713-20.
167. Peters, J.M., et al., *Alterations in lipoprotein metabolism in peroxisome proliferator-activated receptor alpha-deficient mice.* J Biol Chem, 1997. **272**(43): p. 27307-12.
168. Staels, B., et al., *Fibrates influence the expression of genes involved in lipoprotein metabolism in a tissue-selective manner in the rat.* Arterioscler Thromb, 1992. **12**(3): p. 286-94.
169. McKeage, K. and G.M. Keating, *Fenofibrate: a review of its use in dyslipidaemia.* Drugs, 2011. **71**(14): p. 1917-46.
170. Arakawa, R., et al., *Fenofibric acid, an active form of fenofibrate, increases apolipoprotein A-I-mediated high-density lipoprotein biogenesis by enhancing*

*transcription of ATP-binding cassette transporter A1 gene in a liver X receptor-dependent manner.* Arterioscler Thromb Vasc Biol, 2005. **25**(6): p. 1193-7.
171. Schoonjans, K., et al., *Peroxisome proliferator-activated receptors, orphans with ligands and functions.* Curr Opin Lipidol, 1997. **8**(3): p. 159-66.
172. Fruchart, J.C., *Peroxisome proliferator-activated receptor-alpha (PPARalpha): at the crossroads of obesity, diabetes and cardiovascular disease.* Atherosclerosis, 2009. **205**(1): p. 1-8.
173. Fruchart, J.C. and P. Duriez, *Mode of action of fibrates in the regulation of triglyceride and HDL-cholesterol metabolism.* Drugs Today (Barc), 2006. **42**(1): p. 39-64.
174. Haubenwallner, S., et al., *Hypolipidemic activity of select fibrates correlates to changes in hepatic apolipoprotein C-III expression: a potential physiologic basis for their mode of action.* J Lipid Res, 1995. **36**(12): p. 2541-51.
175. Schoonjans, K., B. Staels, and J. Auwerx, *The peroxisome proliferator activated receptors (PPARS) and their effects on lipid metabolism and adipocyte differentiation.* Biochim Biophys Acta, 1996. **1302**(2): p. 93-109.
176. Schoonjans, K., B. Staels, and J. Auwerx, *Role of the peroxisome proliferator-activated receptor (PPAR) in mediating the effects of fibrates and fatty acids on gene expression.* J Lipid Res, 1996. **37**(5): p. 907-25.
177. Guerin, M., et al., *Fenofibrate reduces plasma cholesteryl ester transfer from HDL to VLDL and normalizes the atherogenic, dense LDL profile in combined hyperlipidemia.* Arterioscler Thromb Vasc Biol, 1996. **16**(6): p. 763-72.
178. Caslake, M.J., et al., *Fenofibrate and LDL metabolic heterogeneity in hypercholesterolemia.* Arterioscler Thromb, 1993. **13**(5): p. 702-11.
179. Ikewaki, K., et al., *Fenofibrate effectively reduces remnants, and small dense LDL, and increases HDL particle number in hypertriglyceridemic men - a nuclear magnetic resonance study.* J Atheroscler Thromb, 2004. **11**(5): p. 278-85.
180. Winkler, K., et al., *Qualitative effect of fenofibrate and quantitative effect of atorvastatin on LDL profile in combined hyperlipidemia with dense LDL.* Exp Clin Endocrinol Diabetes, 2004. **112**(5): p. 241-7.
181. Vu-Dac, N., et al., *Fibrates increase human apolipoprotein A-II expression through activation of the peroxisome proliferator-activated receptor.* J Clin Invest, 1995. **96**(2): p. 741-50.
182. Chinetti, G., et al., *CLA-1/SR-BI is expressed in atherosclerotic lesion macrophages and regulated by activators of peroxisome proliferator-activated receptors.* Circulation, 2000. **101**(20): p. 2411-7.
183. Forcheron, F., et al., *Mechanisms of the triglyceride- and cholesterol-lowering effect of fenofibrate in hyperlipidemic type 2 diabetic patients.* Diabetes, 2002. **51**(12): p. 3486-91.
184. McPherson, R., et al., *Role of Lp A-I and Lp A-I/A-II in cholesteryl ester transfer protein-mediated neutral lipid transfer. Studies in normal subjects and in hypertriglyceridemic patients before and after fenofibrate therapy.* Arterioscler Thromb Vasc Biol, 1996. **16**(11): p. 1340-6.
185. Keech, A., et al., *Effects of long-term fenofibrate therapy on cardiovascular events in 9795 people with type 2 diabetes mellitus (the FIELD study): randomised controlled trial.* Lancet, 2005. **366**(9500): p. 1849-61.
186. Insua, A., et al., *Fenofibrate of gemfibrozil for treatment of types IIa and IIb primary hyperlipoproteinemia: a randomized, double-blind, crossover study.* Endocr Pract, 2002. **8**(2): p. 96-101.

187. Duez, H., et al., *Regulation of human apoA-I by gemfibrozil and fenofibrate through selective peroxisome proliferator-activated receptor alpha modulation.* Arterioscler Thromb Vasc Biol, 2005. **25**(3): p. 585-91.
188. Steinmetz, A., et al., *Multicenter comparison of micronized fenofibrate and simvastatin in patients with primary type IIA or IIB hyperlipoproteinemia.* J Cardiovasc Pharmacol, 1996. **27**(4): p. 563-70.
189. Farnier, M., et al., *Comparative efficacy and safety of micronized fenofibrate and simvastatin in patients with primary type IIa or IIb hyperlipidemia.* Arch Intern Med, 1994. **154**(4): p. 441-9.
190. Ducobu, J., L. VanHaelst, and H. Salomon, *Comparison of micronized fenofibrate and pravastatin in patients with primary hyperlipidemia.* J Cardiovasc Pharmacol, 2003. **41**(1): p. 60-7.
191. Despres, J.P., et al., *Effects of micronized fenofibrate versus atorvastatin in the treatment of dyslipidaemic patients with low plasma HDL-cholesterol levels: a 12-week randomized trial.* J Intern Med, 2002. **251**(6): p. 490-9.
192. Ansquer, J.C., et al., *Effects of atorvastatin 10 mg and fenofibrate 200 mg on the low-density lipoprotein profile in dyslipidemic patients: A 12-week, multicenter, randomized, open-label, parallel-group study.* Curr Ther Res Clin Exp, 2009. **70**(2): p. 71-93.
193. Malik, J., et al., *Both fenofibrate and atorvastatin improve vascular reactivity in combined hyperlipidaemia (fenofibrate versus atorvastatin trial--FAT).* Cardiovasc Res, 2001. **52**(2): p. 290-8.
194. Wi, J., et al., *Optimal pharmacologic approach to patients with hypertriglyceridemia and low high-density lipoprotein-cholesterol: randomized comparison of fenofibrate 160 mg and niacin 1500 mg.* Atherosclerosis, 2010. **213**(1): p. 235-40.
195. Group, A.S., et al., *Effects of combination lipid therapy in type 2 diabetes mellitus.* N Engl J Med, 2010. **362**(17): p. 1563-74.
196. Group, A.S., et al., *Action to Control Cardiovascular Risk in Diabetes (ACCORD) trial: design and methods.* Am J Cardiol, 2007. **99**(12A): p. 21i-33i.
197. Farnier, M., et al., *Efficacy and safety of the coadministration of ezetimibe/simvastatin with fenofibrate in patients with mixed hyperlipidemia.* Am Heart J, 2007. **153**(2): p. 335 e1-8.
198. Rhodin, J.A., *[Electron microscopy of the kidney].* Brux Med, 1959. **39**(12): p. 409-26.
199. Rhodin, J., *Electron microscopy of the kidney.* Am J Med, 1958. **24**(5): p. 661-75.
200. De Duve, C. and P. Baudhuin, *Peroxisomes (microbodies and related particles).* Physiol Rev, 1966. **46**(2): p. 323-57.
201. Fahimi, H.D., *Cytochemical localization of peroxidatic activity of catalase in rat hepatic microbodies (peroxisomes).* J Cell Biol, 1969. **43**(2): p. 275-88.
202. Novikoff, A.B. and P.M. Novikoff, *Microperoxisomes and peroxisomes in relation to lipid metabolism.* Ann N Y Acad Sci, 1982. **386**: p. 138-52.
203. Novikoff, A.B., et al., *Organelle relationships in cultured 3T3-L1 preadipocytes.* J Cell Biol, 1980. **87**(1): p. 180-96.
204. Lodhi, I.J. and C.F. Semenkovich, *Peroxisomes: a nexus for lipid metabolism and cellular signaling.* Cell Metab, 2014. **19**(3): p. 380-92.
205. Lazarow, P.B. and Y. Fujiki, *Biogenesis of peroxisomes.* Annu Rev Cell Biol, 1985. **1**: p. 489-530.
206. Legg, P.G. and R.L. Wood, *New observations on microbodies. A cytochemical study on CPIB-treated rat liver.* J Cell Biol, 1970. **45**(1): p. 118-29.

207. Reddy, J. and D. Svoboda, *Proliferation of microbodies and synthesis of catalase in rat liver. Induction in tumor-bearing host by CPIB.* Am J Pathol, 1971. **63**(1): p. 99-108.
208. Tabak, H.F., I. Braakman, and A. van der Zand, *Peroxisome formation and maintenance are dependent on the endoplasmic reticulum.* Annu Rev Biochem, 2013. **82**: p. 723-44.
209. Novikoff, P.M. and A.B. Novikoff, *Peroxisomes in absorptive cells of mammalian small intestine.* J Cell Biol, 1972. **53**(2): p. 532-60.
210. van der Zand, A., et al., *Biochemically distinct vesicles from the endoplasmic reticulum fuse to form peroxisomes.* Cell, 2012. **149**(2): p. 397-409.
211. Subramani, S., *Components involved in peroxisome import, biogenesis, proliferation, turnover, and movement.* Physiol Rev, 1998. **78**(1): p. 171-88.
212. Dimitrov, L., S.K. Lam, and R. Schekman, *The role of the endoplasmic reticulum in peroxisome biogenesis.* Cold Spring Harb Perspect Biol, 2013. **5**(5): p. a013243.
213. Holroyd, C. and R. Erdmann, *Protein translocation machineries of peroxisomes.* FEBS Lett, 2001. **501**(1): p. 6-10.
214. Jones, J.M., J.C. Morrell, and S.J. Gould, *PEX19 is a predominantly cytosolic chaperone and import receptor for class 1 peroxisomal membrane proteins.* J Cell Biol, 2004. **164**(1): p. 57-67.
215. Fang, Y., et al., *PEX3 functions as a PEX19 docking factor in the import of class I peroxisomal membrane proteins.* J Cell Biol, 2004. **164**(6): p. 863-75.
216. Matsuzaki, T. and Y. Fujiki, *The peroxisomal membrane protein import receptor Pex3p is directly transported to peroxisomes by a novel Pex19p- and Pex16p-dependent pathway.* J Cell Biol, 2008. **183**(7): p. 1275-86.
217. Gould, S.G., G.A. Keller, and S. Subramani, *Identification of a peroxisomal targeting signal at the carboxy terminus of firefly luciferase.* J Cell Biol, 1987. **105**(6 Pt 2): p. 2923-31.
218. Swinkels, B.W., et al., *A novel, cleavable peroxisomal targeting signal at the amino-terminus of the rat 3-ketoacyl-CoA thiolase.* EMBO J, 1991. **10**(11): p. 3255-62.
219. Dodt, G. and S.J. Gould, *Multiple PEX genes are required for proper subcellular distribution and stability of Pex5p, the PTS1 receptor: evidence that PTS1 protein import is mediated by a cycling receptor.* J Cell Biol, 1996. **135**(6 Pt 2): p. 1763-74.
220. Braverman, N., et al., *Human PEX7 encodes the peroxisomal PTS2 receptor and is responsible for rhizomelic chondrodysplasia punctata.* Nat Genet, 1997. **15**(4): p. 369-76.
221. Liu, X., C. Ma, and S. Subramani, *Recent advances in peroxisomal matrix protein import.* Curr Opin Cell Biol, 2012. **24**(4): p. 484-9.
222. Osumi, T. and T. Hashimoto, *Purification and properties of mitochondrial and peroxisomal 3-hydroxyacyl-CoA dehydrogenase from rat liver.* Arch Biochem Biophys, 1980. **203**(1): p. 372-83.
223. Vanhove, G.F., et al., *The CoA esters of 2-methyl-branched chain fatty acids and of the bile acid intermediates di- and trihydroxycoprostanic acids are oxidized by one single peroxisomal branched chain acyl-CoA oxidase in human liver and kidney.* J Biol Chem, 1993. **268**(14): p. 10335-44.
224. Wanders, R.J., et al., *Peroxisomes, lipid metabolism and lipotoxicity.* Biochim Biophys Acta, 2010. **1801**(3): p. 272-80.
225. Wanders, R.J., et al., *The peroxisomal ABC transporter family.* Pflugers Arch, 2007. **453**(5): p. 719-34.
226. Kashiwayama, Y., et al., *70-kDa peroxisomal membrane protein related protein (P70R/ABCD4) localizes to endoplasmic reticulum not peroxisomes, and NH2-terminal*

*hydrophobic property determines the subcellular localization of ABC subfamily D proteins.* Exp Cell Res, 2009. **315**(2): p. 190-205.
227. van Roermund, C.W., et al., *The human peroxisomal ABC half transporter ALDP functions as a homodimer and accepts acyl-CoA esters.* Faseb J, 2008. **22**(12): p. 4201-8.
228. van Roermund, C.W., et al., *Differential substrate specificities of human ABCD1 and ABCD2 in peroxisomal fatty acid beta-oxidation.* Biochim Biophys Acta, 2011. **1811**(3): p. 148-52.
229. Cartier, N., et al., *Retroviral-mediated gene transfer corrects very-long-chain fatty acid metabolism in adrenoleukodystrophy fibroblasts.* Proc Natl Acad Sci U S A, 1995. **92**(5): p. 1674-8.
230. Braiterman, L.T., et al., *Suppression of peroxisomal membrane protein defects by peroxisomal ATP binding cassette (ABC) proteins.* Hum Mol Genet, 1998. **7**(2): p. 239-47.
231. Weinhofer, I., et al., *Cholesterol regulates ABCD2 expression: implications for the therapy of X-linked adrenoleukodystrophy.* Hum Mol Genet, 2002. **11**(22): p. 2701-8.
232. Weinhofer, I., et al., *X-linked adrenoleukodystrophy mice demonstrate abnormalities in cholesterol metabolism.* FEBS Lett, 2005. **579**(25): p. 5512-6.
233. Lombard-Platet, G., et al., *A close relative of the adrenoleukodystrophy (ALD) gene codes for a peroxisomal protein with a specific expression pattern.* Proc Natl Acad Sci U S A, 1996. **93**(3): p. 1265-9.
234. Pujol, A., et al., *Functional overlap between ABCD1 (ALD) and ABCD2 (ALDR) transporters: a therapeutic target for X-adrenoleukodystrophy.* Human Molecular Genetics, 2004. **13**(23): p. 2997-3006.
235. Lu, J.F., et al., *A mouse model for X-linked adrenoleukodystrophy.* Proc Natl Acad Sci U S A, 1997. **94**(17): p. 9366-71.
236. Ferrer, I., et al., *Inactivation of the peroxisomal ABCD2 transporter in the mouse leads to late-onset ataxia involving mitochondria, Golgi and endoplasmatic reticulum damage.* Hum Mol Genet, 2005. **14**(23): p. 3565-3577.
237. Lu, J.F., et al., *The role of peroxisomal ABC transporters in the mouse adrenal gland: the loss of Abcd2 (ALDR), Not Abcd1 (ALD), causes oxidative damage.* Laboratory Investigation, 2007. **87**(3): p. 261-272.
238. Fourcade, S., et al., *A key role for the peroxisomal ABCD2 transporter in fatty acid homeostasis.* Am J Physiol Endocrinol Metab, 2009. **296**(1): p. E211-21.
239. Fourcade, S., et al., *Valproic acid induces antioxidant effects in X-linked adrenoleukodystrophy.* Hum Mol Genet, 2010. **19**(10): p. 2005-14.
240. Bremer, J. and K.R. Norum, *Metabolism of very long-chain monounsaturated fatty acids (22:1) and the adaptation to their presence in the diet.* J Lipid Res, 1982. **23**(2): p. 243-56.
241. Liu, J., et al., *ABCD2 is abundant in adipose tissue and opposes the accumulation of dietary erucic acid (C22:1) in fat.* J Lipid Res, 2010. **51**(1): p. 162-8.
242. Liu, J.J., et al., *The absence of ABCD2 sensitizes mice to disruptions in lipid metabolism by dietary erucic acid.* Journal of Lipid Research, 2012. **53**(6): p. 1071-1079.
243. Weinhofer, I., et al., *Distinct modulatory roles for thyroid hormone receptors TRalpha and TRbeta in SREBP1-activated ABCD2 expression.* Eur J Cell Biol, 2008. **87**(12): p. 933-45.
244. Gondcaille, C., et al., *LXR antagonists induce ABCD2 expression.* Biochim Biophys Acta, 2013. **1841**(2): p. 259-266.
245. Park, C.Y., et al., *ABCD2 is a direct target of beta-catenin and TCF-4: implications for X-linked adrenoleukodystrophy therapy.* PLoS One, 2013. **8**(2): p. e56242.

246. Berger, J., et al., *The four murine peroxisomal ABC-transporter genes differ in constitutive, inducible and developmental expression.* European Journal of Biochemistry, 1999. **265**(2): p. 719-727.
247. Imanaka, T., et al., *Characterization of the 70-kDa peroxisomal membrane protein, an ATP binding cassette transporter.* J Biol Chem, 1999. **274**(17): p. 11968-76.
248. Morita, M. and T. Imanaka, *Peroxisomal ABC transporters: structure, function and role in disease.* Biochim Biophys Acta, 2012. **1822**(9): p. 1387-96.
249. Blanchette-Mackie, E.J., et al., *Perilipin is located on the surface layer of intracellular lipid droplets in adipocytes.* J Lipid Res, 1995. **36**(6): p. 1211-26.
250. Ahlabo, I. and T. Barnard, *Observations on peroxisomes in brown adipose tissue of the rat.* J Histochem Cytochem, 1971. **19**(11): p. 670-5.
251. Pavelka, M., et al., *Enzymic and morphological studies on catalase positive particles from brown fat of cold adapted rats.* Histochemistry, 1976. **50**(1): p. 47-55.
252. Bagattin, A., L. Hugendubler, and E. Mueller, *Transcriptional coactivator PGC-1alpha promotes peroxisomal remodeling and biogenesis.* Proc Natl Acad Sci U S A, 2010. **107**(47): p. 20376-81.
253. Martens, K., et al., *Peroxisome deficient aP2-Pex5 knockout mice display impaired white adipocyte and muscle function concomitant with reduced adrenergic tone.* Mol Genet Metab, 2012. **107**(4): p. 735-47.
254. Brites, P., et al., *Alkyl-glycerol rescues plasmalogen levels and pathology of ether-phospholipid deficient mice.* PLoS One, 2011. **6**(12): p. e28539.
255. Staels, B., et al., *Mechanism of action of fibrates on lipid and lipoprotein metabolism.* Circulation, 1998. **98**(19): p. 2088-93.
256. Farnier, M., *Update on the clinical utility of fenofibrate in mixed dyslipidemias: mechanisms of action and rational prescribing.* Vasc Health Risk Manag, 2008. **4**(5): p. 991-1000.
257. Lai, C.Q., et al., *Fenofibrate effect on triglyceride and postprandial response of apolipoprotein A5 variants: the GOLDN study.* Arterioscler Thromb Vasc Biol, 2007. **27**(6): p. 1417-25.
258. Kraja, A.T., et al., *Genetic analysis of 16 NMR-lipoprotein fractions in humans, the GOLDN study.* Lipids, 2013. **48**(2): p. 155-65.
259. Frazier-Wood, A.C., et al., *The PPAR alpha gene is associated with triglyceride, low-density cholesterol and inflammation marker response to fenofibrate intervention: the GOLDN study.* Pharmacogenomics J, 2013. **13**(4): p. 312-7.
260. Irvin, M.R., et al., *Apolipoprotein E polymorphisms and postprandial triglyceridemia before and after fenofibrate treatment in the Genetics of Lipid Lowering and Diet Network (GOLDN) Study.* Circ Cardiovasc Genet, 2010. **3**(5): p. 462-7.
261. Wojczynski, M.K., et al., *Apolipoprotein B genetic variants modify the response to fenofibrate: a GOLDN study.* J Lipid Res, 2010. **51**(11): p. 3316-23.
262. Liu, Y., et al., *The SCARB1 gene is associated with lipid response to dietary and pharmacological interventions.* J Hum Genet, 2008. **53**(8): p. 709-17.
263. Shen, J., et al., *Association of common C-reactive protein (CRP) gene polymorphisms with baseline plasma CRP levels and fenofibrate response: the GOLDN study.* Diabetes Care, 2008. **31**(5): p. 910-5.
264. Aslibekyan, S., et al., *Variants identified in a GWAS meta-analysis for blood lipids are associated with the lipid response to fenofibrate.* PLoS One, 2012. **7**(10): p. e48663.

265. Weber, F.D., et al., *X-linked adrenoleukodystrophy: very long-chain fatty acid metabolism is severely impaired in monocytes but not in lymphocytes.* Hum Mol Genet, 2014.
266. Wanders, R.J. and H.R. Waterham, *Biochemistry of mammalian peroxisomes revisited.* Annu Rev Biochem, 2006. **75**: p. 295-332.
267. Mosser, J., et al., *Putative X-linked adrenoleukodystrophy gene shares unexpected homology with ABC transporters.* Nature, 1993. **361**(6414): p. 726-30.
268. Schluter, A., et al., *Functional genomic analysis unravels a metabolic-inflammatory interplay in adrenoleukodystrophy.* Human Molecular Genetics, 2012. **21**(5): p. 1062-1077.
269. Gentleman, R.C., et al., *Bioconductor: open software development for computational biology and bioinformatics.* Genome Biology, 2004. **5**(10).
270. Smyth, G.K., *Limma: linear models for microarray data*, in *Statistics for Biology and Health*. 2005. p. 397-420.
271. Robert Gentleman, V.J.C., Wolfgang Huber, Rafael A. Irizarry, Sandrine Dudoit, *Bioinformatics and Computational Biology Solutions Using R and Bioconductor*, in *Statistics for Biology and Health*. 2005. p. 397-420.
272. Kanehisa, M. and S. Goto, *KEGG: Kyoto Encyclopedia of Genes and Genomes.* Nucleic Acids Research, 2000. **28**(1): p. 27-30.
273. Mootha, V.K., et al., *PGC-1 alpha-responsive genes involved in oxidative phosphorylation are coordinately downregulated in human diabetes.* Nature Genetics, 2003. **34**(3): p. 267-273.
274. Corella, D., et al., *The-256T > C polymorphism in the apolipoprotein A-II gene promoter is associated with body mass index and food intake in the genetics of lipid lowering drugs and diet network study.* Clinical Chemistry, 2007. **53**(6): p. 1144-1152.
275. Aslibekyan, S., et al., *A genome-wide association study of inflammatory biomarker changes in response to fenofibrate treatment in the Genetics of Lipid Lowering Drug and Diet Network.* Pharmacogenet Genomics, 2012. **22**(3): p. 191-7.
276. Matsson, P., et al., *Discovery of regulatory elements in human ATP-binding cassette transporters through expression quantitative trait mapping.* Pharmacogenomics J, 2012. **12**(3): p. 214-26.
277. Brun, R.P., et al., *Differential activation of adipogenesis by multiple PPAR isoforms.* Genes & Development, 1996. **10**(8): p. 974-984.
278. Chaput, E., et al., *Fenofibrate and rosiglitazone lower serum triglycerides with opposing effects on body weight.* Biochem Biophys Res Commun, 2000. **271**(2): p. 445-50.
279. Raabe, M., et al., *Analysis of the role of microsomal triglyceride transfer protein in the liver of tissue-specific knockout mice.* Journal of Clinical Investigation, 1999. **103**(9): p. 1287-1298.
280. Mead, J.R., S.A. Irvine, and D.P. Ramji, *Lipoprotein lipase: structure, function, regulation, and role in disease.* Journal of Molecular Medicine-Jmm, 2002. **80**(12): p. 753-769.
281. Van Veldhoven, P.P. and M. Baes, *Peroxisome deficient invertebrate and vertebrate animal models.* Front Physiol, 2013. **4**: p. 335.
282. Weinhofer, I., et al., *Liver X receptor alpha interferes with SREBP1c-mediated Abcd2 expression. Novel cross-talk in gene regulation.* J Biol Chem, 2005. **280**(50): p. 41243-51.
283. Liu, J., et al., *The absence of ABCD2 sensitizes mice to disruptions in lipid metabolism by dietary erucic acid.* J Lipid Res, 2012. **53**(6): p. 1071-9.
284. Zhen, Y., et al., *Nuclear import of exogenous FGF1 requires the ER-protein LRRC59 and the importins Kpnalpha1 and Kpnbeta1.* Traffic, 2012. **13**(5): p. 650-64.

285. Alexson, S.E., H. Osmundsen, and R.K. Berge, *The presence of acyl-CoA hydrolase in rat brown-adipose-tissue peroxisomes.* Biochem J, 1989. **262**(1): p. 41-6.
286. Graham, J.M., *Isolation of peroxisomes from tissues and cells by differential and density gradient centrifugation.* Curr Protoc Cell Biol, 2001. **Chapter 3**: p. Unit 3 5.
287. Luers, G.H., et al., *Immuno-isolation of highly purified peroxisomes using magnetic beads and continuous immunomagnetic sorting.* Electrophoresis, 1998. **19**(7): p. 1205-10.
288. American Academy of Pediatrics Steering Committee on Quality, I., et al., *Toward transparent clinical policies.* Pediatrics, 2008. **121**(3): p. 643-6.
289. Schrader, M., N.A. Bonekamp, and M. Islinger, *Fission and proliferation of peroxisomes.* Biochim Biophys Acta, 2012. **1822**(9): p. 1343-57.
290. Koch, A., et al., *Dynamin-like protein 1 is involved in peroxisomal fission.* J Biol Chem, 2003. **278**(10): p. 8597-605.
291. Jourdain, I., et al., *Dynamin-dependent biogenesis, cell cycle regulation and mitochondrial association of peroxisomes in fission yeast.* Traffic, 2008. **9**(3): p. 353-65.
292. Neuspiel, M., et al., *Cargo-selected transport from the mitochondria to peroxisomes is mediated by vesicular carriers.* Curr Biol, 2008. **18**(2): p. 102-8.
293. Kim, P.K., et al., *The origin and maintenance of mammalian peroxisomes involves a de novo PEX16-dependent pathway from the ER.* J Cell Biol, 2006. **173**(4): p. 521-32.
294. Toro, A.A., et al., *Pex3p-dependent peroxisomal biogenesis initiates in the endoplasmic reticulum of human fibroblasts.* J Cell Biochem, 2009. **107**(6): p. 1083-96.
295. Yonekawa, S., et al., *Sec16B is involved in the endoplasmic reticulum export of the peroxisomal membrane biogenesis factor peroxin 16 (Pex16) in mammalian cells.* Proc Natl Acad Sci U S A, 2011. **108**(31): p. 12746-51.
296. Boukh-Viner, T., et al., *Dynamic ergosterol- and ceramide-rich domains in the peroxisomal membrane serve as an organizing platform for peroxisome fusion.* J Cell Biol, 2005. **168**(5): p. 761-73.
297. Ye, Y., et al., *A membrane protein complex mediates retro-translocation from the ER lumen into the cytosol.* Nature, 2004. **429**(6994): p. 841-7.
298. Curran, J.E., et al., *Genetic variation in selenoprotein S influences inflammatory response.* Nat Genet, 2005. **37**(11): p. 1234-41.
299. Turanov, A.A., et al., *Selenoprotein S is Involved in Maintenance and Transport of Multiprotein Complexes.* Biochem J, 2014.
300. Jonker, J.W., et al., *A PPARgamma-FGF1 axis is required for adaptive adipose remodelling and metabolic homeostasis.* Nature, 2012. **485**(7398): p. 391-4.

## VITA

## PERSONAL INFORMATION

Name: Xiaoxi Liu

## EDUCATION

August 2009 – August 2014

Department of Pharmaceutical Sciences

College of Pharmacy, University of Kentucky

Lexington, Kentucky, USA

July 2005 – July 2009

Bachelor Degree of Biological Sciences

University of Science and Technology of China

Hefei, Anhui, China

## PUBLICATIONS

1. Yuhuan Wang, Xiaoxi Liu, Gregory A. Graf. An Urso-EZ combination therapy that simultaneously increases biliary secretion and reduces cholesterol absorption actively promotes cholesterol elimination in mice. (In preparation for submission).
2. Xiaoxi Liu, Jingjing Liu, Joshua D. Lester, Gregory A. Graf. ABCD2 identifies a novel subcellular organelle in mouse adipose tissue. (submitted to BMC Cell Biology)
3. Xiaoxi Liu, Jingjing Liu, Shuang Liang, Agatha Schlüter, Stephane Fourcade, Stella Aslibekyan, Aurora Pujol, Gregory A. ABCD2 alters PPARα signaling in vitro, but does not impair responses to fenofibrate therapy in a mouse model of diet-induced obesity. (Submitted to MolPharm)
4. Kai Su, Nadezhda S. Sabeva, Yuhuan Wang, Xiaoxi Liu, Joshua D. Lester, Jingjing Liu, Shuang Liang, Gregory A. Graf. Acceleration of biliary cholesterol secretion restores glycemic control and alleviates hypertriglyceridemia in obese db/db mice. Arterioscler Thromb Vasc Biol. 2014 Jan; 34(1):26-33. doi: 10.1161

5. Chaohua Lai, Xiaoxi Liu, Changlin Tian, Fangming Wu. Integrin α1 has a long helix, extending from the transmembrane region to the cytoplasmic tail in detergent micelles. PLoS One. 2013 Apr 30; 8(4):e62954. doi: 10.1371
6. Jingjing Liu, Shuang Liang, Xiaoxi Liu, J. Andrew Brown, Kylie E. Newman, Manjula Sunkara, Andrew J. Morris, Saloni Bhatnagar, Xiangan Li, Aurora Pujol and Gregory A. Graf. The absence of ABCD2 sensitizes mice to disruptions in lipid metabolism by dietary erucic acid." J Lipid Res. 2012 Jun; 53(6):1071-9. doi: 10.1194